Study on Potassium Dihydrogen Phosphate and Potassium Dideuterium Phosphate by Single-Crystal Neutron Structural Analyses

単結晶中性子構造解析による燐酸二水素カリウムおよび燐酸二重水素カリウムの研究

Tatsuki MIYOSHI
Graduate school of Science and Engineering, Yamaguchi University

三好　烈麗
山口大学大学院　理工学研究科

Supervisor: Prof. Hiroyuki MASHIYAMA

指導教員：　増山　博行 教授

March, 2011
2011 年 3 月

Abstract

Potassium dihydrogen phosphate (KDP) is paraelectric with a tetragonal system ($I\bar{4}2d$, $Z = 4$) at room temperature. The crystal is grown from a water solution by the slow evaporation method, colorless, transparent, and stable in atmospheric condition. It is useful in piezoelectric and nonlinear optic devices. In 1935, ferroelectricity of KDP along the c-axis was discovered below the Curie temperature $T_c = 123\,\mathrm{K}$, where the crystal takes the face-centered orthorhombic system ($Fdd2$, $Z = 8$). The deuterated crystal potassium dideuterium phosphate (DKDP) is isomorphous to KDP, and T_c rises about 100 K, which is known as the deuteration effect or isotope effect. Under high pressure (hydrostatic pressure), T_c decreases and finally disappears at about 2 and 6 GPa for KDP and DKDP, respectively, around which the dielectric constant shows a quantum paraelectric character. Although the phenomena of the ferroelectric transition have been investigated widely by many researchers, the dynamical mechanism of the phase transition in KDP/DKDP is not conclusive yet.

To the authors' knowledge, structural studies of KDP are limited down to the liquid nitrogen temperature, and those of DKDP down to 210 K. In addition to the structural parameters in the paraelectric phase, those in the ferroelectric phase are important in the comprehensive understanding of the phase transition mechanism. Therefore, we perform the single-crystal neutron diffraction experiments of both KDP and DKDP in a wide temperature range (down to 10 K) for both ferroelectric and paraelectric phases and refine the structure parameters, in order to elucidate the essential difference between KDP and DKDP. The neutron diffraction experiments were performed using a four-circle-off-center-type diffractometer, FONDER (T2-2) of JRR-3M, JAEA, Tokai.

The structural changes at the ferroelectric phase transition and their differences of both KDP and DKDP are summarized as follows:

(i) Protons/deuterons are in disorder in the paraelectric phase, while the K and P atoms are not from the crystallographic viewpoints. Below T_c, the K and P atoms displace along the c-axis in connection with the ordering of protons/deuterons.

(ii) In DKDP, the atomic coordinates show no remarkable temperature dependence except for the stepwise change during the ferroelectric phase transition. On the other hand, the 'precursor' behavior in the paraelectric phase and the continuous changes of the atomic coordinates just below T_c are confirmed in KDP.

(iii) The displacements of the atoms below T_c are considered in keeping a common center-of-gravity of the unit cell. In the ferroelectric phase, the K and P atoms display remarkable translations, and the O and H/D atoms tiny shifts along the c-axis in comparison with their positions in the paraelectric phase. The antiparallel displacements of the K and P atoms assure keeping the center-of-gravity of the unit cell throughout the phase transition.

(iv) The spontaneous polarization is calculated from the structural parameters using the point-charge method (K:$+e$, P:$+5e$, O:$-2e$, and H/D:$+e$). The calculated magnitudes of the polarization are in agreement with the previous values measured directly. The contribution from the P atom to the total polarization is predominant because of its large charge. As reported previously, the spontaneous polarization of DKDP is about 1.2 times larger than that of KDP, and this difference arises from the slightly larger displacement of the P atom in DKDP than in KDP.

(v) In KDP, the atomic shifts along the c-axis indicate gradual increases due to the ordering of proton with decreasing temperature just below T_c. This character is consequently associated with the temperature dependence of the spontaneous polarization. At very low temperatures, the thermal contraction of the unit cell affects the magnitudes of the displacements, that is, the spontaneous polarizations decrease a little. In DKDP, the atomic displacements and the polarization change take place rapidly; the phase transition must be just of the first-order type.

(vi) All the atomic distances and angles are examined in both KDP and DKDP. From the result, remarkable differences are confirmed in the geometrical parameters relevant to the hydrogen bonds (O–H/D$\cdots$O bond), while no significant difference is confirmed in the other quantities. Except for the temperature dependence just below T_c in KDP, the continuous thermal contractions of the unit cells are only observed, and no remarkable change is found in the crystal structure below the liquid-nitrogen temperature.

(vii) In the paraelectric phases, the split distance between two equilibrium sites of the H/D atom, δ, is about 0.13 Å longer in DKDP than in KDP. The distance between two oxygen atoms of the hydrogen bond, $R_{O\text{–}O}$, has a difference of about 0.04 Å between KDP and DKDP; these two are reconfirmed in our study.

It is also found that the deuteron has a smaller distance from the acceptor O atom; the distance r_D is about 0.04 Å shorter than r_H in both paraelectric and ferroelectric phases. r_D depends little on temperature, while r_H rather largely.

Even if the proton and deuteron are located within the same double minimum potential, the remarkable difference should appear in their reciprocating motions between two equilibrium positions because of the zero-point energies due to the mass difference. Consequently, it generates a difference in the strength of the hydrogen bond; if the proton vibrates more frequently, it makes the distance R_{O-O} shorter. Therefore, the isotope effect on KDP and DKDP can be explained as a result of such a mass effect. Additionally, the difference between the behaviors of proton and deuteron is found to increase definitely the difference of the spontaneous polarizations; a heavy deuteron attaches closer to the acceptor O1, and induces the larger charge redistribution in P–O bond and the D atom, so that the shift of the P atom can become larger. (Refer to (iv).)

These structural analyses support a scenario in which the differences of the hydrogen mass and the potentials associated with different distances between the two O atoms cause the differences in the transition temperature, the spontaneous polarization, and the vanishing of the ferroelectric phases at different critical pressures, in KDP and DKDP. Namely, 'tunneling' hydrogen is the key to understanding the phase transition of KDP-type ferroelectrics, though 'tunneling' may be a dynamical disorder without quantum coherency.

In this thesis, the author presents the results of the single-crystal neutron diffraction experiments of both KDP and DKDP in a wide temperature range (down to 10 K) for the ferroelectric and paraelectric phases and refine the structure parameters, in order to discuss the essential difference between KDP and DKDP. The briefing introduction onto the distinguished ferroelectrics, KDP and DKDP, is presented in chapter 1, which would provide beginners of both ferroelectrics with some and simple explanations. If the reader has enough knowledges about KDP and DKDP, he/she may skip chapter 1 for economy with time. Next, The experimental process is described in chapter 2. Results of the structure refinement are presented in chapter 3, and discussed in chapter 4. Finally, conclusions are presented in chapter 5.

要旨

リン酸二水素カリウム（略称 KDP）は 1935 年に強誘電性が発見されて以来，多数の研究がなされている化合物である．KDP は無色透明なイオン性結晶であり，水溶液蒸発法などにより良質な単結晶ができ，非線形光学素子，圧電素子として有用な物質である．常圧下，室温で常誘電相（正方晶系；$I\bar{4}2d$, $Z = 4$）であり，123 K 以下で強誘電相（斜方晶系；$Fdd2$, $Z = 8$）に相転移する．KDP の大きな特徴は，組成中の軽水素を重水素に置換したリン酸二重水素カリウム（略称 DKDP）での常誘電—強誘電相転移点が常圧下で約 100 K 近く上昇することであり，この重水素置換効果の原因について諸説あり，現在でも決着をみていない．また，高圧（静水圧）下では KDP，DKDP ともに転移点が降下し，それぞれ約 2 GPa と 6 GPa において強誘電相が消失し，また量子常誘電性を示すことも極めて重要な特徴と言える．

化合物の微視的構造を調べ，物性との関連性を議論することは相転移機構を理解する上で重要である．KDP と DKDP における重水素置換効果及び高圧下の挙動の原因解明に繋がり得る知見が両物質の詳細な構造解析によって得られると考えられるので，強誘電相の全温度領域での単結晶中性子回折実験を行った．日本原子力研究開発機構（JAEA）の原子力科学研究所（茨城県東海村）内の改造 3 号炉に設置の 4 軸型回折計（FONDER）を共同利用により使用し、実験を行った．転移点近傍を含む広い温度域における両物質の結晶構造解析から，詳細な結晶構造パラメータの温度依存性を得，KDP と DKDP の比較を行った．

以下に得られた知見をまとめる．

(1) 常誘電相でカリウム及びリン原子核は結晶学的に無秩序状態であると結論することは出来なかった．強誘電相では（重）水素の秩序化に伴い，両原子核の変位が生ずる．

(2) DKDP では転移点での不連続な変化以外，構造に顕著な温度依存性はないが，KDP では常誘電相での前駆的挙動と転移点直下での原子座標の連続的変化が認められた．

(3) 相転移前後における原子核の変位を単位胞中の重心を一致させて比較した．常誘電相に対して，強誘電相ではカリウム及びリン原子核が顕著な変位を起こし，それ以外の酸素，軽水素もしくは重水素原子核はほとんど変位していなかった．相転移による重心の均衡はカリウム及びリン原子核の反平行の変位により保たれている．

(4) 点電荷（カリウム：$+1e$，リン：$+5e$，酸素：$-2e$，水素：$+1e$）を仮定して構造パラメータから c 軸方向に発生する自発分極を計算すると，過去に誘電的測定で報告されている実験値と良く一致した．自発分極に対する各原子の寄与は価数の大きいリンの変位によるものが大半である．DKDP の自発分極は KDP に対して 1.2 倍ほど大きな値をもつことが知られているが，この差は PO_4 四面体中のリン原子核の変位量が KDP に対して DKDP では若干大きいためであることがわかった．

(5) KDP では転移点直下で秩序化が進むにつれて，原子変位が大きくなり，これが自発分極の温度依存性を表している．極低温では格子の熱収縮が変位量，従って分極値を僅かだが減少させる．DKDP は転移に伴い直ちに原子変位が起こり，1 次転移の様相が強い．

(6) 結晶構造中の隣接する原子間距離，角度を調べた．その結果 KDP と DKDP では単位胞中の水素結合（O–H/D$\cdots$O 結合）に関連する幾何学的パラメータに注目すべき差が認められたのに対し，それ以外のものについては有意の差は認めらなかった．上述の転移点直下の温度依存以外は，連続的な熱収縮による温度依存があるのみで，窒素温度以下の構造は極低温まで変化はなかった．

(7) 従来は常誘電相で水素が位置する 2 つのサイト間の距離 δ が軽水素より重水素においては 0.13 Å ほど大きいこと，及び酸素間距離 $R_{O\text{–}O}$ に差（約 0.04 Å）があるという幾何学的同位体効果のみが注目されていた．今回，これを再確認するとともに，常誘電，強誘電の両相において，重水素原子核はアクセプター原子である酸素原子核からの距離 r がより小さい値（軽水素原子核に対して約 0.04 Å）をとり，強誘電相ではほとんど温度依存がないことが新たに見出された．

軽水素原子核と重水素原子核で同じポテンシャル中にあっても，質量の差に起因して重水素の零点エネルギーは軽水素より 0.7 倍ほど低いため，2 つのサイトを行き来する頻度に大きな差が出る．その結果は水素結合力の差となり，重水素では $R_{O\text{–}O}$ が大きくなり，その反動で r が小さくなると考えることで同位体効果は説明がつく．このような軽水素原子核と重水素原子核の振る舞いの差異は (4) で挙げた自発分極の差を生むことに深く関連する．つまり重い重水素原子核は O1 原子により近づき，そして P–O 結合と重水素原子核の間にて電子密度分布のより大きな変化を誘起する。これにより P 原子はより大きく変位する。

水素の質量の差と酸素間距離の違いによるポテンシャルの差とが相俟って，KDP と DKDP の転移温度の差，自発分極の差，さらには静水圧下での強誘電相の喪失というシナリオを，本構造解析結果はサポートしている．すなわち，KDP 系強誘電体の相転移における水素結合の重要性を構造的に明らかにすることが出来た．

本博士論文において、著者は最低温度 10 K までに至る幅広い温度域での KDP 及び DKDP 両結晶の単結晶中性子回折実験の結果を提示し、そしてその結果を元に両結晶の間での本質的な結晶構造の差を議論している。第 1 章では著名な強誘電体である KDP と DKDP について、その肝要な特徴を平易に解説している。若し KDP 及び DKDP につい

ての知識を有する読者であれば、第 1 章は読み飛ばして頂いても構わない。第 2 章では実験に関する事項が、第 3 章では実験結果について、そして第 4 章ではその考察について述べられている。そして最後に、第 5 章において本論文のまとめが記されている。

Acknowledgements

The author thanks Dr. Kazuo Gesi for providing KDP single crystals of fine quality.

The author expresses his deepest gratitude to Prof. Hiroyuki Mashiyama for his supervision onto the author.

Deep appreciation goes to Prof. Takanao Asahi and Dr. Hironobu Kasano. Prof. Takanao Asahi provided his own manuals for DABEX and RADIEL making the smooth study to the author. Dr. Hironobu Kasano feed his fruitful comments about chemical bonding and displacement of each atom through paraelectric-ferroelectric phase transitions of KDP and DKDP, and helpful advices on the preparation method of DKDP single crystal to the author.

The author extends his grateful thanks to Dr. Hirotake Shigematsu for carefull assistance in the single-crystal neutron diffraction experiment of DKDP.

The author also received warm encouragements for writing this paper from Prof. Terutake Tazawa, Prof. Toru Shigeoka, Prof. Isao Kiuchi, Prof. Kiyoshi Shiraishi, Prof. Koji Nozaki, Mr. Naohiro Koshiji, Dr. Masaki Takesada, Dr. Yukihiko Kawamura, Dr. Nahomi Kan, Dr. Ko-ichiro Kobayashi, and Mr. Kazuhiko Shinoda. A crystallographic visualization software VESTA [1] provided fine drawings of the KDP/DKDP crystal structure and accurate and reliable sense to the author in this study.

The neutron diffraction experiments at JRR-3M were supported by the Institute for Solid State Physics (The University of Tokyo) and JAEA under experiment-project Nos. 6746, 7780, 8777, and 9736. The author would like to express his grateful thanks to Prof. Yukio Noda, Dr. Hiroyuki Kimura, and the dedicated and credible staffs of Tokai Research and Development Center, JAEA.

Mr. Tomoshi Akimoto, Mr. Fumihiro Ishimura, Mr. Shuji Enokida, Mr. Koji Kanegae, Mr. Yoshihiko Sako, Mr. Takuya Tsunehiro, and Ms. Ayaka Fujita gave cheerful and noisy laboratory life to the author. He would like to gave his gentlemanly and silent thanksgivings to them.

For the memory of Mr. Teruki Hanada.

GOD BLESS YOU!

Table of Contents

Chapter 1

Introduction

dubium sapientiae initium.
— René Descartes, in 'Mediationes de Prima Philosophia'

In this thesis, the author reports about results of single-crystal neutron diffraction experiments of potassium dihydrogen phosphate (KH_2PO_4, KDP) and its deuterated crystal isomorph KD_2PO_4 (DKDP) as well-known ferroelectrics.

Since discoveries of the ferroelectricity in them, many investigators made their works for these ferroelectrics from their experimental and theoretical viewpoints.

The crystals have some interesting and striking features: transition temperature rise of *ca.* 100 K by deuteration, ferroelectric transition vanishing under high pressures, etc.

Although those crystals are the typical ferroelectrics which have long history for more than seventy years, the interpretations of their ferroelectric phase transition mechanism have been in controversy for a long time. Except for the paraelectric phases, there are not enough and detail research reports about the crystal structures of the ferroelectric phases which will play important and effective roles in the discussion. Therefore, we performed single-crystal neutron structural analyses both of KDP and DKDP, and then compared particularly the crystal structures of the ferroelectric phases. As the results, the author present the discussions about the ferroelectric phase transitions of them from structural viewpoints.

Potassium dihydrogen phosphate (KH_2PO_4, hereafter abbreviated to KDP) is one of the well-known ferroelectrics discovered by Busch and Scherrer. [2–5]. The crystal is easily grown from a water solution by the slow evaporation method, stable

in atmospheric condition, useful in piezoelectric and nonlinear optic devices, and well known as a typical ferroelectric with a Curie temperature $T_c = 123\,\mathrm{K}$, where the paraelectric-ferroelectric phase transition takes place. Its paraelectric and ferroelectric phases have body-centered tetragonal ($I\bar{4}2d$, D_{2d}^{12}, $Z = 4$) and face-centered orthorhombic ($Fdd2$, C_{2v}^{19}, $Z = 8$) systems, respectively, and its ferroelectricity appears along the c-axis. (Refer Figs. 1.1–1.9.) KDP is often categorized in KDP family ferroelectrics or hydrogen-bond-type ferroelectrics, in which a proton in an O–H···O bond is considered to play an important role in ferroelectric phase transition. [6] *1

The deuterated crystal potassium dideuterium phosphate (KD_2PO_4, hereafter abbreviated to DKDP) is isomorphous to KDP, and its paraelectric-ferroelectric phase transition takes place at *ca.* 220 K. Both KDP and DKDP come up frequently in

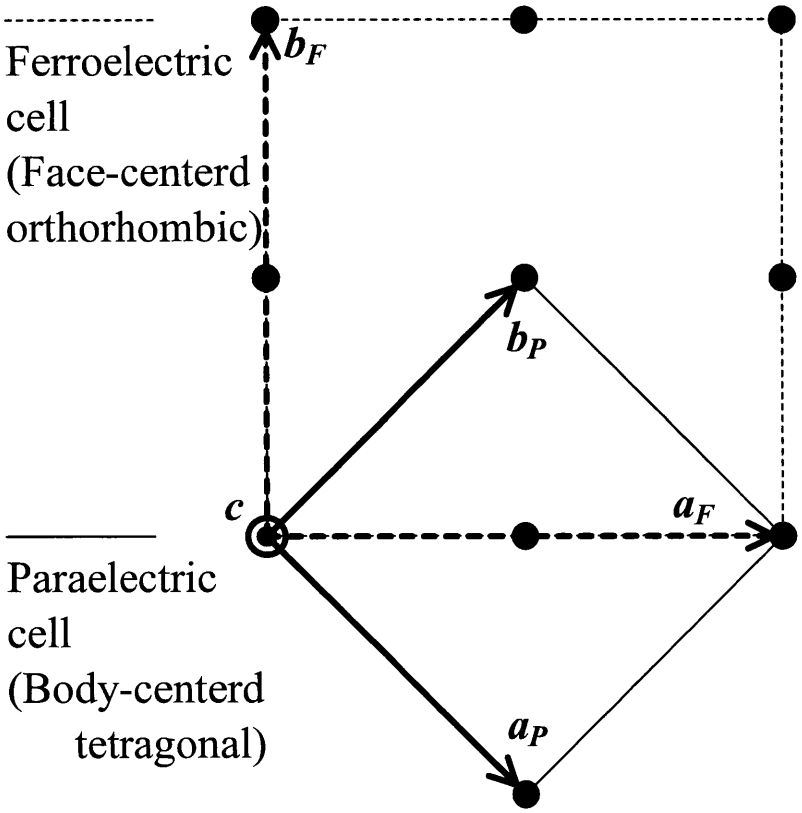

Figure 1.1 Schematic view of the lattice points of ferroelectric and paraelectric phases. Those cells have a common c-axis, which is ferroelectric and perpendicular to the page space. The ferroelectric lattice ($Fdd2$, C_{2v}^{19}, $Z = 8$) has a rotation angle of *ca.* 45° to the paraelectric phase ($I\bar{4}2d$, D_{2d}^{12}, $Z = 4$). The cell volume of the ferroelectric phase is two times larger than the paraelectric one.

*1 The author has been presented a report on other hydrogen-bond-type ferroelectric, pyridinium periodate. [7]

discussions about KDP-type ferroelectrics together, as if they are permanently inseparable counterparts. They are known for the deuteration effect or isotope effect showing that the Curie temperatures of their deuteron compounds are *ca.* 100 K higher than their proton compounds. [8–10]

In the paraelectric (tetragonal) phase of KDP, a proton occupies two sites related by a symmetry operation with equal probability. The disordered distribution of the proton between two oxygen atoms of the hydrogen bond in KDP was confirmed by neutron diffraction study. [11] Each PO_4 tetrahedron is linked to four adjacent PO_4 tetrahedra by hydrogen bonds, which lie along the *a*- or *b*-direction of the tetragonal cell perpendicular to the ferroelectric *c*-axis. The O-to-O distance R_{O-O} linked by the proton is *ca.* 2.5 Å, and the distance r between the oxygen atom and the nearby proton is *ca.* 1 Å. In the ferroelectric phase (orthorhombic phase), a proton attaches to an acceptor oxygen atom. Accordingly, the symmetry is lowered, and the ordered proton is observed directly also by single-crystal neutron diffraction study. (Refer Fig 1.10.) [12]

It is well known that only two protons attach to a PO_4 tetrahedron, which is known as the ice rule. [6] In the ferroelectric phase, the distance between two acceptors (named O1) decreases slightly, and the distance between two donors (named O2) increases slightly, in comparison with that in the tetragonal phase. The symmetry of the $H_2PO_4^-$ cluster is C_2, and the S_4 symmetry of the PO_4 tetrahedron should be lowered at low temperatures. [12]

Although the structural change from the paraelectric phase to the ferroelectric phase is accepted by every researcher, the dynamical mechanism of the ferroelectric phase transition in KDP is not conclusive yet. Blinc took the quantum effect in the order-disorder transition of the proton configuration into account, while assuming proton tunneling to explain the isotope effect. [13] Other researchers followed this proton tunneling model, and then gave some theoretical works including the model. [14–20]

Ichikawa and coworkers noticed geometrical isotope effects among hydrogen-bond-type ferroelectrics and their deuterated isomorphs; the hydrogen-bond lengths seem to have unique systematic differences between hydrogen and deuterium compounds. [21–26] More concretely, the distance R_{O-O} is *ca.* 0.05 Å longer in DKDP than in KDP. This longer R_{O-O} induces ordering at high temperatures, which is the key to understand the isotope effects in KDP family crystals.

Moreover, Tominaga *et al.* claimed that the tunneling model is inadequate since no evidence of the softening of the proton tunneling mode has been detected directly. [27, 28] Additionally, they found forbidden Raman lines in the paraelectric phase, which indicated that the point symmetry of a PO_4 tetrahedron was C_2, the orthorhombic symmetry, but not the tetragonal S_4. [29] Therefore, they proposed an order-disorder-

type transition mechanism on the basis of a mean structure including the locally and momentarily distorted PO_4 tetrahedron. [27–34] Fig. 1.11 shows a schematic view of the claimed model by Tominaga *et al.*

On the other hand, the quantum motion of protons within a double-well potential has been analyzed by many authors. The tunneling frequencies, if they exist independently, are estimated at *ca.* 500 and 50 cm^{-1} in KDP and DKDP, respectively. [20, 35–38]

The crystal structures of KDP and DKDP around the paraelectric-ferroelectric phase transition temperature were refined by Nelmes and his coworkers. [39–44] The main results are as follows:

(i) In the paraelectric phase, the density distribution of protons has two peaks

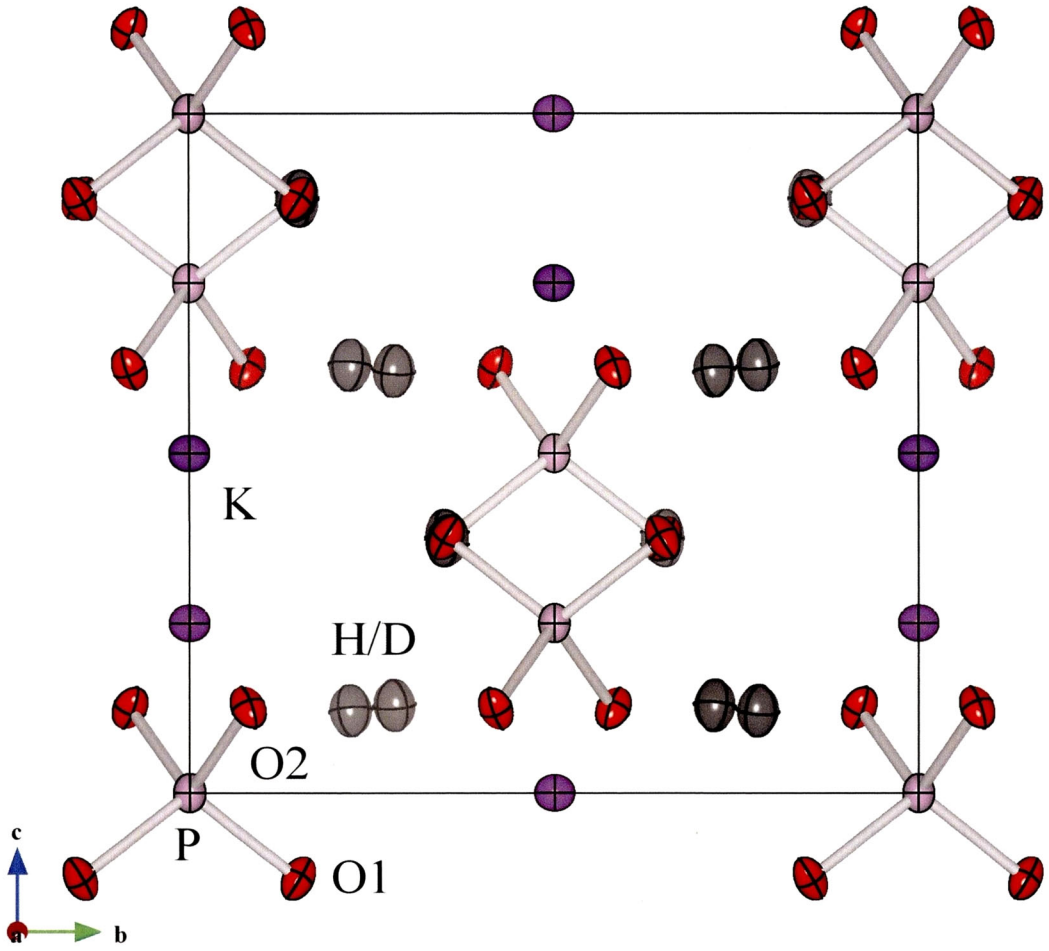

Figure 1.2 Crystal structure in the paraelectric phase of KDP/DKDP on the *a*-axis projection. Although O1 and O2 atoms are indicated separately for comparison with the ferroelectric phase, those atoms are crystallographically equivalent to each other in the paraelectric phase; only one independent oxygen atom exists in the asymmetric unit of the paraelectric unit cell.

separated by a distance δ, which is *ca.* 0.32 Å in KDP or 0.45 Å in DKDP just above T_c.

(ii) In the ferroelectric phase, the proton distribution becomes an unbalanced one just below T_c, and finally appears as a single peak at the acceptor O1 side.

(iii) With decreasing temperature, the atomic displacement parameter decreases linearly in the paraelectric phase. However, the U_{33} of the phosphorus atom has a positive cut point in the zero-temperature extrapolation, which may indicate the disorder of the phosphorus atom along the polar axis in the paraelectric phase.

For determination of structural parameters of crystal containing light element as hydrogen and/or deuterium atom, neutron diffraction method has greater confidence

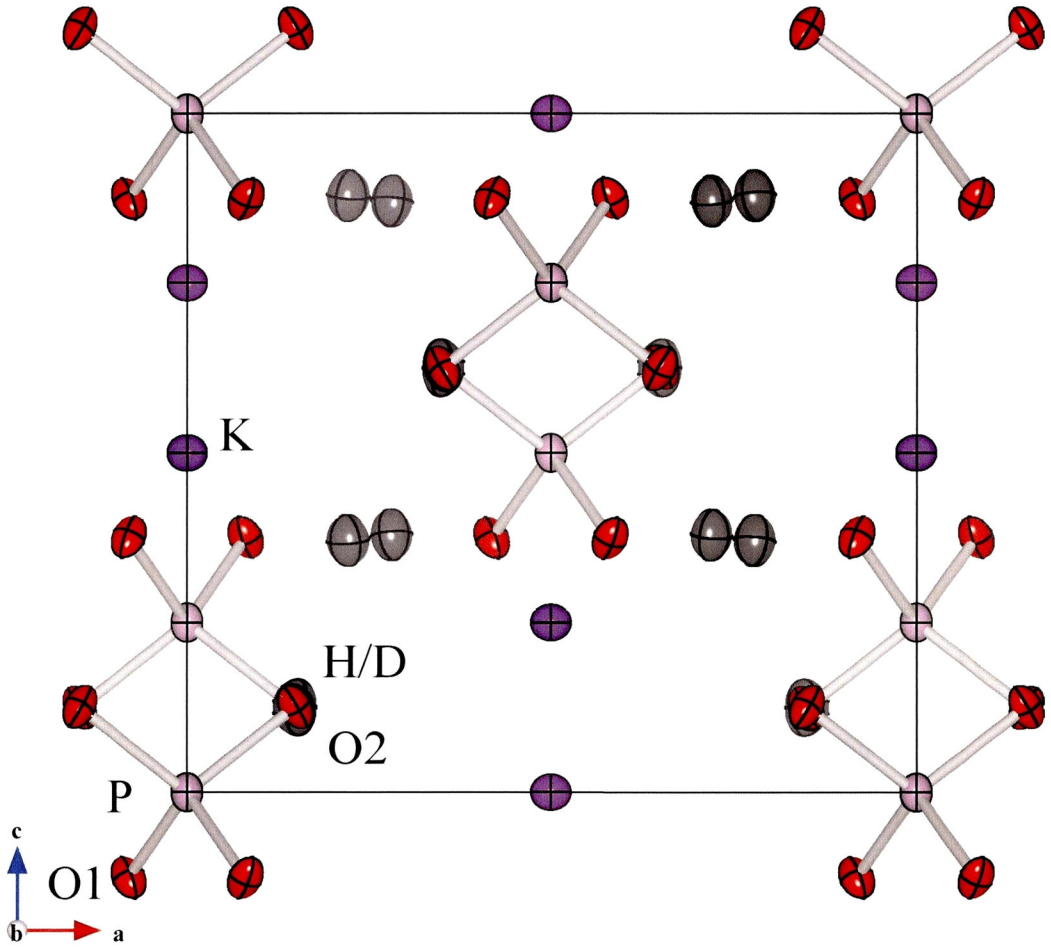

Figure 1.3 Crystal structure in the paraelectric phase of KDP/DKDP on the *b*-axis projection. Although O1 and O2 atoms are indicated separately for comparison with the ferroelectric phase, those atoms are crystallographically equivalent to each other in the paraelectric phase; only one independent oxygen atom exists in the asymmetric unit of the paraelectric unit cell.

than X-ray diffraction method. [11, 12, 45–54] Nelmes and his coworkers, who performed their single-crystal neutron diffraction experiments with high resolution, presented many reports about the detail crystal structures of KDP and DKDP. [39–44, 55–59]

The coherent neutron scattering used in structural analysis reflects only the mean structure of the crystal, so that it is difficult to distinguish between a dynamic disorder and a static or quasi-static disorder. The former may be called a quantum tunnel, while the latter a classical disorder. In order to see the dynamical motion of protons directly, incoherent neutron scattering experiments were performed by Ikeda *et al.*, who refuted proton tunneling. [60] Therefore, the order-disorder transition mechanism

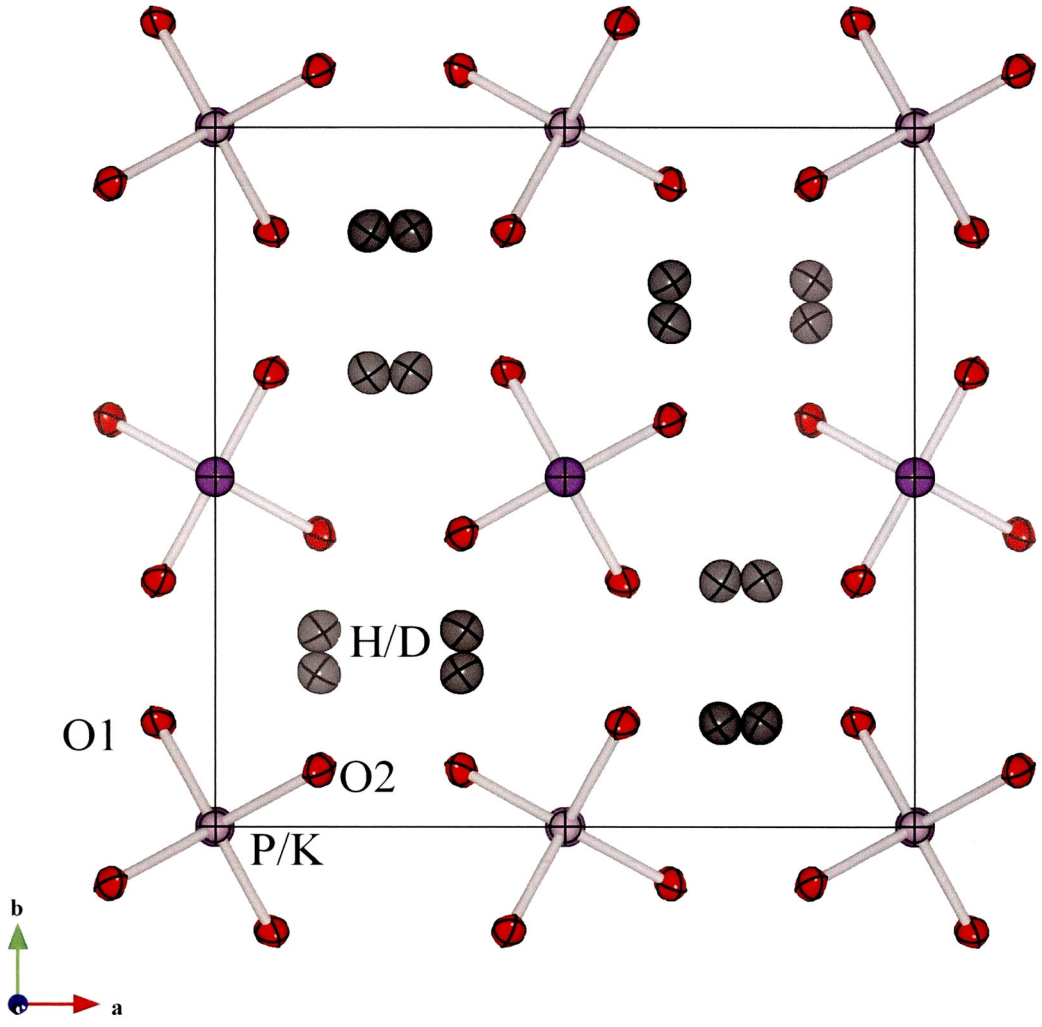

Figure 1.4 Crystal structure in the paraelectric phase of KDP/DKDP on the *c*-axis projection. Although O1 and O2 atoms are indicated separately for comparison with the ferroelectric phase, those atoms are crystallographically equivalent to each other in the paraelectric phase; only one independent oxygen atom exists in the asymmetric unit of the paraelectric unit cell.

not of a proton tunneling but of a disordered PO_4 tetrahedron was accepted widely.

The pressure effect on T_c is also well-known. [61–71] Samara proposed an empirical criterion to specify the character of the phase transition in ferroelectrics; the transition temperature increases with the application of hydrostatic pressure if the transition is of the order-disorder type, while for displacive-type ferroelectrics the temperature dependence is reversed. [66] It has been noted that the ferroelectric phase transition temperature of both KDP and DKDP decreases with the application of hydrostatic pressure, which is in contrast to typical substances that exhibit an order-disorder type transition. Moreover, the ferroelectric phase transition disappears down to zero temperature at the respective critical pressures, around which the dielectric constant shows a quantum paraelectric character, as if the transition is displacive. [71]

Such confusing situations were resolved partially. In 2002, Reiter *et al.* carefully

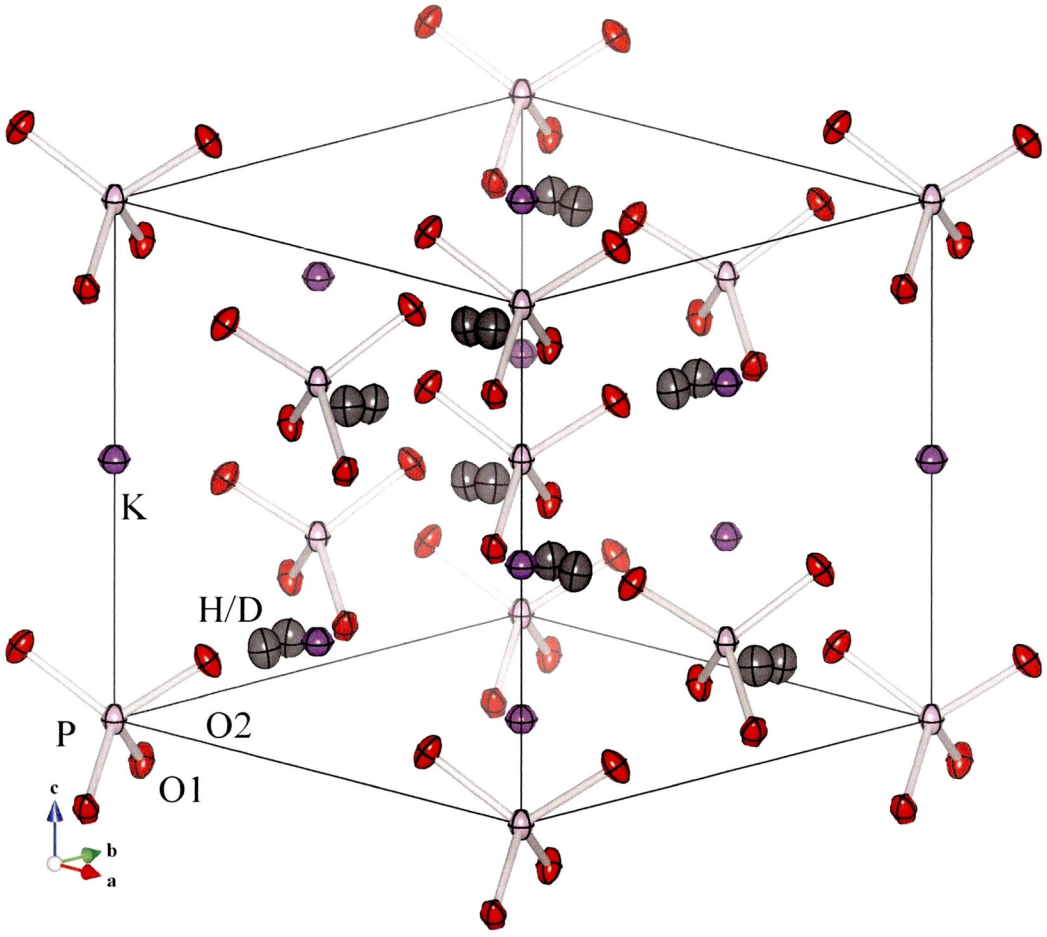

Figure 1.5 Crystal structure in the paraelectric phase of KDP/DKDP on a bird's-eye view. Although O1 and O2 atoms are indicated separately for comparison with the ferroelectric phase, those atoms are crystallographically equivalent to each other in the paraelectric phase; only one independent oxygen atom exists in the asymmetric unit of the paraelectric unit cell.

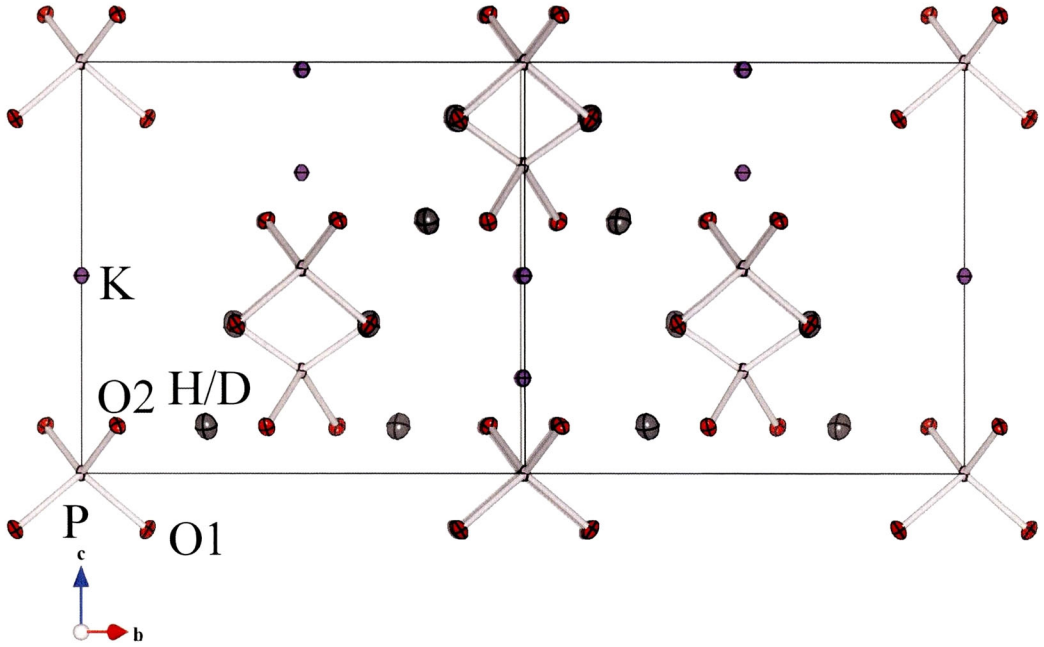

Figure 1.6 Crystal structure in the ferroelectric phase of KDP/DKDP on the paraelectric *a*-axis projection. O1 and O2 atoms are crystallographically independent to each other in the ferroelectric phase; only two independent oxygen atoms exist in the asymmetric unit of the ferroelectric unit cell.

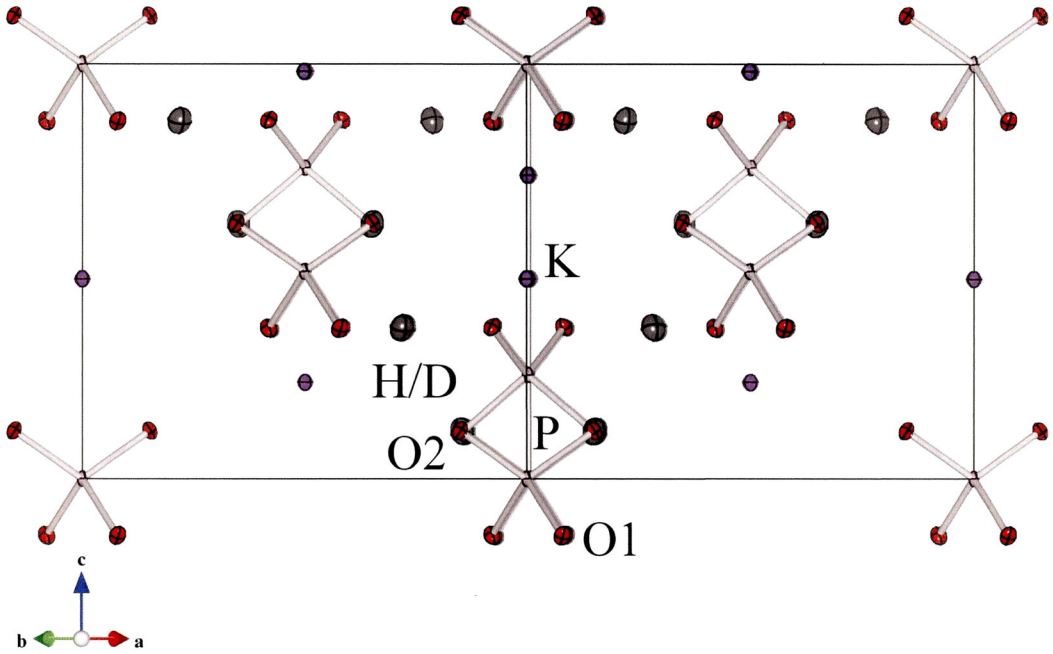

Figure 1.7 Crystal structure in the ferroelectric phase of KDP/DKDP on the paraelectric *b*-axis projection. O1 and O2 atoms are crystallographically independent to each other in the ferroelectric phase; only two independent oxygen atoms exist in the asymmetric unit of the ferroelectric unit cell.

observed the incoherent scattering from KDP and found evidence of proton tunneling, *i.e.*, protons are coherent over the two sites in the paraelectric phase. [72]

First-principles calculations have been developed to investigate rather complex systems such as KDP and DKDP. [73] It was revealed that structural transition accompanies electronic charge redistribution and ionic displacement as a consequence of proton ordering. Moreover, proton tunneling is coupled with heavier ions that exhibit cluster collective motion, but not single-particle dynamics. A simplified model of KDP also explained the displacive character of KDP on the basis of the tunneling motion of a 'particle' with half of the effective mass of the $H_2PO_4^-$ cluster. [74]

The refined structural parameters of ferroelectric phases in the low-temperature

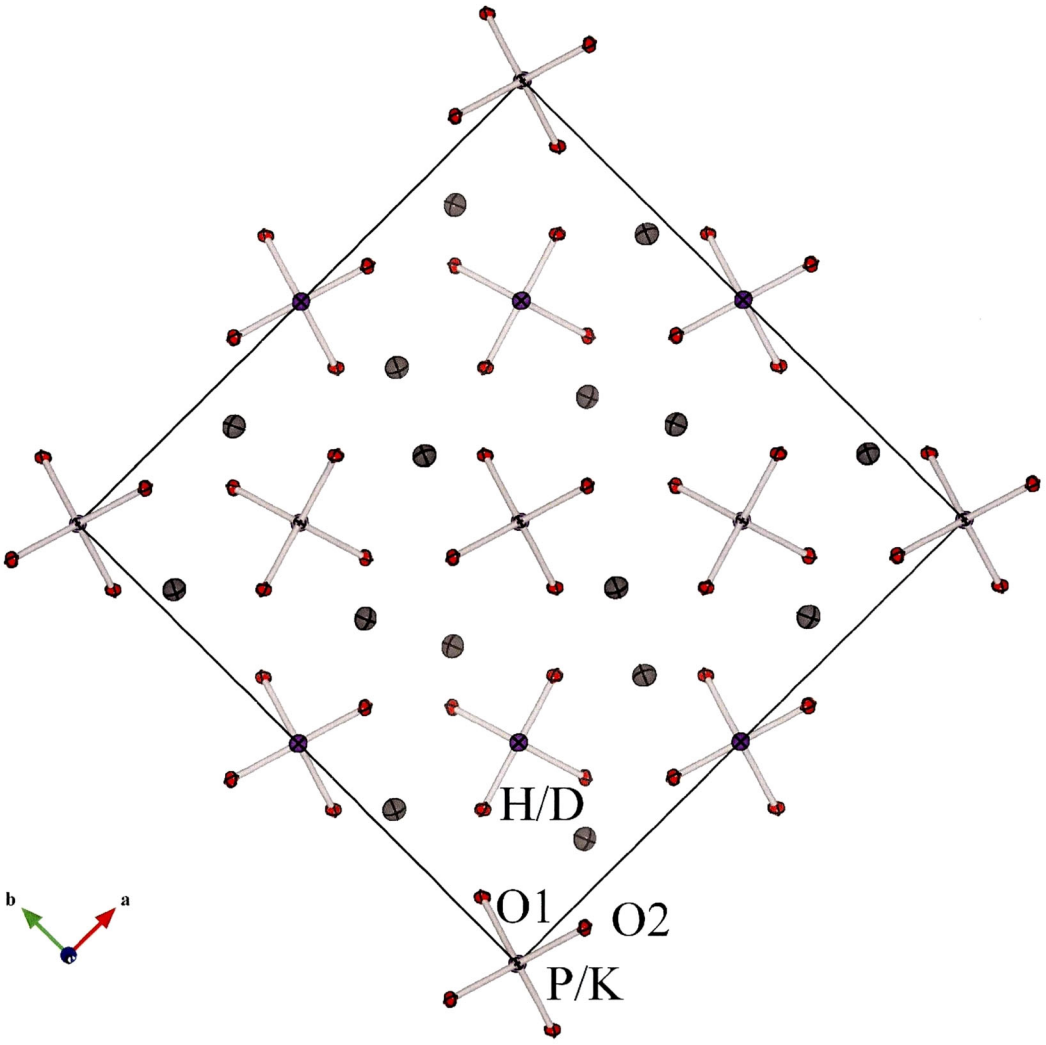

Figure 1.8 Crystal structure in the ferroelectric phase of KDP/DKDP on the paraelectric *c*-axis projection. O1 and O2 atoms are crystallographically independent to each other in the ferroelectric phase; only two independent oxygen atoms exist in the asymmetric unit of the ferroelectric unit cell.

region were reported at $T_c - 20\,K$ and $T_c - 10\,K$ for KDP and DKDP, respectively, by Nelmes *et al.* [42] To the authors' knowledge, structural studies of KDP are limited down to the liquid nitrogen temperature, and those of DKDP down to 210 K. In addition to the structural parameters in the paraelectric phase, those in the ferroelectric phase are effective and important in the comprehensive understanding of the phase transition mechanism.

Therefore, the author performed the single-crystal neutron diffraction experiments of both KDP and DKDP in a wide temperature range (down to 10 K) for the ferroelectric and paraelectric phases and refine the structure parameters, in order to examine the essential difference between KDP and DKDP. [75] The experimental process is described in chapter 2. Results of the structure refinement are presented in chapter 3, and discussed in chapter 4. Finally, conclusions are presented in chapter 5.

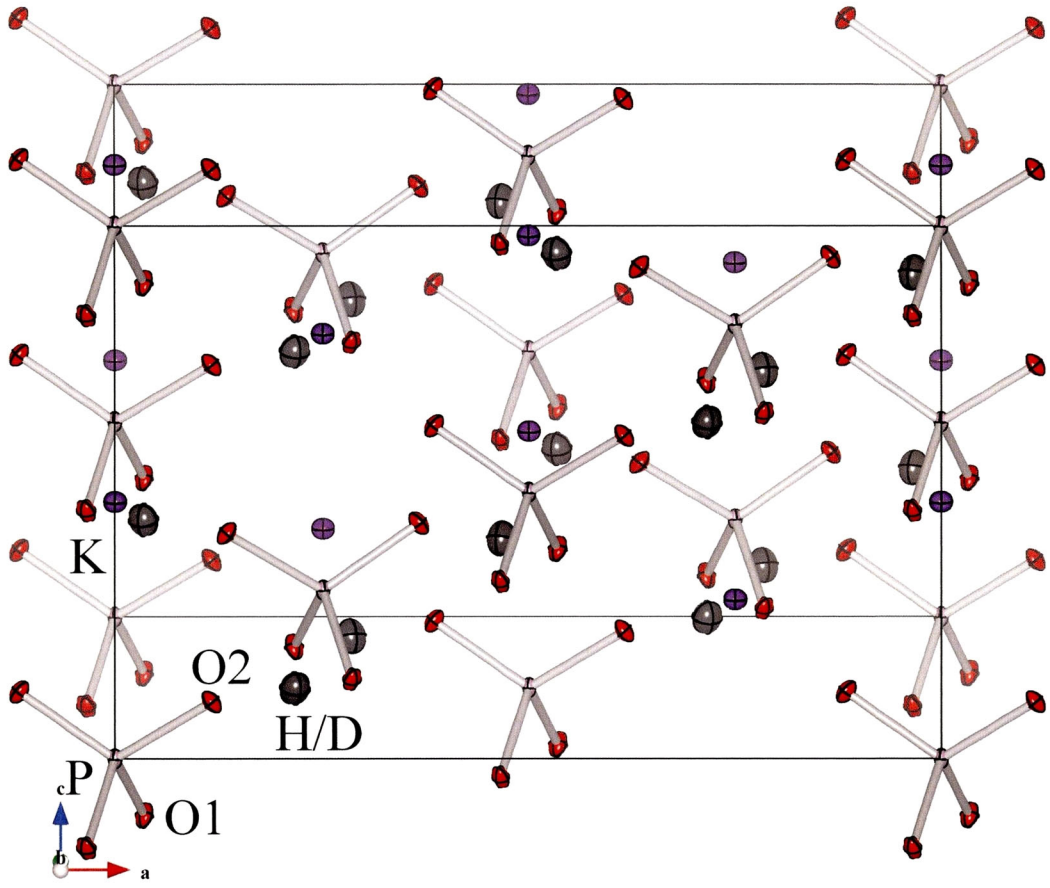

Figure 1.9 Crystal structure in the ferroelectric phase of KDP/DKDP on a bird's-eye view. O1 and O2 atoms are crystallographically independent to each other in the ferroelectric phase; only two independent oxygen atoms exist in the asymmetric unit of the ferroelectric unit cell.

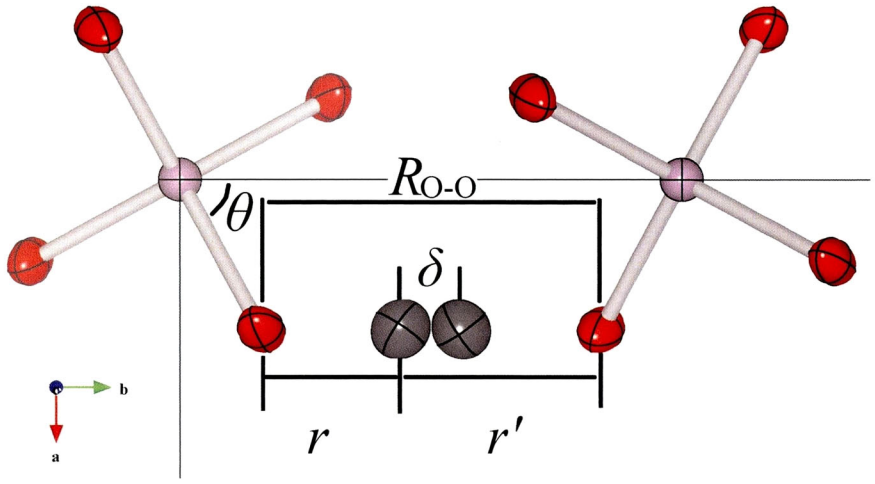

Figure 1.10 Interatomic distances and angle about hydrogen bond in the paraelectric phase of KDP/DKDP. In the paraelectric phase, the accept O1 and the donor O2 atoms are crystallographically equivalent to each other, and the hydrogen atom occupies the two equilibrium site with a equal probability. In the Ferroelectric phase, the two independent oxygen atoms become crystallographically independent, and the nuclear distribution of the hydrogen atom unbalanced.

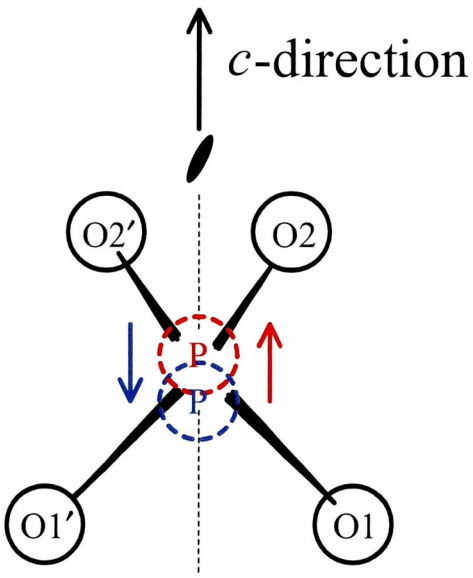

Figure 1.11 Schematic view of the locally and momentarily distorted PO_4 tetrahedron and its dipole moment derived from the distortion in the paraelectric phase of KDP/DKDP. The dipole moments are parallel or anti-parallel to the c-axis, which has 2-fold symmetry along it.

Chapter 2

Experimental Process

If I have been able to see further, it was only because I stood on the shoulders of giants.

— Isaac Newton, in the letter to Robert Hooke

Any measurement has its strong and weak points in itself. Firstly, investigators must know methods enough before experiments. Deep considerations about the methods could yield the reliable, rigid, and effective results for the investigators. On the other hand, shallow considerations take the investigators to the HELL.

2.1 Single-crystal specimens

An experimental specimen of KDP with rectangular dimensions of 3.1 × 3.2 × 2.1 mm^3 (along the tetragonal *a*-, *b*-, and *c*- axes) was cut from a transparent region of a grown parent crystal provided by Dr. K. Gesi. The paraelectric-ferroelectric transition temperature was 123 K.

A single crystal of DKDP was grown by the slow evaporation method from a heavy water solution kept in a desiccator at room temperature for about two weeks. The reagent with a deuteration ratio of 98 % was supplied from Cambridge Isotope Laboratories, Inc., and heavy water with a deuteration ratio of 99.9 % from ISOTEC, commercially. The obtained crystal is shown in Fig 2.1.

Fig 2.2 shows the result of differential scanning calorimetry (DSC) of a transparent and tiny plate from the crystal grown by the author. Scan speed (heating rate) was 5 K/min on heating process. Specimen-mass was 9.2 mg and reference to the specimen was α-alumina (Al_2O_3), of which mass was 7.1 mg. The DSC specimen was prepared with a small platy fragment from a part of the DKDP crystal obtained. The

residual part of the crystal was cut into a few blocks as specimens for dielectric constant and neutron single-crystal diffraction experiments. In order to prevent moisture absorption in atmospheric vapors with light water (H_2O), the small platy fragment was not crushed into fine powder like conventional DSC specimen, and put into a hermetically closed Al pan. The transition point is determined 214 K from the peak position in dielectric constant measurement performed separately, which is almost in good agreement with the transition point determined from this DSC curve. The heating DSC line yields the transition entropy of 3.68 J/(mol K) which is corresponding to $0.442R$, in which R denotes gas constant of 8.314510 J/(mol K). The obtained transition entropy is similar to the value of $R \ln (3/2) = 0.405R$.

As an experimental specimen, a block with rectangular dimensions of 2.8 × 2.6 × 2.5 mm^3 (along the tetragonal *a*-, *b*-, and *c*- axes) was cut from a transparent region of the grown parent crystal. The deuterium replacement ratio of the crystal was estimated to be 95.8 % from the peak position of the dielectric constant at transition point of 214 K. [28] Figs. 2.3–2.8 show temperature dependences of dielectric constants ϵ's (left ordinate) and reciprocal dielectric constants ϵ^{-1}'s (right ordinate) at 50, 10, and 5 kHz of the DKDP crystal obtained in cooling or heating processes. The specimen painted Ag-paste on its crystallographic *c*-planes as electrodes was held in a closed-cycle He-gas cryostat, MiniStat (Iwatani Plantech Corporation), with a coldhead (D510 type) and a compressor unit (CW303 type), and then temperature control of the specimen was carried out by temperature controller, TCU-4 (Iwatani Plantech Corporation) on cooling speed of ±0.83 K/min. The measurement was per-

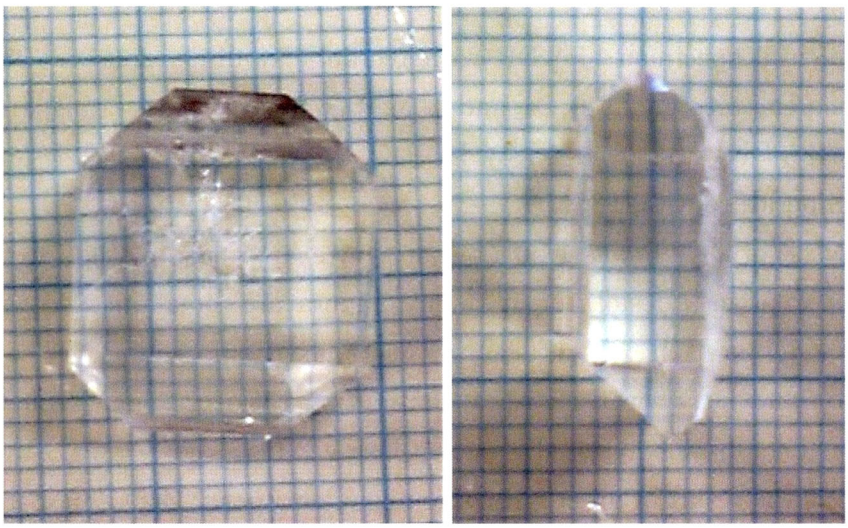

Figure 2.1 External view of a single crystal of DKDP grown by the slow evaporation method from a heavy water solution, which was kept in a desiccator at room temperature for about two weeks.

formed by using of LCR meter AG-4311 (ANDO). The regular and inverted triangle symbols denote the values of dielectric constant ϵ and reciprocal dielectric constant ϵ^{-1}, respectively. The behavior of reciprocal dielectric constant ϵ^{-1} obeys Curie-Weiss law. The transition point is determined 214 K from the peak position of the dielectric constant, which is in good agreement with the transition point determined from DSC curve on heating process obtained separately. Shoulder-like anomaly is also recognized in lower temperature region from transition point of the crystal as already reported by other investigators.

The surfaces of the specimens were polished carefully using filter paper wet with distilled or heavy water. As an electrode, silver paste or evaporated aluminum was attached on the c-planes of the specimens, and DC bias fields of 240–360 V/mm were applied by a power supply (Glassman High Voltage INC.) in order to keep the single domain states only in the ferroelectrics phases of KDP and DKDP. The specimens were glued on vanadium sticks using insulating varnish (GE low-temperature varnish). A schematic view of the single-crystal specimen for neutron diffraction experiment are shown in Fig. 2.9.

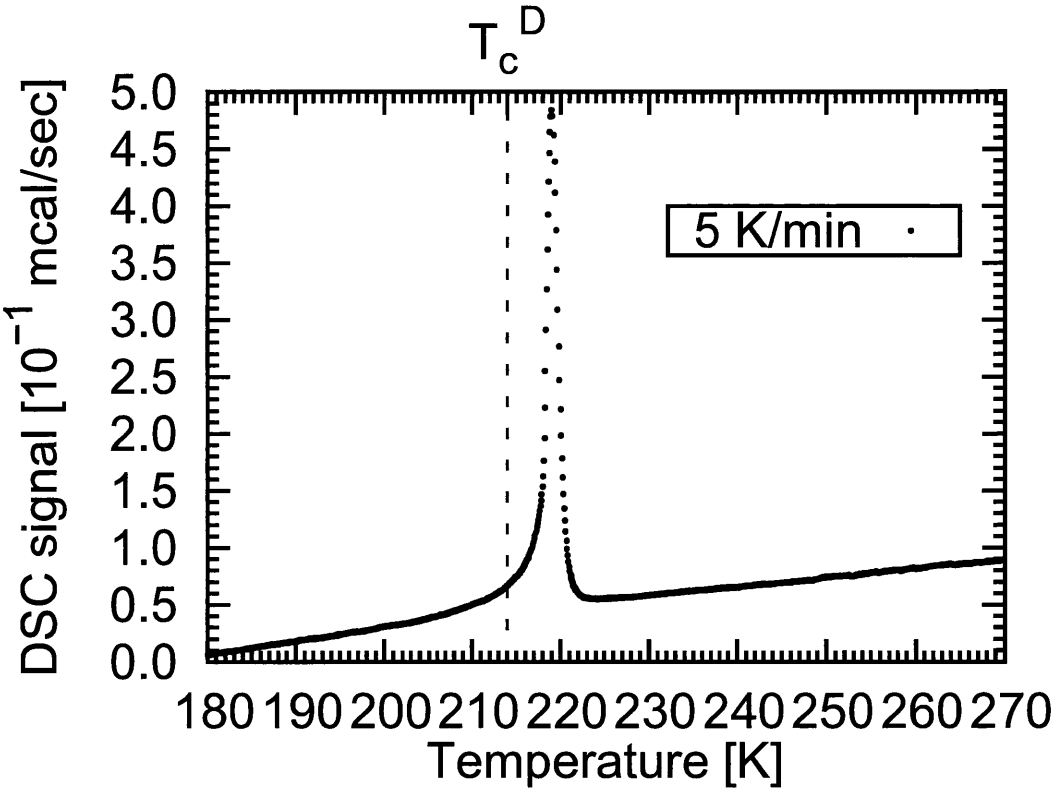

Figure 2.2 Heating DSC curve of the DKDP crystal grown by slow evaporation method of heavy water solution in this study.

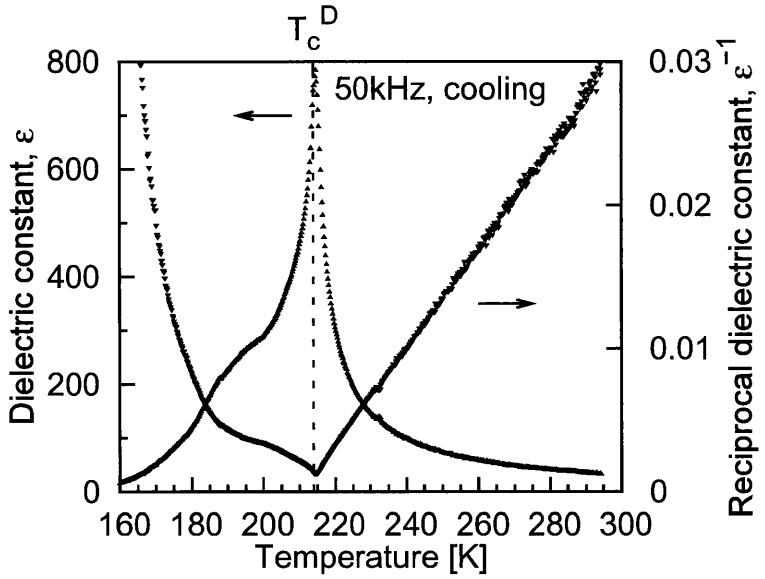

Figure 2.3 Temperature dependences of dielectric constant ϵ (left ordinate) and reciprocal dielectric constant ϵ^{-1} (right ordinate) at 50 kHz of the DKDP crystal obtained in cooling process. Deuterium replacement rate of the single crystal prepared in this study is estimated 95.8 % from the transition point of 214 K.

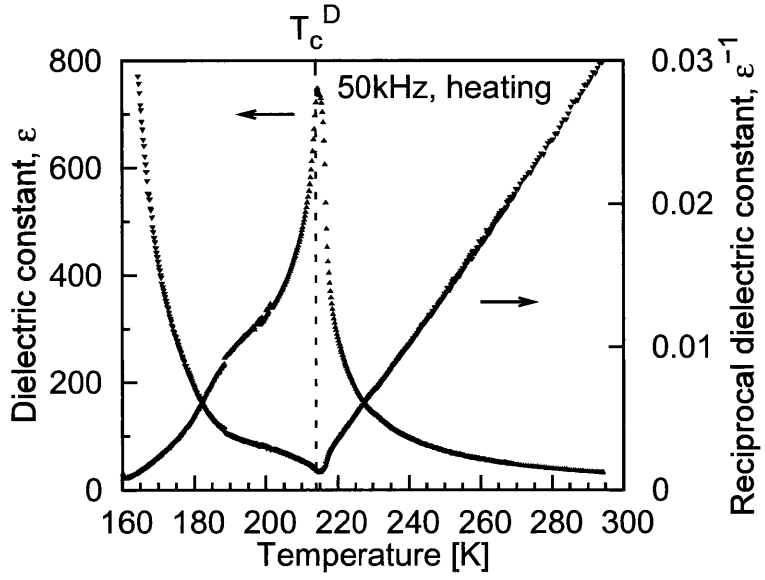

Figure 2.4 Temperature dependences of dielectric constant ϵ (left ordinate) and reciprocal dielectric constant ϵ^{-1} (right ordinate) at 50 kHz of the DKDP crystal obtained in heating process.

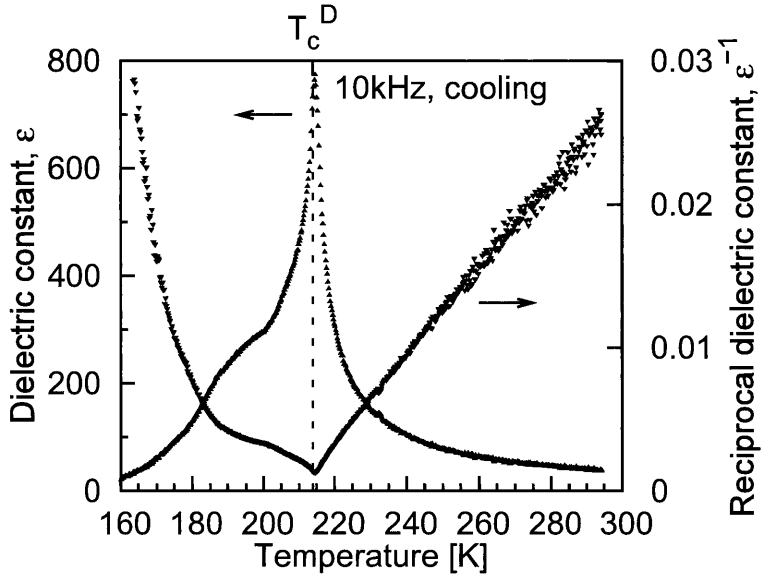

Figure 2.5 Temperature dependences of dielectric constant ϵ (left ordinate) and reciprocal dielectric constant ϵ^{-1} (right ordinate) at 10 kHz of the DKDP crystal obtained in cooling process.

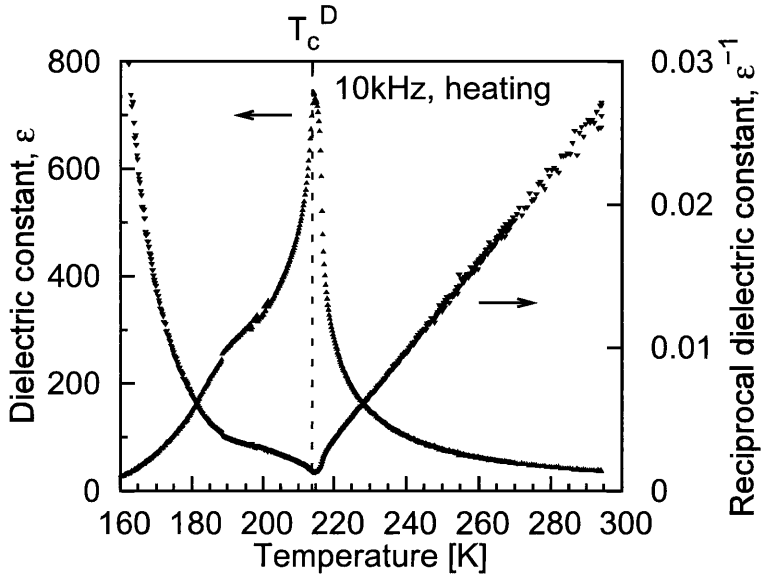

Figure 2.6 Temperature dependences of dielectric constant ϵ (left ordinate) and reciprocal dielectric constant ϵ^{-1} (right ordinate) at 10 kHz of the DKDP crystal obtained in heating process.

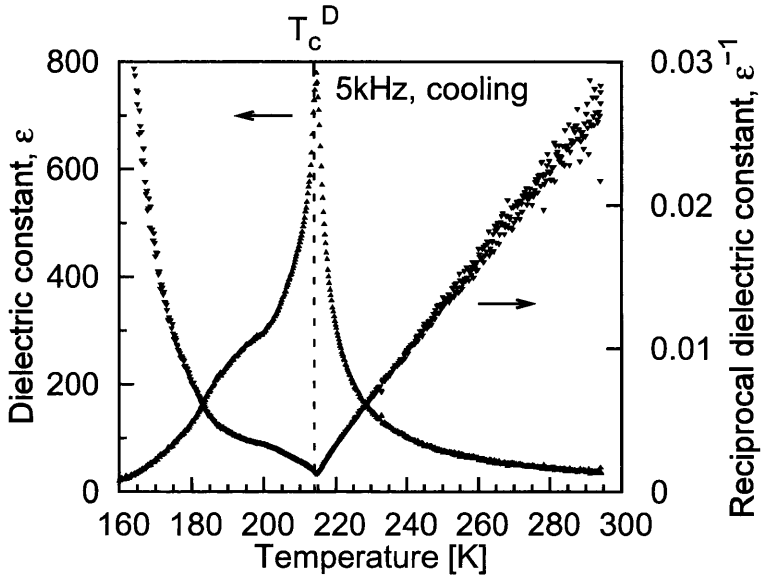

Figure 2.7 Temperature dependences of dielectric constant ϵ (left ordinate) and reciprocal dielectric constant ϵ^{-1} (right ordinate) at 5 kHz of the DKDP crystal obtained in cooling process.

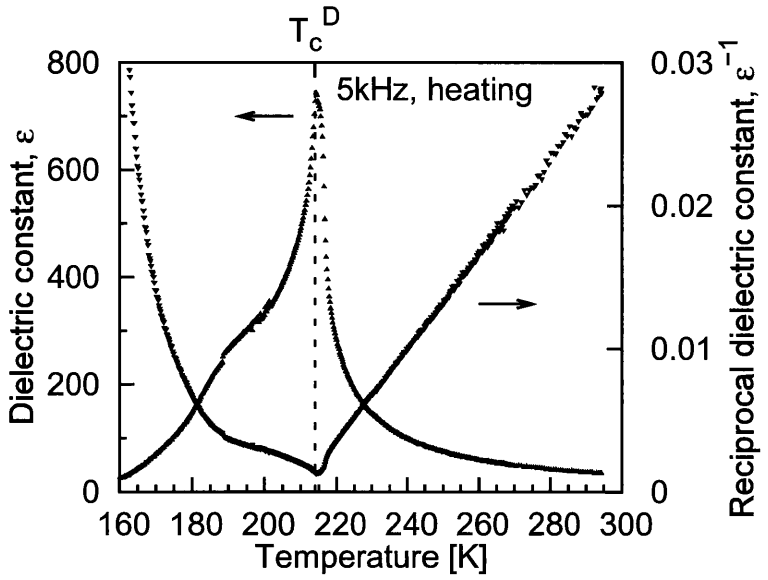

Figure 2.8 Temperature dependences of dielectric constant ϵ (left ordinate) and reciprocal dielectric constant ϵ^{-1} (right ordinate) at 5 kHz of the DKDP crystal obtained in heating process.

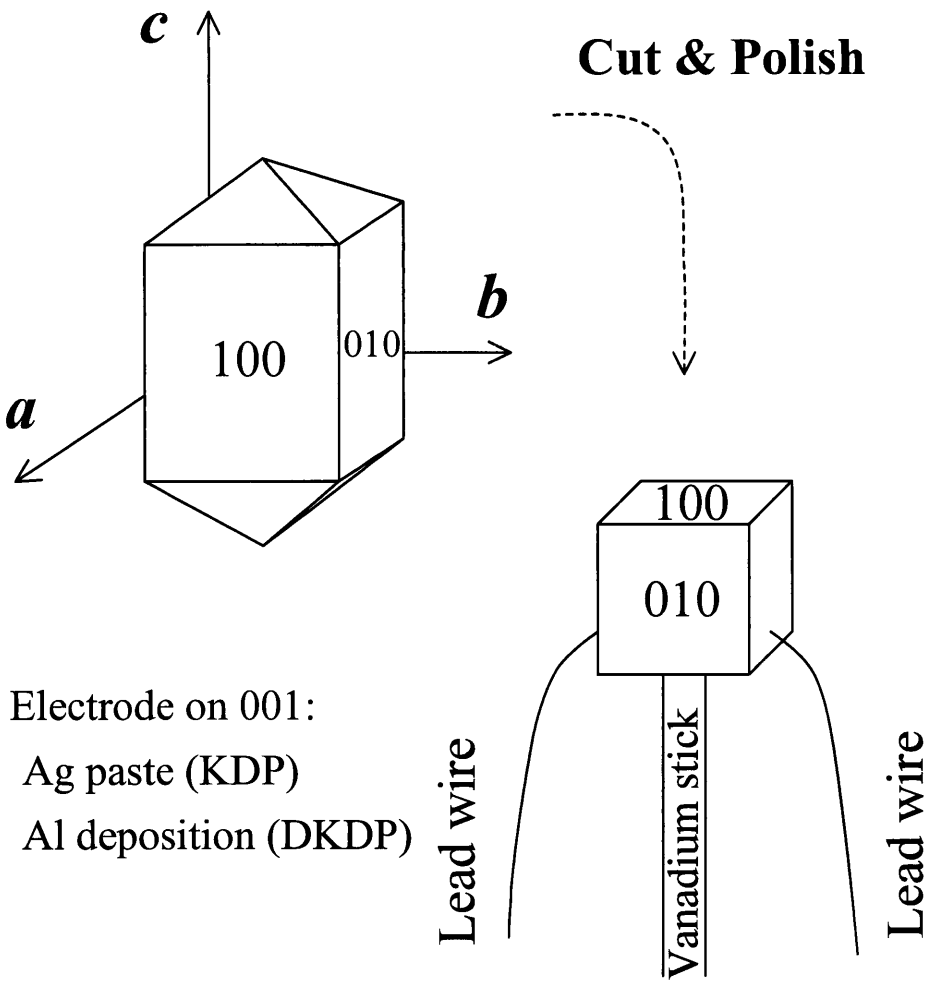

Figure 2.9 Schematic view of the single-crystal specimen for present neutron diffraction experiments. KDP/DKDP crystal has a simple and easy crystal habit with it. The specimens of both KDP and DKDP crystals with rectangular shapes were cut carefully from a transparent and clear region in the parent crystal. The elctrode were attached for application of the poling electric field. The size of specimen is recommended to be as *ca.* $3.0 \times 3.0 \times 3.0\,\mathrm{mm}^3$ for the experiment at FONDER. [76]

2.2 Single-crystal neutron diffraction experiment

Single-crystal neutron diffraction experiments were performed using a four-circle-off-center-type diffractometer, FONDER [76] (T2-2) of JRR-3M, JAEA, Tokai. Fig. 2.10 shows the reactor building and the guide hall of JRR-3M. The neutron wavelengths in those experiments were 1.245 2 and 1.239 6 Å for KDP and DKDP, respectively, and the diffraction angle was $2\theta < 156°$.

The temperature of the specimens was controlled using a TEMCON system of the cryostat accessory of FONDER. (Refer Fig. 2.11, 2.12.) Fluctuation of temperature control of the cryostat was enough small for the present experiments, and took a value up to *ca.* $\pm$ 0.1 K. The diffraction experiments were performed at ten temperatures for each compound: 10, 30, 70, 110, 115, 118, 120, 125, 150, and 200 K for KDP, and 10, 70, 130, 160, 190, 205, 210, 220, 250, and 298 K for DKDP. About 220 and 420 unique reflections were measured in the paraelectric and ferroelectric phases, respectively.

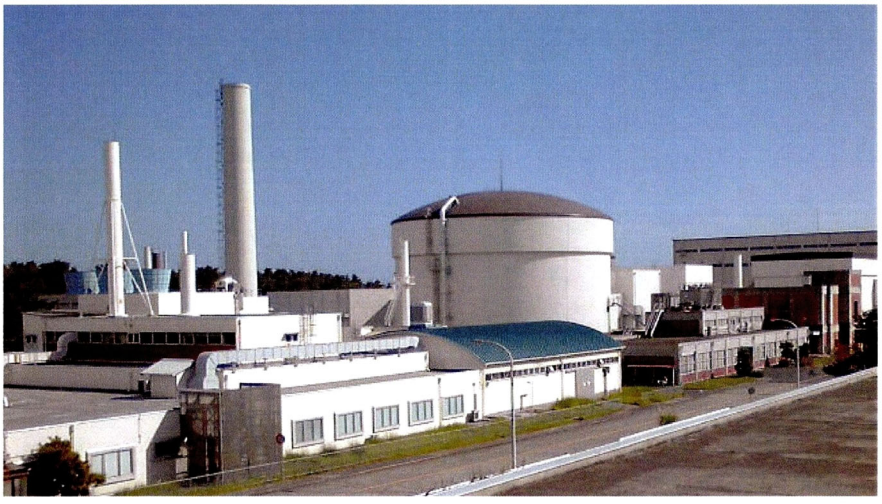

Figure 2.10 External view of the reactor building (center) containing the nuclear reactor, JRR-3M, of JAEA at Tokai. The experiment at neutron diffractometer FONDER is performed using neutron beam from this reactor. [76] FONDER has been installed not in this building, but in guide hall for experiment. The guide hall is built beside the reactor building.

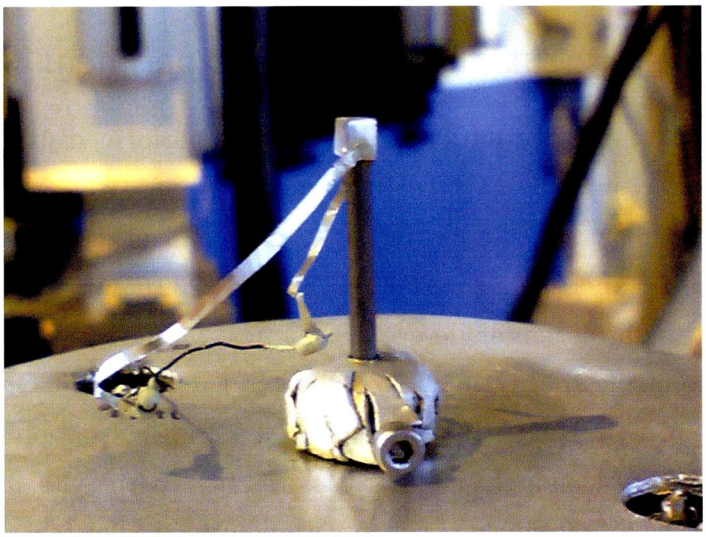

Figure 2.11 External view of the single-crystal specimen mounted on the sample stage of FONDER. The cryostat is not in sealed state. The mounting stage was covered by Cadmium sheet in order to prevent and suppress the extra scattering of back ground, and equipped with terminals for external DC bias field. Aluminum foils were used for lead wires.

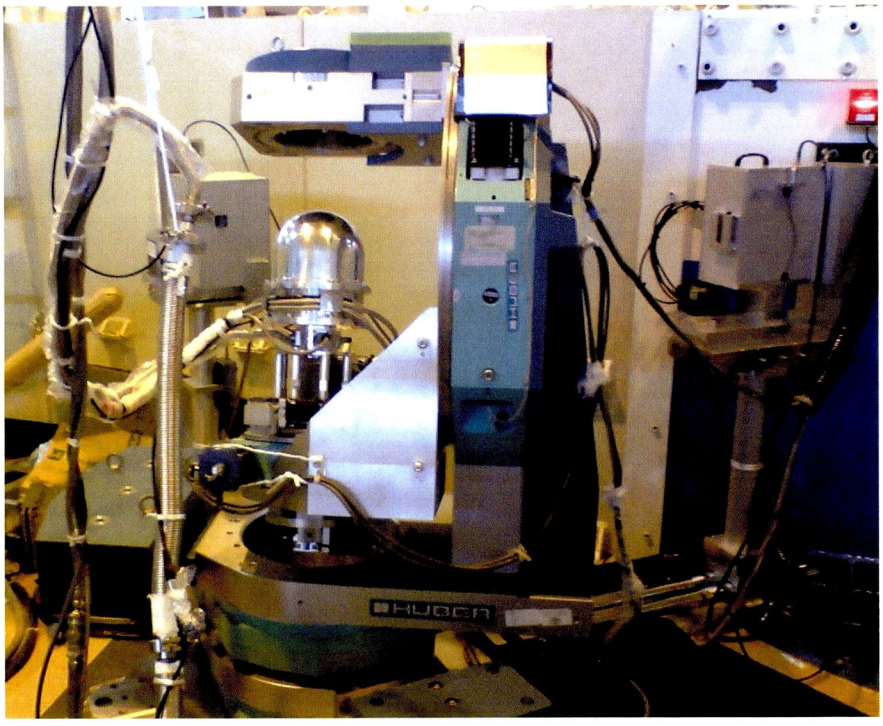

Figure 2.12 External view of FONDER. The aluminum cryostat is in sealed state. The neutron counter is in left top beyond the cryostat dome. A neutron beam hole is confirmed in right top of the picture. The neutron beam shutter is open, in which the red lamp is turning on.

2.3 Data analysis

Using the fractional coordinates, x_j, y_j, and z_j, the occupation factor, g_j, the bound coherent scattering length, $b_{c,j}$, and the Debye-Waller factor, $T_j(\boldsymbol{h})$, of the nuclei (*i.e.*, atomic species) specified with subscript j in the unit cell of the crystal, the crystal structure factor, $F(\boldsymbol{h})$, is expressed as follows:

$$F(\boldsymbol{h}) = \sum_{j=1}^{n} g_j b_{c,j} T_j(\boldsymbol{h}) \exp\left[2\pi i \left(hx_j + ky_j + lz_j\right)\right] \tag{2.3.1}$$

From the least-squares calculations with the experimental dataset, we obtain the Debye-Waller factor $T(\boldsymbol{h})$ and the atomic displacement parameters U_{ij};

$$\begin{aligned} T(\boldsymbol{h}) = \exp\big[-2\pi^2 \big(&h^2 a^{*2} U_{11} + k^2 b^{*2} U_{22} + l^2 c^{*2} U_{33} \\ &+ 2hka^* b^* U_{12} + 2hla^* c^* U_{13} + 2klb^* c^* U_{23}\big)\big]. \end{aligned} \tag{2.3.2}$$

The atomic displacement parameters are directly related to the mean square displacements if the atom vibrates within a harmonic potential, *i.e.*,

$$U_{11} = a^2 \left\langle (x - \bar{x})^2 \right\rangle, \tag{2.3.3}$$

$$U_{22} = b^2 \left\langle (y - \bar{y})^2 \right\rangle, \tag{2.3.4}$$

$$U_{33} = c^2 \left\langle (z - \bar{z})^2 \right\rangle, \tag{2.3.5}$$

$$U_{12} = ab \left\langle (x - \bar{x})(y - \bar{y}) \right\rangle, \tag{2.3.6}$$

$$U_{13} = ac \left\langle (x - \bar{x})(z - \bar{z}) \right\rangle, \tag{2.3.7}$$

$$U_{23} = bc \left\langle (y - \bar{y})(z - \bar{z}) \right\rangle, \tag{2.3.8}$$

which are hold only on orthogonal crystal systems, *i.e.*, orthorhombic, tetragonal, and cubic systems.

Additionally, equivalent isotropic atomic displacement parameter is directly calculated as follows: [77]

$$\begin{aligned} U_{\mathrm{eq}} &= \frac{1}{3} \sum_i \sum_j U_{ij} a_i^* a_j^* \boldsymbol{a}_i \cdot \boldsymbol{a}_j \\ &= \frac{1}{3} \Big[U_{11} (aa^*)^2 + U_{22} (bb^*)^2 + U_{33} (cc^*)^2 \\ &\quad + 2U_{12} a^* b^* ab \cos\gamma + 2U_{13} a^* c^* ac \cos\beta + 2U_{23} b^* c^* bc \cos\alpha \Big]. \end{aligned} \tag{2.3.9}$$

Firstly, each reflection profile was checked, and the net intensity and standard deviation were reduced using a Profile Check program of FONDER. Absorption and extinction corrections were applied to the analysis of the raw diffraction data using the programs of DABEXN and RADIELN [78, 79], and then equivalent reflections of

those corrected ones were averaged. The index ranges were $h, k \leq 11, l \leq 10$ and $h, k \leq 15, l \leq 10$ in the paraelectric and ferroelectric phases, respectively.

For the obtained diffraction datasets, the structural parameters were refined using the full-matrix least-squares program *SHELXL-97* [80], *via* WinGX [81]. The initial parameters of the fractional coordinates of atoms were those reported by Bacon and Pease [11, 12]. In the author's analyses, the space groups of the paraelectric and ferroelectric phases are $I\bar{4}2d$ and $Fdd2$, respectively, and the standard symmetry coordinates are used. In the final processes of all the structure refinements, anisotropic Debye-Waller factors were used for all the atoms.

A split-atom method was applied to the analysis of protons/deuterons in the paraelectric phases of KDP/DKDP. Finally, All the least-squares refinements converged, and yielded R_1-factors of 2.73–3.90 and 3.19–5.16 % for KDP and DKDP, respectively. Here, the R_1-, wR_2-, and S-factors are defined by

$$R_1 = \frac{\sum_{\boldsymbol{h}} ||F_o(\boldsymbol{h})| - |F_c(\boldsymbol{h})||}{\sum_{\boldsymbol{h}} |F_o(\boldsymbol{h})|}, \tag{2.3.10}$$

$$wR_2 = \left\{ \frac{\sum w(\boldsymbol{h}) \left(|F_o(\boldsymbol{h})|^2 - |F_c(\boldsymbol{h})|^2 \right)^2}{\sum w(\boldsymbol{h}) |F_o^2(\boldsymbol{h})|^2} \right\}^{1/2}, \tag{2.3.11}$$

$$GooF = S = \left\{ \frac{\sum w(\boldsymbol{h}) \left(|F_o(\boldsymbol{h})|^2 - |F_c(\boldsymbol{h})|^2 \right)^2}{n - p} \right\}^{1/2}, \tag{2.3.12}$$

respectively, where $F_o(\boldsymbol{h})$ and $F_c(\boldsymbol{h})$ are the observed and calculated structure factors for the index $\boldsymbol{h}$, respectively, and $w(\boldsymbol{h})$, n, and p are the weight scheme for the index $\boldsymbol{h}$, the number of reflections, and the number of parameters refined in analysis, respectively.

The weight scheme for the index $\boldsymbol{h}$ in this thesis, $w(\boldsymbol{h})$, is expressed as,

$$w(\boldsymbol{h}) \equiv \frac{1}{\sigma^2 (F_o^2(\boldsymbol{h})) + (aP(\boldsymbol{h}))^2 + bP(\boldsymbol{h})}, \tag{2.3.13}$$

where a and b are the parameters set by trial and error for the variance with no marked systematic trends on the magnitude of F_c^2 or of resolution. [80]

$$P \equiv \frac{2F_c^2 + \mathrm{Max}\left(F_o^2(\boldsymbol{h}), 0\right)}{3}, \tag{2.3.14}$$

The measurement conditions and the obtained R_1-, wR_2-, and S-factors are tabulated in Table 3.1.

Chapter 3

Results

Since then I never pay attention to anything by "experts". I calculate everything myself.

— Richard Phillips Feynman, in 'Surely You're Joking, Mr. Feynman!'

God gave the humans a easy and difficult toys, which are names by them 'SCIENCE'. The toys create much satisfaction and distress on the humans. In a stroke of good fortune, or bad one, it is non-breakable.

3.1 Atomic parameters

The unit cell and atomic parameters in ferroelectric and paraelectric phases for both KDP and DKDP are presented in Table 3.2–3.21. The parameters a, b, and c in Å and the angles α, β, and γ in degree are the lattice constants. The dimensionless parameters x, y, and z are fractional coordinates. The term g denotes the occupation factor of each atom as a dimensionless parameter. U_{eq} and U_{ij} in Å^2 are isotropic and anisotropic atomic displacement parameters, respectively. The values in parentheses are the estimated standard deviations (e.s.d.'s), and the parameters without e.s.d.'s are fixed ones. The lattice parameter a of DKDP is *ca.* 0.05 Å longer than that of KDP, while b and c are almost the same, as described at the tables.

The views of the crystal structures of the paraelectric phase have been drwan in Fig. 1.2– 1.5. The views of the crystal structures of the ferroelectric phase have been drwan in Fig. 1.6– 1.9.

Table 3.1 Measured temperatures [K], numbers of independent reflections, R_1-, wR_2-, and S-factors in structural analyses of KDP and DKDP.

KDP				
Temp. [K]	No. Refs.	R_1 [%]	wR_2 [%]	S
200	197	3.90	10.43	0.700
150	215	3.28	8.23	0.802
125	208	2.73	7.33	0.595
120	388	3.54	9.52	0.722
118	390	3.51	9.50	0.694
115	390	3.27	8.94	0.724
110	380	3.22	8.17	0.909
70	374	3.44	8.87	0.963
30	382	3.81	9.62	1.064
10	375	3.26	8.55	1.029
DKDP				
Temp. [K]	No. Refs.	R_1 [%]	wR_2 [%]	S
298	222	3.19	8.81	0.579
250	220	4.24	11.32	0.762
220	219	4.23	10.90	0.771
210	366	4.64	11.46	8.64
205	398	4.73	11.94	0.931
190	373	5.06	12.68	0.910
160	397	4.83	12.62	1.088
130	403	4.55	11.46	0.999
70	390	4.57	11.93	1.055
10	381	5.16	13.07	1.033

Table 3.2 Unit cell and atomic parameters of orthorhombic KDP at 10 K. The parameters a, b, and c in Å and the angles α, β, and γ in degree are the lattice constants. The dimensionless parameters x, y, and z are fractional coordinates. The term g denotes the occupation factor of each atom as a dimensionless parameter. U_{eq} and U_{ij} in Å^2 are isotropic and anisotropic atomic displacement parameters, respectively. The principal mean square atomic displacements of each atom are also described. The values in parentheses are the estimated standard deviations (e.s.d.'s), and the parameters without e.s.d.'s are fixed ones.

Crystal system	Space group	a	b	c	α $(= \beta = \gamma)$
Orthorhombic	$Fdd2$	10.544(7)	10.481(6)	6.920(5)	90

Atom	x	y	z	g	U_{eq}
K	0	0	0.483 7(5)	0.5	0.004 5(4)
P	0	0	0	0.5	0.003 4(3)
O1	0.033 99(9)	0.115 49(9)	−0.136 9(3)	1	0.005 3(2)
O2	0.116 17(9)	−0.034 4(1)	0.116 9(4)	1	0.005 0(2)
H	0.212 7(2)	0.063 2(2)	0.113 8(6)	1	0.016 6(4)

Atom	U_{11}	U_{22}	U_{33}	U_{23}	U_{13}	U_{12}
K	0.003 3(7)	0.004 8(8)	0.005 3(8)	0	0	0.000 1(7)
P	0.002 4(5)	0.003 2(6)	0.004 6(6)	0	0	−0.000 1(5)
O1	0.004 1(4)	0.004 9(4)	0.007 0(4)	0.000 9(4)	0.000 9(4)	−0.000 3(3)
O2	0.004 2(3)	0.004 6(4)	0.006 2(4)	0.000 1(4)	−0.001 1(4)	0.000 2(3)
H	0.015 5(8)	0.014 7(8)	0.019 6(9)	−0.001 4(9)	0.000 8(9)	−0.000 7(6)

Atom	Principal mean square atomic displacements		
K	0.0053	0.0048	0.0033
P	0.0046	0.0033	0.0024
O1	0.0075	0.0049	0.0036
O2	0.0066	0.0046	0.0037
H	0.0201	0.0154	0.0141

Table 3.3 Unit cell and atomic parameters of orthorhombic KDP at 30 K. The parameters a, b, and c in Å and the angles α, β, and γ in degree are the lattice constants. The dimensionless parameters x, y, and z are fractional coordinates. The term g denotes the occupation factor of each atom as a dimensionless parameter. U_{eq} and U_{ij} in Å^2 are isotropic and anisotropic atomic displacement parameters, respectively. The principal mean square atomic displacements of each atom are also described. The values in parentheses are the estimated standard deviations (e.s.d.'s), and the parameters without e.s.d.'s are fixed ones.

Crystal system	Space group	a	b	c	α $(= \beta = \gamma)$
Orthorhombic	$Fdd2$	10.539(5)	10.478(4)	6.917(3)	90

Atom	x	y	z	g	U_{eq}
K	0	0	0.483 9(6)	0.5	0.005 3(4)
P	0	0	0	0.5	0.004 2(3)
O1	0.034 1(1)	0.115 4(1)	−0.136 4(4)	1	0.005 9(3)
O2	0.116 1(1)	−0.034 5(1)	0.117 4(4)	1	0.005 8(2)
H	0.212 8(2)	0.063 2(2)	0.114 6(7)	1	0.017 5(4)

Atom	U_{11}	U_{22}	U_{33}	U_{23}	U_{13}	U_{12}
K	0.004 1(9)	0.004 8(9)	0.007 0(9)	0	0	0.000 7(8)
P	0.002 6(6)	0.005 0(7)	0.005 2(7)	0	0	−0.000 2(5)
O1	0.004 5(4)	0.005 3(4)	0.007 9(5)	0.001 1(4)	0.000 6(4)	−0.000 2(3)
O2	0.004 7(4)	0.005 6(4)	0.007 0(4)	0.000 3(4)	−0.000 7(5)	0.000 1(3)
H	0.015 9(9)	0.015 8(9)	0.021(1)	−0.002(1)	0.000(1)	0.000 3(7)

Atom	Principal mean square atomic displacements		
K	0.0070	0.0052	0.0036
P	0.0052	0.0050	0.0025
O1	0.0084	0.0050	0.0042
O2	0.0072	0.0056	0.0045
H	0.0215	0.0160	0.0149

Table 3.4 Unit cell and atomic parameters of orthorhombic KDP at 70 K. The parameters a, b, and c in Å and the angles α, β, and γ in degree are the lattice constants. The dimensionless parameters x, y, and z are fractional coordinates. The term g denotes the occupation factor of each atom as a dimensionless parameter. U_{eq} and U_{ij} in Å^2 are isotropic and anisotropic atomic displacement parameters, respectively. The principal mean square atomic displacements of each atom are also described. The values in parentheses are the estimated standard deviations (e.s.d.'s), and the parameters without e.s.d.'s are fixed ones.

Crystal system	Space group	a	b	c	α $(= \beta = \gamma)$
Orthorhombic	$Fdd2$	10.544(6)	10.484(5)	6.924(4)	90

Atom	x	y	z	g	U_{eq}
K	0	0	0.483 8(5)	0.5	0.006 8(4)
P	0	0	0	0.5	0.005 1(3)
O1	0.034 0(1)	0.115 5(1)	−0.136 1(4)	1	0.007 1(2)
O2	0.116 3(1)	−0.034 5(1)	0.117 6(4)	1	0.007 0(2)
H	0.213 0(2)	0.063 3(2)	0.114 9(6)	1	0.019 0(4)

Atom	U_{11}	U_{22}	U_{33}	U_{23}	U_{13}	U_{12}
K	0.005 7(8)	0.007 3(9)	0.007 5(9)	0	0	0.000 9(7)
P	0.002 7(6)	0.006 7(6)	0.006 0(6)	0	0	−0.000 2(5)
O1	0.005 1(4)	0.007 7(4)	0.008 6(4)	0.001 5(4)	0.001 2(4)	0.000 0(3)
O2	0.006 0(4)	0.006 4(4)	0.008 8(4)	0.000 2(4)	−0.001 8(4)	−0.000 1(3)
H	0.018 7(9)	0.016 3(9)	0.022(1)	−0.003(1)	0.001(1)	−0.001 2(7)

Atom	Principal mean square atomic displacements		
K	0.0077	0.0075	0.0053
P	0.0067	0.0060	0.0027
O1	0.0099	0.0069	0.0047
O2	0.0097	0.0064	0.0051
H	0.0234	0.0186	0.0150

Table 3.5 Unit cell and atomic parameters of orthorhombic KDP at 110 K. The parameters a, b, and c in Å and the angles α, β, and γ in degree are the lattice constants. The dimensionless parameters x, y, and z are fractional coordinates. The term g denotes the occupation factor of each atom as a dimensionless parameter. U_{eq} and U_{ij} in Å^2 are isotropic and anisotropic atomic displacement parameters, respectively. The principal mean square atomic displacements of each atom are also described. The values in parentheses are the estimated standard deviations (e.s.d.'s), and the parameters without e.s.d.'s are fixed ones.

Crystal system	Space group	a	b	c	α $(= \beta = \gamma)$
Orthorhombic	$Fdd2$	10.549(7)	10.484(5)	6.930(5)	90

Atom	x	y	z	g	U_{eq}
K	0	0	0.483 4(5)	0.5	0.008 2(4)
P	0	0	0	0.5	0.006 4(3)
O1	0.033 8(1)	0.115 4(1)	−0.135 7(4)	1	0.008 5(2)
O2	0.116 2(1)	−0.034 2(1)	0.117 4(4)	1	0.008 3(2)
H	0.211 9(2)	0.062 7(2)	0.116 4(6)	1	0.019 9(4)

Atom	U_{11}	U_{22}	U_{33}	U_{23}	U_{13}	U_{12}
K	0.007 0(8)	0.008 5(8)	0.009 3(8)	0	0	0.000 6(7)
P	0.004 5(5)	0.006 7(6)	0.007 9(6)	0	0	−0.000 4(5)
O1	0.006 0(4)	0.008 3(4)	0.011 1(4)	0.002 0(4)	0.001 2(4)	−0.000 1(3)
O2	0.007 2(4)	0.007 5(4)	0.010 1(4)	0.000 5(3)	−0.002 5(4)	−0.000 2(3)
H	0.019 9(8)	0.017 5(8)	0.022 3(7)	−0.002(1)	0.001 5(9)	−0.000 2(6)

Atom	Principal mean square atomic displacements		
K	0.0093	0.0087	0.0067
P	0.0079	0.0068	0.0045
O1	0.0123	0.0075	0.0056
O2	0.0116	0.0074	0.0057
H	0.0237	0.0194	0.0166

Table 3.6 Unit cell and atomic parameters of orthorhombic KDP at 115 K. The parameters a, b, and c in Å and the angles α, β, and γ in degree are the lattice constants. The dimensionless parameters x, y, and z are fractional coordinates. The term g denotes the occupation factor of each atom as a dimensionless parameter. U_{eq} and U_{ij} in Å^2 are isotropic and anisotropic atomic displacement parameters, respectively. The principal mean square atomic displacements of each atom are also described. The values in parentheses are the estimated standard deviations (e.s.d.'s), and the parameters without e.s.d.'s are fixed ones.

Crystal system	Space group	a	b	c	α $(= \beta = \gamma)$
Orthorhombic	$Fdd2$	10.534(4)	10.471(5)	6.942(5)	90

Atom	x	y	z	g	U_{eq}
K	0	0	0.486 2(4)	0.5	0.006 7(4)
P	0	0	0	0.5	0.004 0(3)
O1	0.033 73(8)	0.115 53(9)	−0.135 7(3)	1	0.006 5(2)
O2	0.116 16(8)	−0.033 82(8)	0.117 8(3)	1	0.006 3(2)
H	0.211 2(2)	0.062 3(2)	0.115 2(5)	1	0.019 8(4)

Atom	U_{11}	U_{22}	U_{33}	U_{23}	U_{13}	U_{12}
K	0.006 2(7)	0.004 2(7)	0.009 7(8)	0	0	0.000 5(7)
P	0.001 9(5)	0.002 9(5)	0.007 2(6)	0	0	−0.000 8(4)
O1	0.004 5(3)	0.005 3(4)	0.009 6(4)	0.002 2(3)	0.001 6(3)	0.000 6(3)
O2	0.005 5(3)	0.003 2(4)	0.010 1(4)	−0.000 2(3)	−0.003 0(4)	0.000 3(3)
H	0.019 3(7)	0.016 4(8)	0.023 8(9)	−0.001 9(9)	0.002 0(6)	0.002 6(6)

Atom	Principal mean square atomic displacements		
K	0.0097	0.0064	0.0041
P	0.0072	0.0033	0.0015
O1	0.0109	0.0044	0.0041
O2	0.0115	0.0041	0.0031
H	0.0247	0.0207	0.0141

Table 3.7 Unit cell and atomic parameters of orthorhombic KDP at 118 K. The parameters a, b, and c in Å and the angles α, β, and γ in degree are the lattice constants. The dimensionless parameters x, y, and z are fractional coordinates. The term g denotes the occupation factor of each atom as a dimensionless parameter. U_{eq} and U_{ij} in Å^2 are isotropic and anisotropic atomic displacement parameters, respectively. The principal mean square atomic displacements of each atom are also described. The values in parentheses are the estimated standard deviations (e.s.d.'s), and the parameters without e.s.d.'s are fixed ones.

Crystal system	Space group	a	b	c	α $(= \beta = \gamma)$
Orthorhombic	$Fdd2$	10.533(5)	10.479(6)	6.941(6)	90

Atom	x	y	z	g	U_{eq}
K	0	0	0.487 0(5)	0.5	0.006 8(4)
P	0	0	0	0.5	0.005 0(3)
O1	0.033 62(9)	0.115 35(9)	−0.135 1(4)	1	0.007 3(2)
O2	0.116 31(8)	−0.033 83(9)	0.118 3(4)	1	0.007 1(2)
H	0.211 0(2)	0.061 9(2)	0.115 8(6)	1	0.020 6(4)

Atom	U_{11}	U_{22}	U_{33}	U_{23}	U_{13}	U_{12}
K	0.006 4(7)	0.005 3(8)	0.008 8(9)	0	0	0.001 1(7)
P	0.003 0(5)	0.002 6(6)	0.009 4(6)	0	0	−0.001 2(4)
O1	0.004 8(4)	0.006 2(4)	0.010 9(4)	0.002 1(4)	0.001 1(4)	0.000 3(3)
O2	0.006 1(3)	0.003 9(4)	0.011 2(4)	0.000 0(4)	−0.002 9(4)	0.000 4(3)
H	0.019 6(8)	0.019 8(9)	0.022 5(9)	−0.001(1)	0.001(1)	0.003 5(6)

Atom	Principal mean square atomic displacements		
K	0.0088	0.0070	0.0045
P	0.0094	0.0040	0.0016
O1	0.0119	0.0054	0.0046
O2	0.0125	0.0049	0.0037
H	0.0232	0.0226	0.0160

Table 3.8 Unit cell and atomic parameters of orthorhombic KDP at 120 K. The parameters a, b, and c in Å and the angles α, β, and γ in degree are the lattice constants. The dimensionless parameters x, y, and z are fractional coordinates. The term g denotes the occupation factor of each atom as a dimensionless parameter. U_{eq} and U_{ij} in Å^2 are isotropic and anisotropic atomic displacement parameters, respectively. The principal mean square atomic displacements of each atom are also described. The values in parentheses are the estimated standard deviations (e.s.d.'s), and the parameters without e.s.d.'s are fixed ones.

Crystal system	Space group	a	b	c	α $(= \beta = \gamma)$
Orthorhombic	$Fdd2$	10.533(5)	10.488(6)	6.939(6)	90

Atom	x	y	z	g	U_{eq}
K	0	0	0.487 9(5)	0.5	0.007 0(4)
P	0	0	0	0.5	0.005 3(3)
O1	0.033 52(9)	0.115 60(9)	−0.134 9(4)	1	0.007 2(2)
O2	0.116 33(9)	−0.033 78(9)	0.118 8(4)	1	0.007 3(2)
H	0.210 4(2)	0.061 5(2)	0.116 0(6)	1	0.021 5(4)

Atom	U_{11}	U_{22}	U_{33}	U_{23}	U_{13}	U_{12}
K	0.005 7(7)	0.006 9(8)	0.008 5(9)	0	0	0.001 2(7)
P	0.003 7(5)	0.002 8(6)	0.009 4(6)	0	0	−0.001 1(5)
O1	0.005 0(4)	0.006 3(4)	0.010 4(4)	0.001 8(4)	0.000 6(4)	0.000 1(3)
O2	0.006 4(4)	0.004 4(4)	0.011 1(4)	−0.000 1(4)	−0.003 3(4)	0.001 2(3)
H	0.020 9(8)	0.020 2(9)	0.023(1)	0.000(1)	0.002(1)	0.004 6(7)

Atom	Principal mean square atomic displacements		
K	0.0085	0.0076	0.0050
P	0.0094	0.0045	0.0020
O1	0.0111	0.0057	0.0049
O2	0.0129	0.0055	0.0035
H	0.0256	0.0230	0.0157

Table 3.9 Unit cell and atomic parameters of tetragonal KDP at 125 K. The parameters a, b, and c in Å and the angles α, β, and γ in degree are the lattice constants. The dimensionless parameters x, y, and z are fractional coordinates. The term g denotes the occupation factor of each atom as a dimensionless parameter. U_{eq} and U_{ij} in Å^2 are isotropic and anisotropic atomic displacement parameters, respectively. The principal mean square atomic displacements of each atom are also described. The values in parentheses are the estimated standard deviations (e.s.d.'s), and the parameters without e.s.d.'s are fixed ones.

Crystal system	Space group	$a(=b)$	c	$\alpha\ (=\beta=\gamma)$
Tetragonal	$I\bar{4}2d$	7.421(3)	6.943(5)	90

Atom	x	y	z	g	U_{eq}
K	0	0	0.5	0.25	0.009 1(4)
P	0	0	0	0.25	0.007 8(3)
O	0.149 3(1)	0.082 7(1)	0.126 9(1)	1	0.008 6(2)
H	0.148 2(5)	0.231(2)	0.120(3)	0.5	0.023(2)

Atom	U_{11}	U_{22}	U_{33}	U_{23}	U_{13}	U_{12}
K	0.009 4(6)	0.009 4(6)	0.008 7(9)	0	0	0
P	0.005 3(4)	0.005 3(4)	0.012 8(7)	0	0	0
O	0.006 6(3)	0.006 8(4)	0.012 5(3)	−0.001 3(3)	−0.002 6(3)	0.001 4(2)
H	0.015 9(9)	0.027(7)	0.025(2)	−0.004(4)	−0.006(3)	0.000(1)

Atom	Principal mean square atomic displacements		
K	0.0094	0.0094	0.0086
P	0.0128	0.0053	0.0053
O	0.0139	0.0069	0.0051
H	0.0314	0.0239	0.0129

Table 3.10 Unit cell and atomic parameters of tetragonal KDP at 150 K. The parameters a, b, and c in Å and the angles α, β, and γ in degree are the lattice constants. The dimensionless parameters x, y, and z are fractional coordinates. The term g denotes the occupation factor of each atom as a dimensionless parameter. U_{eq} and U_{ij} in Å^2 are isotropic and anisotropic atomic displacement parameters, respectively. The principal mean square atomic displacements of each atom are also described. The values in parentheses are the estimated standard deviations (e.s.d.'s), and the parameters without e.s.d.'s are fixed ones.

Crystal system	Space group	$a(=b)$	c	$\alpha\ (=\beta=\gamma)$
Tetragonal	$I\bar{4}2d$	7.429(3)	6.935(2)	90

Atom	x	y	z	g	U_{eq}
K	0	0	0.5	0.25	0.010 4(5)
P	0	0	0	0.25	0.008 7(4)
O	0.149 2(1)	0.082 7(1)	0.126 4(2)	1	0.010 1(3)
H	0.148 2(5)	0.229(2)	0.128(2)	0.5	0.021(2)

Atom	U_{11}	U_{22}	U_{33}	U_{23}	U_{13}	U_{12}
K	0.012 4(7)	0.012 4(7)	0.006 5(9)	0	0	0
P	0.008 5(5)	0.008 5(5)	0.009 1(7)	0	0	0
O	0.009 3(4)	0.010 0(4)	0.011 1(4)	−0.002 0(3)	−0.003 4(4)	0.000 9(3)
H	0.017(1)	0.026(7)	0.020(2)	0.006(3)	0.009(3)	0.000(1)

Atom	Principal mean square atomic displacements		
K	0.0124	0.0124	0.0065
P	0.0091	0.0085	0.0085
O	0.0146	0.0091	0.0066
H	0.0317	0.0229	0.0078

Table 3.11 Unit cell and atomic parameters of tetragonal KDP at 200 K. The parameters a, b, and c in Å and the angles α, β, and γ in degree are the lattice constants. The dimensionless parameters x, y, and z are fractional coordinates. The term g denotes the occupation factor of each atom as a dimensionless parameter. U_{eq} and U_{ij} in Å^2 are isotropic and anisotropic atomic displacement parameters, respectively. The principal mean square atomic displacements of each atom are also described. The values in parentheses are the estimated standard deviations (e.s.d.'s), and the parameters without e.s.d.'s are fixed ones.

Crystal system	Space group	$a(=b)$	c	$\alpha\ (=\beta=\gamma)$
Tetragonal	$I\bar{4}2d$	7.433(3)	6.958(6)	90

Atom	x	y	z	g	U_{eq}
K	0	0	0.5	0.25	0.012 7(7)
P	0	0	0	0.25	0.008 2(5)
O	0.148 5(2)	0.082 4(2)	0.126 4(2)	1	0.010 2(3)
H	0.146 8(7)	0.227(1)	0.117(3)	0.5	0.020(2)

Atom	U_{11}	U_{22}	U_{33}	U_{23}	U_{13}	U_{12}
K	0.013(1)	0.013(1)	0.012(1)	0	0	0
P	0.005 7(6)	0.005 7(6)	0.013(1)	0	0	0
O	0.008 1(5)	0.007 9(5)	0.014 8(5)	−0.001 6(5)	−0.003 5(5)	0.001 0(3)
H	0.018(1)	0.018(6)	0.023(3)	−0.008(4)	−0.005(3)	0.006(2)

Atom	Principal mean square atomic displacements		
K	0.0128	0.0128	0.0124
P	0.0132	0.0057	0.0057
O	0.0167	0.0075	0.0065
H	0.0334	0.0142	0.0110

Table 3.12 Unit cell and atomic parameters of orthorhombic DKDP at 10 K. The parameters a, b, and c in Å and the angles α, β, and γ in degree are the lattice constants. The dimensionless parameters x, y, and z are fractional coordinates. The term g denotes the occupation factor of each atom as a dimensionless parameter. U_{eq} and U_{ij} in Å^2 are isotropic and anisotropic atomic displacement parameters, respectively. The principal mean square atomic displacements of each atom are also described. The values in parentheses are the estimated standard deviations (e.s.d.'s), and the parameters without e.s.d.'s are fixed ones.

Crystal system	Space group	a	b	c	α $(= \beta = \gamma)$
Orthorhombic	$Fdd2$	10.595(9)	10.487(6)	6.922(4)	90

Atom	x	y	z	g	U_{eq}
K	0	0	0.482 4(6)	0.5	0.004 4(6)
P	0	0	0	0.5	0.002 4(4)
O1	0.035 4(1)	0.114 9(1)	−0.137 3(5)	1	0.004 2(3)
O2	0.115 8(1)	−0.035 2(1)	0.116 6(5)	1	0.004 0(3)
D	0.216 0(2)	0.065 1(2)	0.114 1(6)	1	0.014 2(4)

Atom	U_{11}	U_{22}	U_{33}	U_{23}	U_{13}	U_{12}
K	0.006(1)	0.007(1)	0.001(1)	0	0	−0.000 3(9)
P	0.002 0(8)	0.002 3(9)	0.002 8(9)	0	0	−0.000 5(6)
O1	0.004 5(6)	0.004 5(6)	0.003 5(6)	0.001 8(5)	0.002 3(5)	0.001 3(4)
O2	0.003 1(6)	0.006 0(6)	0.003 0(6)	0.000 5(5)	−0.001 7(5)	0.000 5(4)
D	0.014 0(7)	0.013 6(7)	0.015 1(7)	−0.001 5(7)	0.000 4(7)	−0.000 0(6)

Atom	Principal mean square atomic displacements		
K	0.0066	0.0057	0.0009
P	0.0028	0.0027	0.0017
O1	0.0078	0.0033	0.0015
O2	0.0061	0.0047	0.0012
D	0.0160	0.0140	0.0126

Table 3.13 Unit cell and atomic parameters of orthorhombic DKDP at 70 K. The parameters a, b, and c in Å and the angles α, β, and γ in degree are the lattice constants. The dimensionless parameters x, y, and z are fractional coordinates. The term g denotes the occupation factor of each atom as a dimensionless parameter. U_{eq} and U_{ij} in Å^2 are isotropic and anisotropic atomic displacement parameters, respectively. The principal mean square atomic displacements of each atom are also described. The values in parentheses are the estimated standard deviations (e.s.d.'s), and the parameters without e.s.d.'s are fixed ones.

Crystal system	Space group	a	b	c	α $(= \beta = \gamma)$
Orthorhombic	$Fdd2$	10.58(2)	10.49(1)	6.920(3)	90

Atom	x	y	z	g	U_{eq}
K	0	0	0.482 7(6)	0.5	0.004 8(6)
P	0	0	0	0.5	0.002 9(4)
O1	0.035 0(1)	0.115 0(1)	−0.137 7(5)	1	0.004 9(3)
O2	0.115 6(1)	−0.035 2(1)	0.116 1(5)	1	0.005 3(3)
D	0.216 3(2)	0.065 5(2)	0.114 1(6)	1	0.015 3(4)

Atom	U_{11}	U_{22}	U_{33}	U_{23}	U_{13}	U_{12}
K	0.008(1)	0.004(1)	0.003(1)	0	0	−0.000 2(9)
P	0.004 2(8)	0.001 1(8)	0.003 4(9)	0	0	0.000 6(6)
O1	0.006 3(6)	0.003 3(5)	0.005 2(5)	0.001 9(5)	0.002 0(5)	−0.000 1(4)
O2	0.006 9(6)	0.004 3(5)	0.004 8(6)	−0.000 0(5)	−0.001 8(6)	0.000 4(4)
D	0.016 9(7)	0.012 5(6)	0.016 5(7)	−0.001 8(7)	−0.000 4(7)	0.000 6(6)

Atom	Principal mean square atomic displacements		
K	0.0076	0.0042	0.0026
P	0.0044	0.0034	0.0010
O1	0.0081	0.0049	0.0018
O2	0.0079	0.0043	0.0037
D	0.0177	0.0165	0.0118

Table 3.14 Unit cell and atomic parameters of orthorhombic DKDP at 130 K. The parameters a, b, and c in Å and the angles α, β, and γ in degree are the lattice constants. The dimensionless parameters x, y, and z are fractional coordinates. The term g denotes the occupation factor of each atom as a dimensionless parameter. U_{eq} and U_{ij} in Å^2 are isotropic and anisotropic atomic displacement parameters, respectively. The principal mean square atomic displacements of each atom are also described. The values in parentheses are the estimated standard deviations (e.s.d.'s), and the parameters without e.s.d.'s are fixed ones.

Crystal system	Space group	a	b	c	α $(= \beta = \gamma)$
Orthorhombic	$Fdd2$	10.584(5)	10.485(4)	6.943(4)	90

Atom	x	y	z	g	U_{eq}
K	0	0	0.481 8(5)	0.5	0.007 5(5)
P	0	0	0	0.5	0.004 3(4)
O1	0.034 9(1)	0.114 9(1)	−0.137 2(5)	1	0.007 6(3)
O2	0.115 8(1)	−0.035 3(1)	0.115 6(5)	1	0.007 0(3)
D	0.216 0(2)	0.065 9(2)	0.114 1(6)	1	0.016 6(3)

Atom	U_{11}	U_{22}	U_{33}	U_{23}	U_{13}	U_{12}
K	0.008(1)	0.007(1)	0.007(1)	0	0	0.000 0(8)
P	0.003 0(7)	0.003 7(7)	0.006 3(8)	0	0	0.000 2(5)
O1	0.006 0(5)	0.007 3(5)	0.009 4(5)	0.003 2(5)	0.001 5(5)	−0.000 2(4)
O2	0.007 0(5)	0.005 8(5)	0.008 3(5)	0.000 7(5)	−0.002 6(5)	0.000 5(4)
D	0.015 2(6)	0.015 0(6)	0.019 7(6)	−0.001 9(6)	0.000 7(6)	0.000 2(5)

Atom	Principal mean square atomic displacements		
K	0.0082	0.0073	0.0070
P	0.0062	0.0038	0.0029
O1	0.0119	0.0065	0.0043
O2	0.0103	0.0063	0.0044
D	0.0204	0.0153	0.0142

Table 3.15 Unit cell and atomic parameters of orthorhombic DKDP at 160 K. The parameters a, b, and c in Å and the angles α, β, and γ in degree are the lattice constants. The dimensionless parameters x, y, and z are fractional coordinates. The term g denotes the occupation factor of each atom as a dimensionless parameter. U_{eq} and U_{ij} in Å^2 are isotropic and anisotropic atomic displacement parameters, respectively. The principal mean square atomic displacements of each atom are also described. The values in parentheses are the estimated standard deviations (e.s.d.'s), and the parameters without e.s.d.'s are fixed ones.

Crystal system	Space group	a	b	c	α $(= \beta = \gamma)$
Orthorhombic	$Fdd2$	10.589(7)	10.489(6)	6.945(5)	90

Atom	x	y	z	g	U_{eq}
K	0	0	0.482 5(6)	0.5	0.009 6(6)
P	0	0	0	0.5	0.006 5(4)
O1	0.034 7(2)	0.114 8(2)	−0.137 6(5)	1	0.010 0(3)
O2	0.115 5(2)	−0.035 0(2)	0.115 3(5)	1	0.009 3(3)
D	0.216 0(2)	0.065 8(2)	0.114 1(6)	1	0.019 1(4)

Atom	U_{11}	U_{22}	U_{33}	U_{23}	U_{13}	U_{12}
K	0.013(1)	0.010(1)	0.007(1)	0	0	0.000(1)
P	0.006 7(9)	0.005 2(9)	0.008(1)	0	0	0.000 3(6)
O1	0.009 9(6)	0.009 4(6)	0.010 8(6)	0.003 8(6)	0.003 0(6)	−0.000 1(5)
O2	0.010 6(6)	0.008 0(6)	0.009 3(6)	0.000 6(6)	−0.003 9(6)	0.000 4(4)
D	0.019 8(7)	0.017 5(7)	0.020 1(7)	−0.002 5(8)	−0.001 0(8)	0.001 1(6)

Atom	Principal mean square atomic displacements		
K	0.0126	0.0095	0.0067
P	0.0076	0.0067	0.0051
O1	0.0151	0.0098	0.0052
O2	0.0139	0.0082	0.0058
D	0.0224	0.0190	0.0159

Table 3.16 Unit cell and atomic parameters of orthorhombic DKDP at 190 K. The parameters a, b, and c in Å and the angles α, β, and γ in degree are the lattice constants. The dimensionless parameters x, y, and z are fractional coordinates. The term g denotes the occupation factor of each atom as a dimensionless parameter. U_{eq} and U_{ij} in Å^2 are isotropic and anisotropic atomic displacement parameters, respectively. The principal mean square atomic displacements of each atom are also described. The values in parentheses are the estimated standard deviations (e.s.d.'s), and the parameters without e.s.d.'s are fixed ones.

Crystal system	Space group	a	b	c	α $(= \beta = \gamma)$
Orthorhombic	$Fdd2$	10.60(1)	10.50(1)	6.962(4)	90

Atom	x	y	z	g	U_{eq}
K	0	0	0.481 7(6)	0.5	0.007 9(7)
P	0	0	0	0.5	0.003 9(4)
O1	0.034 5(2)	0.114 6(2)	−0.137 1(5)	1	0.008 8(4)
O2	0.115 4(2)	−0.035 2(2)	0.114 4(5)	1	0.007 6(3)
D	0.216 0(2)	0.066 0(2)	0.112 6(6)	1	0.017 1(4)

Atom	U_{11}	U_{22}	U_{33}	U_{23}	U_{13}	U_{12}
K	0.005(1)	0.012(2)	0.006(1)	0	0	−0.001(1)
P	0.003 9(9)	0.003(1)	0.005(1)	0	0	−0.000 9(6)
O1	0.005 2(6)	0.010 0(8)	0.011 2(6)	0.003 8(6)	0.002 7(6)	−0.000 0(5)
O2	0.006 9(6)	0.007 2(7)	0.008 6(6)	0.001 3(6)	−0.003 4(6)	0.000 4(5)
D	0.016 4(7)	0.016 0(8)	0.019 0(8)	−0.000 8(8)	0.001 1(7)	0.001 5(6)

Atom	Principal mean square atomic displacements		
K	0.0126	0.0061	0.0050
P	0.0051	0.0043	0.0022
O1	0.0149	0.0078	0.0038
O2	0.0114	0.0074	0.0038
D	0.0194	0.0176	0.0144

Table 3.17 Unit cell and atomic parameters of orthorhombic DKDP at 205 K. The parameters a, b, and c in Å and the angles α, β, and γ in degree are the lattice constants. The dimensionless parameters x, y, and z are fractional coordinates. The term g denotes the occupation factor of each atom as a dimensionless parameter. U_{eq} and U_{ij} in Å^2 are isotropic and anisotropic atomic displacement parameters, respectively. The principal mean square atomic displacements of each atom are also described. The values in parentheses are the estimated standard deviations (e.s.d.'s), and the parameters without e.s.d.'s are fixed ones.

Crystal system	Space group	a	b	c	α $(=\beta=\gamma)$
Orthorhombic	$Fdd2$	10.590(5)	10.499(4)	6.964(2)	90

Atom	x	y	z	g	U_{eq}
K	0	0	0.482 5(6)	0.5	0.012 6(6)
P	0	0	0	0.5	0.008 4(4)
O1	0.034 5(2)	0.114 6(2)	−0.136 4(5)	1	0.012 8(3)
O2	0.115 5(2)	−0.034 9(1)	0.115 4(5)	1	0.011 5(3)
D	0.215 7(2)	0.065 9(2)	0.114 6(6)	1	0.021 6(4)

Atom	U_{11}	U_{22}	U_{33}	U_{23}	U_{13}	U_{12}
K	0.014(1)	0.013(1)	0.011(1)	0	0	0.000(1)
P	0.008(1)	0.007 2(8)	0.010(1)	0	0	0.000 3(6)
O1	0.010 4(6)	0.013 0(6)	0.015 0(6)	0.004 8(6)	0.003 3(6)	−0.000 3(5)
O2	0.011 8(6)	0.010 1(6)	0.012 7(6)	0.000 6(6)	−0.004 3(6)	0.000 5(4)
D	0.021 0(7)	0.020 3(7)	0.023 6(7)	−0.002 5(8)	0.000 3(8)	0.002 3(6)

Atom	Principal mean square atomic displacements		
K	0.0139	0.0131	0.0107
P	0.0100	0.0082	0.0071
O1	0.0196	0.0117	0.0072
O2	0.0165	0.0103	0.0077
D	0.0252	0.0222	0.0175

Table 3.18 Unit cell and atomic parameters of orthorhombic DKDP at 210 K. The parameters a, b, and c in Å and the angles α, β, and γ in degree are the lattice constants. The dimensionless parameters x, y, and z are fractional coordinates. The term g denotes the occupation factor of each atom as a dimensionless parameter. U_{eq} and U_{ij} in Å^2 are isotropic and anisotropic atomic displacement parameters, respectively. The principal mean square atomic displacements of each atom are also described. The values in parentheses are the estimated standard deviations (e.s.d.'s), and the parameters without e.s.d.'s are fixed ones.

Crystal system	Space group	a	b	c	α $(= \beta = \gamma)$
Orthorhombic	$Fdd2$	10.59(1)	10.51(1)	6.965(5)	90

Atom	x	y	z	g	U_{eq}
K	0	0	0.482 7(6)	0.5	0.011 3(6)
P	0	0	0	0.5	0.006 3(4)
O1	0.034 3(2)	0.114 9(2)	−0.136 7(5)	1	0.011 4(3)
O2	0.115 4(2)	−0.035 1(2)	0.115 4(5)	1	0.009 9(3)
D	0.215 5(2)	0.065 7(2)	0.114 3(6)	1	0.020 1(4)

Atom	U_{11}	U_{22}	U_{33}	U_{23}	U_{13}	U_{12}
K	0.012(1)	0.016(2)	0.006(1)	0	0	−0.000(1)
P	0.005 3(8)	0.005(1)	0.008 6(9)	0	0	−0.000 7(6)
O1	0.008 0(6)	0.012 1(7)	0.014 0(6)	0.004 7(6)	0.002 6(6)	0.000 0(5)
O2	0.008 9(5)	0.009 7(6)	0.011 2(5)	0.000 9(5)	−0.004 9(6)	0.000 4(5)
D	0.018 9(7)	0.020 9(8)	0.020 6(7)	−0.001 8(7)	0.000 2(7)	0.002 8(6)

Atom	Principal mean square atomic displacements		
K	0.0160	0.0114	0.0065
P	0.0086	0.0059	0.0044
O1	0.0183	0.0096	0.0062
O2	0.0151	0.0098	0.0048
D	0.0235	0.0203	0.0165

Table 3.19 Unit cell and atomic parameters of tetragonal DKDP at 220 K. The parameters a, b, and c in Å and the angles α, β, and γ in degree are the lattice constants. The dimensionless parameters x, y, and z are fractional coordinates. The term g denotes the occupation factor of each atom as a dimensionless parameter. U_{eq} and U_{ij} in Å^2 are isotropic and anisotropic atomic displacement parameters, respectively. The principal mean square atomic displacements of each atom are also described. The values in parentheses are the estimated standard deviations (e.s.d.'s), and the parameters without e.s.d.'s are fixed ones.

Crystal system	Space group	$a(=b)$	c	$\alpha\ (=\beta=\gamma)$
Tetragonal	$I\bar{4}2d$	7.458(2)	6.959(2)	90

Atom	x	y	z	g	U_{eq}
K	0	0	0.5	0.25	0.009 3(8)
P	0	0	0	0.25	0.007 2(6)
O	0.149 0(2)	0.080 7(2)	0.126 0(3)	1	0.009 5(3)
D	0.149 5(4)	0.219 7(3)	0.122(1)	0.5	0.017 0(8)

Atom	U_{11}	U_{22}	U_{33}	U_{23}	U_{13}	U_{12}
K	0.010(1)	0.010(1)	0.007(2)	0	0	0
P	0.005 4(7)	0.005 4(7)	0.011(1)	0	0	0
O	0.008 1(5)	0.007 6(6)	0.013 0(5)	−0.002 3(5)	−0.005 4(6)	0.002 7(4)
D	0.014(1)	0.014(2)	0.023(1)	0.003(3)	0.001(2)	−0.001 4(8)

Atom	Principal mean square atomic displacements		
K	0.0104	0.0104	0.0073
P	0.0108	0.0054	0.0054
O	0.0176	0.0068	0.0042
D	0.0240	0.0153	0.0116

Table 3.20 Unit cell and atomic parameters of tetragonal DKDP at 250 K. The parameters a, b, and c in Å and the angles α, β, and γ in degree are the lattice constants. The dimensionless parameters x, y, and z are fractional coordinates. The term g denotes the occupation factor of each atom as a dimensionless parameter. U_{eq} and U_{ij} in Å^2 are isotropic and anisotropic atomic displacement parameters, respectively. The principal mean square atomic displacements of each atom are also described. The values in parentheses are the estimated standard deviations (e.s.d.'s), and the parameters without e.s.d.'s are fixed ones.

Crystal system	Space group	$a(=b)$	c	$\alpha\ (=\beta=\gamma)$
Tetragonal	$I\bar{4}2d$	7.46(2)	6.954(8)	90

Atom	x	y	z	g	U_{eq}
K	0	0	0.5	0.25	0.011 7(8)
P	0	0	0	0.25	0.009 9(6)
O	0.149 0(2)	0.081 0(2)	0.126 4(3)	1	0.012 4(4)
D	0.148 7(4)	0.219 9(3)	0.121(1)	0.5	0.017 7(8)

Atom	U_{11}	U_{22}	U_{33}	U_{23}	U_{13}	U_{12}
K	0.013(1)	0.013(1)	0.009(2)	0	0	0
P	0.007 4(7)	0.007 4(7)	0.015(1)	0	0	0
O	0.010 2(5)	0.010 3(6)	0.016 7(6)	−0.003 0(5)	−0.005 1(6)	0.002 1(4)
D	0.017(1)	0.012(2)	0.024(1)	0.000(2)	0.000(2)	−0.000 1(7)

Atom	Principal mean square atomic displacements		
K	0.0132	0.0132	0.0088
P	0.0149	0.0074	0.0074
O	0.0207	0.0091	0.0073
D	0.0244	0.0169	0.0119

Table 3.21 Unit cell and atomic parameters of tetragonal DKDP at 298 K. The parameters a, b, and c in Å and the angles α, β, and γ in degree are the lattice constants. The dimensionless parameters x, y, and z are fractional coordinates. The term g denotes the occupation factor of each atom as a dimensionless parameter. U_{eq} and U_{ij} in Å^2 are isotropic and anisotropic atomic displacement parameters, respectively. The principal mean square atomic displacements of each atom are also described. The values in parentheses are the estimated standard deviations (e.s.d.'s), and the parameters without e.s.d.'s are fixed ones.

Crystal system	Space group	$a(=b)$	c	$\alpha\ (=\beta=\gamma)$
Tetragonal	$I\bar{4}2d$	7.471(2)	6.977(4)	90

Atom	x	y	z	g	U_{eq}
K	0	0	0.5	0.25	0.015 9(6)
P	0	0	0	0.25	0.012 3(4)
O	0.148 7(2)	0.081 0(1)	0.125 7(2)	1	0.015 3(3)
D	0.148 4(3)	0.220 2(3)	0.121 0(8)	0.5	0.023 1(6)

Atom	U_{11}	U_{22}	U_{33}	U_{23}	U_{13}	U_{12}
K	0.017 1(9)	0.017 1(9)	0.014(1)	0	0	0
P	0.010 5(5)	0.010 5(5)	0.016(1)	0	0	0
O	0.012 9(4)	0.013 3(4)	0.019 8(4)	−0.003 7(4)	−0.005 8(4)	0.001 8(4)
D	0.021 0(8)	0.020(2)	0.029(1)	−0.001(2)	−0.002(1)	−0.001 3(7)

Atom	Principal mean square atomic displacements		
K	0.0171	0.0171	0.0137
P	0.0158	0.0105	0.0105
O	0.0246	0.0118	0.0096
D	0.0290	0.0216	0.0186

3.2 Interatomic distances and angles

Hereafter, interatomic distances and angles are compared between KDP and DKDP in figures, where the solid and open symbols represent KDP and DKDP, respectively.

A K atom is surrounded by eight oxygen atoms; four of them are the nearest-neighbor (NN) atoms, and the other four are the next-nearest-neighbor (NNN) atoms. Below T_c, K displaces along the c-axis, so that these distances between K and O change, as shown in Fig. 3.1. In the ferroelectric phase, the NN distance splits into K–$O2_{NN}$ and K–$O1_{NN}$, and the NNN distance into K–$O2_{NNN}$ and K–$O1_{NNN}$. [43] Strictly, K–$O2_{NN}$, K–$O1_{NN}$, K–$O2_{NNN}$, and K–$O1_{NNN}$ indicate K–$O2^a$, K–$O1^b$, K–O2, and K–$O1^c$, respectively; the superscripts a, b, and c denote the symmetry coordinates $-x+1/4, y+1/4, z+1/4$; $x-1/4, -y+1/4, z+3/4$; and $x, y, z+1$,

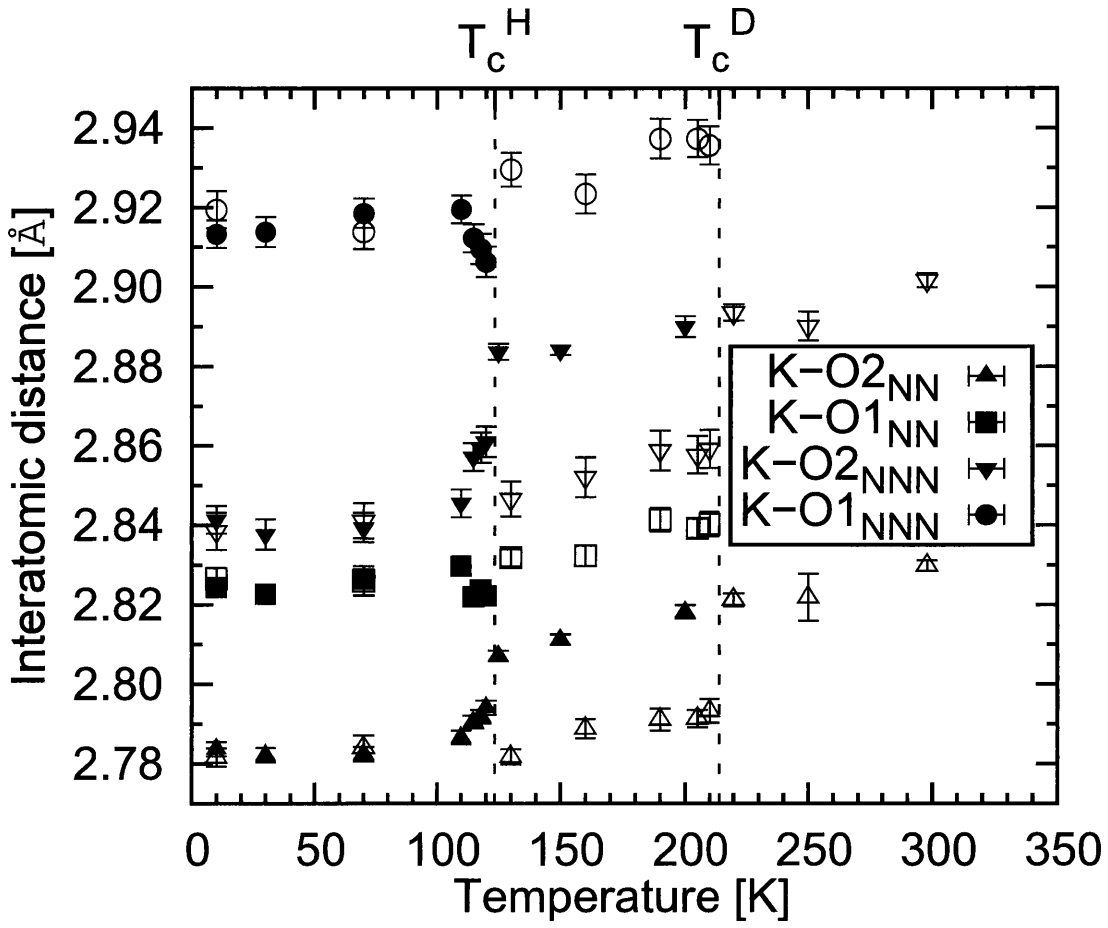

Figure 3.1 Temperature dependences of the interatomic distances K–$O2_{NN}$, K–$O1_{NN}$, K–$O2_{NNN}$, and K–$O1_{NNN}$. The solid and open symbols denote the values of KDP and DKDP, respectively. 'NN' and 'NNN' mean 'nearest-neighbor' and 'next-nearest-neighbor', respectively. [43]

respectively.

The O–K–O angles are shown in Fig. 3.2; the primed and normal O's are NN and NNN ones, respectively. At each angle, O atoms are related to the two-fold symmetry through the K atom along the c-axis. The four interatomic angles in the ferroelectric phase turn into two interatomic angles in the paraelectric phase, which are crystallographically independent of each other. Strictly, O2′–K–O2′, O1′–K–O1′, O2–K–O2, and O1–K–O1 indicate $O2^{a}$–K–$O2^{d}$, $O1^{b}$–K–$O1^{e}$, O2–K–$O2^{f}$, and $O1^{c}$–K–$O1^{g}$, respectively; the superscripts d, e, f, and g denote the symmetry operations $x-1/4, -y-1/4, z+1/4$; $-x+1/4, y-1/4, z+3/4$; $-x, -y, z$; and $-x, -y, z+1$, respectively. Except for the gradual changes just below the T_c of KDP, their interatomic distances and angles change in the same fashion, although the transition temperatures are quite different between KDP and DKDP. With decreasing temperature, the atomic distances slightly decrease as shown in Fig. 3.1, however, the angles do not show such changes. So, the atomic distance of K–O contracts homogeneously within each phase.

Each K atom is surrounded by six PO_4 tetrahedra. Two of them are above and below K along the c-axis, and four around the c-axis. The distances between K and P for the former neighbors are shorter than for the latter neighbors.

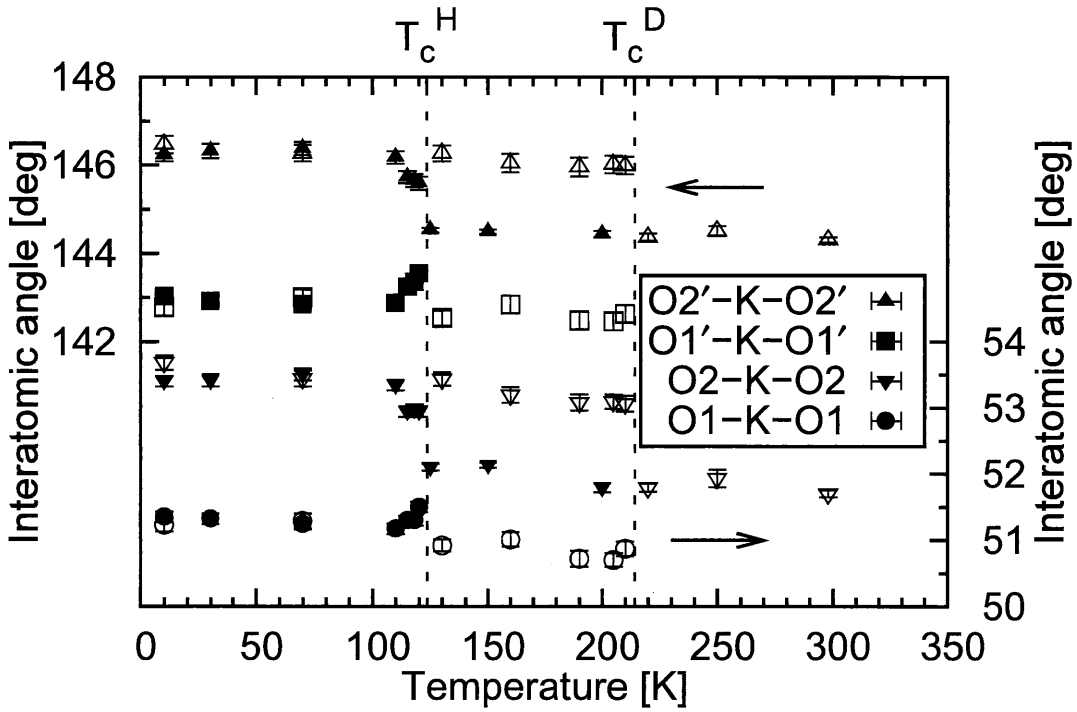

Figure 3.2 Temperature dependences of interatomic angles, O2′–K–O2′ (left ordinate), O1′–K–O1′ (left ordinate), O2–K–O2 (right ordinate), and O1–K–O1 (right ordinate) in both KDP (solid symbols) and DKDP (open symbols).

Fig. 3.3 shows temperature dependences of the interatomic distances, K–P_1 (left ordinate), K–$P_{1'}$ (left ordinate), K–P_2 (right ordinate), and K–$P_{2'}$ (right ordinate). The solid and open symbols denote the values of KDP and DKDP, respectively. These four interatomic distances in ferroelectric phase turn into two interatomic distances in paraelectric phase, which are crystallographically independent of each other. Strictly, K–P_1, K–$P_{1'}$, K–P_2, and K–$P_{2'}$ indicate K–P, K–P^c, K–P^h, and K–P^b in the ferroelectric phase of KDP and DKDP, respectively; the superscript h denotes symmetry operations, $x+1/4, -y+1/4, z+1/4$. In addition to recognition of Curie point increase up to *ca.* 100 K between KDP and DKDP, the differences between KDP and DKDP in these four interatomic distances are also negligible, except for rounded change just below T_c. The temperature dependences of the K–P distances are similar to those of K–O distances shown in Fig. 3.1.

As shown in Figs. 3.1–3.3, no notable difference between KDP and DKDP can be recognized in the interatomic distances and angles of K–O and K–P, except for the

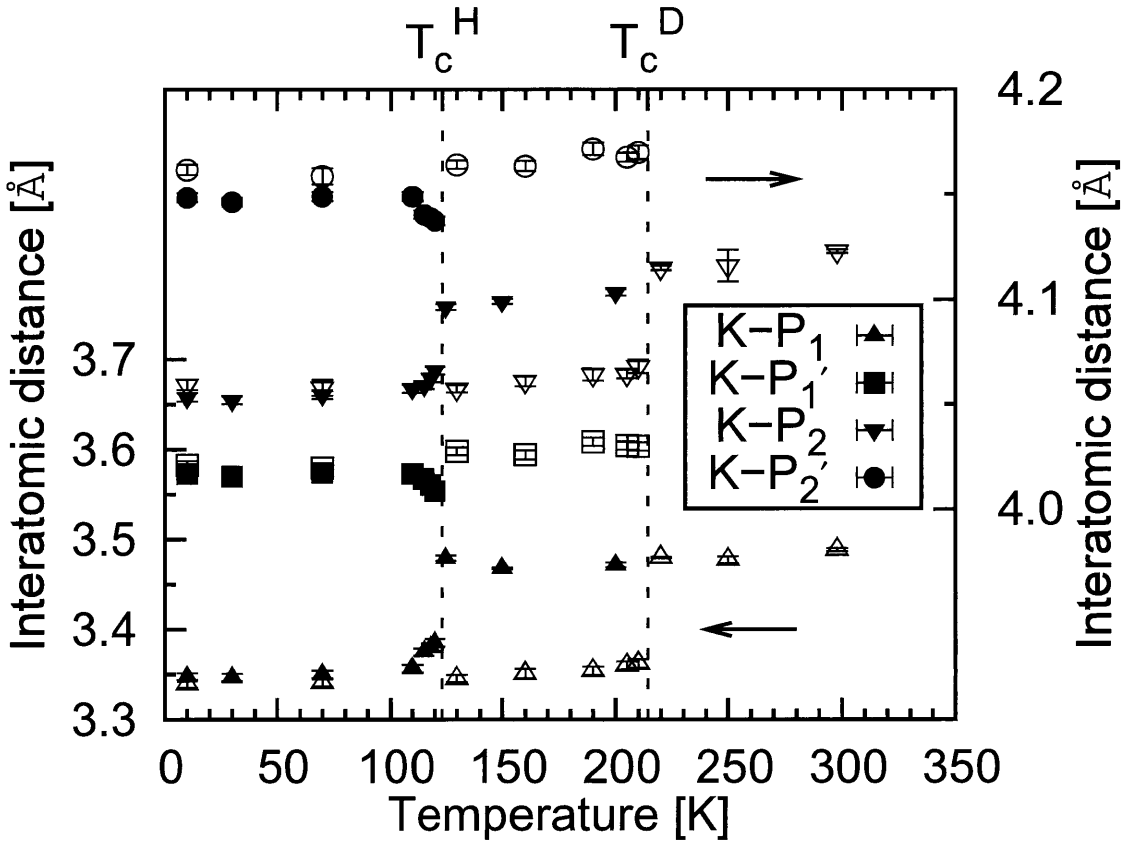

Figure 3.3 Temperature dependences of the interatomic distances, K–P_1 (left ordinate), K–$P_{1'}$ (left ordinate), K–P_2 (right ordinate), and K–$P_{2'}$ (right ordinate). The solid and open symbols denote the values of KDP and DKDP, respectively.

gradual changes just below the T_c of KDP.

Next, the author describes the deformation of the PO_4 tetrahedron. In the paraelectric phase, the molecule has an S_4 symmetry, which is reduced to C_2 in the ferroelectric phase. (Refer Fig. ??.) Therefore, the unique P–O distance splits into P–O1 and P–O2, where O1 is the acceptor for the hydrogen atom and O2 the donor.

Figure ?? shows the temperature dependences of the interatomic distances for KDP and DKDP. If the hydrogen atom attaches to O1, then the P–O1 distance increases by *ca.* 0.03 Å, while the P–O2 distance decreases by *ca.* 0.03 Å; the distance change in DKDP is almost the same as or slightly larger than that in KDP. The difference between P–O2 and P–O1 indicates that the PO_4 tetrahedron distorts slightly in the ferroelectrics phase. Except for the gradual changes just below T_c of KDP, the values of both ferroelectric and paraelectric phases in KDP and DKDP are almost the same.

As shown in the schematic picture in Fig. 3.4, there are two interatomic angles in the paraelectric phase: O–P–O′ $\sim$ 110.3° and O1–P–O2 $\sim$ 109.0°. These angles are almost the same for KDP and DKDP. In the ferroelectric phase, the angle O–P–O′ splits into O1–P–O1′ and O2–P–O2′; the former O1 atom is the acceptor of H/D and the former angle decreases to 106°, and the latter angle increases to 115.5°, as shown in Fig. 3.6.

The interatomic distances within a PO_4 tetrahedron are plotted in Figs. 3.7 and 3.8. In Fig. 3.7, one of two oxygen atoms is symmetrically related to another oxygen atom

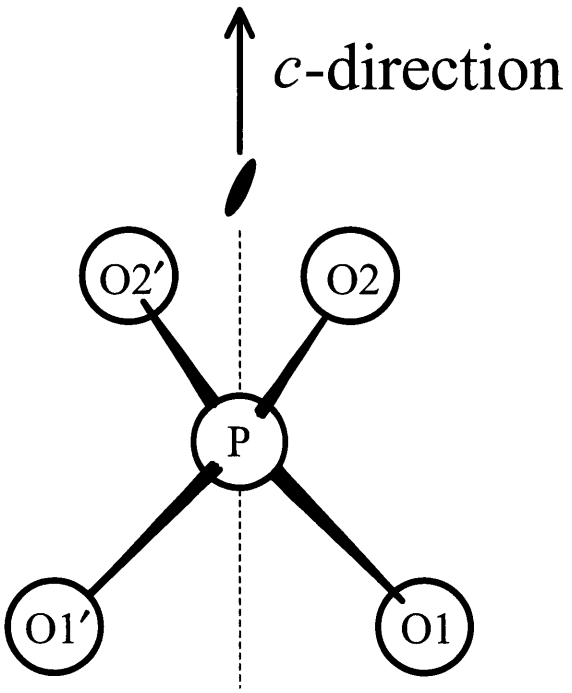

Figure 3.4 Schematic view of the PO_4 tetrahedron and the two-fold axis along the *c*-axis.

as counterpart with two-fold symmetry through phosphorus atom along c-axis. Moreover, these O1–O1 and O2–O2 in ferroelectric phase, which are crystallographically independent of each other, turn into the common interatomic distance in paraelectric phase. This relationship is corresponding to that symmetry of PO_4 tetrahedron changes from C_2 in the ferroelectric phase into S_4 in the paraelectric phase. The difference between O1–O1 and O2–O2 indicates that shape of PO_4 tetrahedron distorts slightly in the ferroelectrics phase. Strictly, O1–O1 and O2–O2 indicate O1–O1^{f} and O2–O2^{f} in the ferroelectric phase, respectively. Although it is natural to recognize Curie point increase up to *ca.* 100 K between KDP and DKDP, the values of both ferroelectric and paraelectric phases in KDP and DKDP are almost in accordance. In Fig. 3.8, one of two oxygen atoms is symmetrically related to another oxygen atom as counterpart with two-fold symmetry through phosphorus atom along c-axis. Moreover, these O1–O2 and O1–O2′ in ferroelectric phase, which are crystallographically independent of each other, turn into the common interatomic distance in paraelectric phase. This relationship is corresponding to that symmetry of PO_4 tetrahedron changes from C_2 in the ferroelectric phase into S_4 in the paraelectric phase. The difference between O1–O2 and O1–O2′ indicates that shape of PO_4 tetrahedron distorts

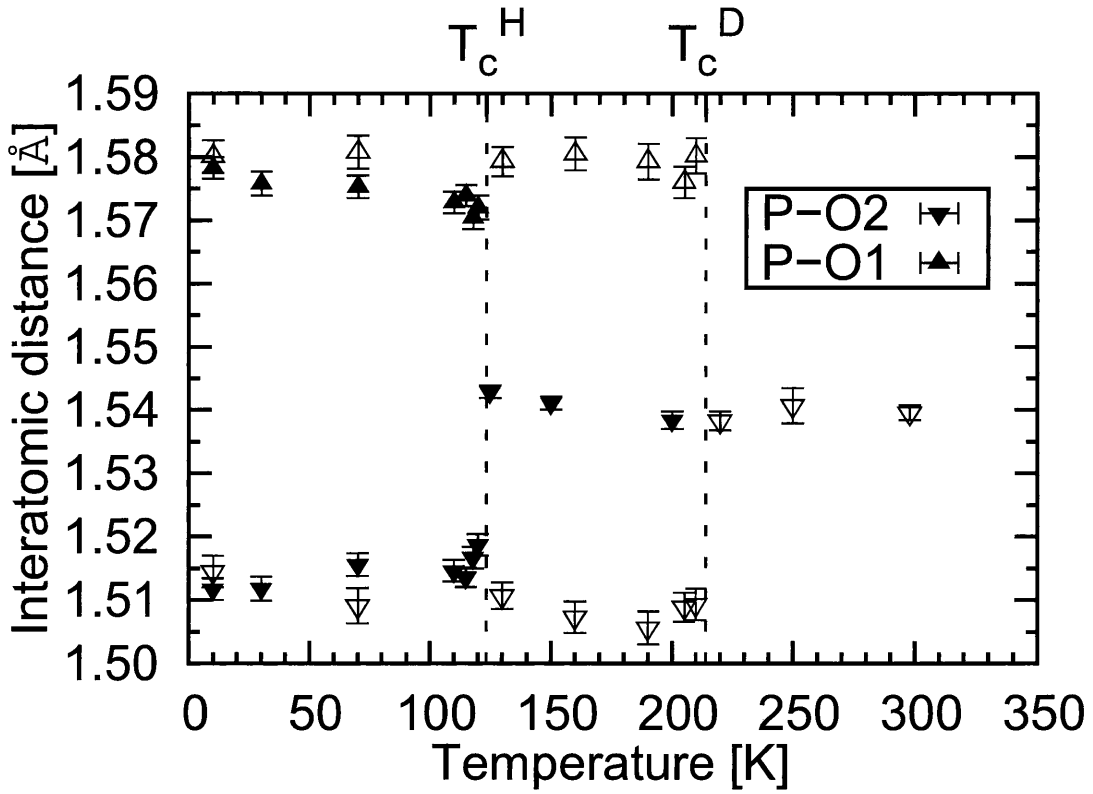

Figure 3.5 Temperature dependences of the interatomic distances P–O2 and P–O1 in both KDP (solid symbols) and DKDP (open symbols).

slightly in the ferroelectrics phase. Strictly, O1–O2′ in the legend indicates O1–O2^{f} in the ferroelectric phase of KDP and DKDP, respectively. Although it is natural to recognize Curie point increase up to *ca.* 100 K between KDP and DKDP, the values of both ferroelectric and paraelectric phases in KDP and DKDP are almost in accordance.

The angles O–P–O also depend on temperature as shown in Fig. 3.9. One of two oxygen atoms is symmetrically related to another oxygen atom as counterpart with two-fold symmetry through phosphorus atom along *c*-axis. Moreover, these O1–P–O2 and O1–P–O2′ in ferroelectric phase, which are crystallographically independent of each other, turn into the common interatomic angle in paraelectric phase. This relationship is corresponding to that symmetry of PO_4 tetrahedron changes from C_2 in the ferroelectric into S_4 in the paraelectric phase. The difference between O1–P–O2 and O1–P–O2′ indicates that shape of PO_4 tetrahedron consequently has slight distortion in the ferroelectrics phase. Strictly, O1–P–O2′ in the legend indicates O1–P–O2^{f} in the ferroelectric phase of KDP and DKDP, respectively. Although it is natural to recognize Curie point increase up to *ca.* 100 K between KDP and DKDP,

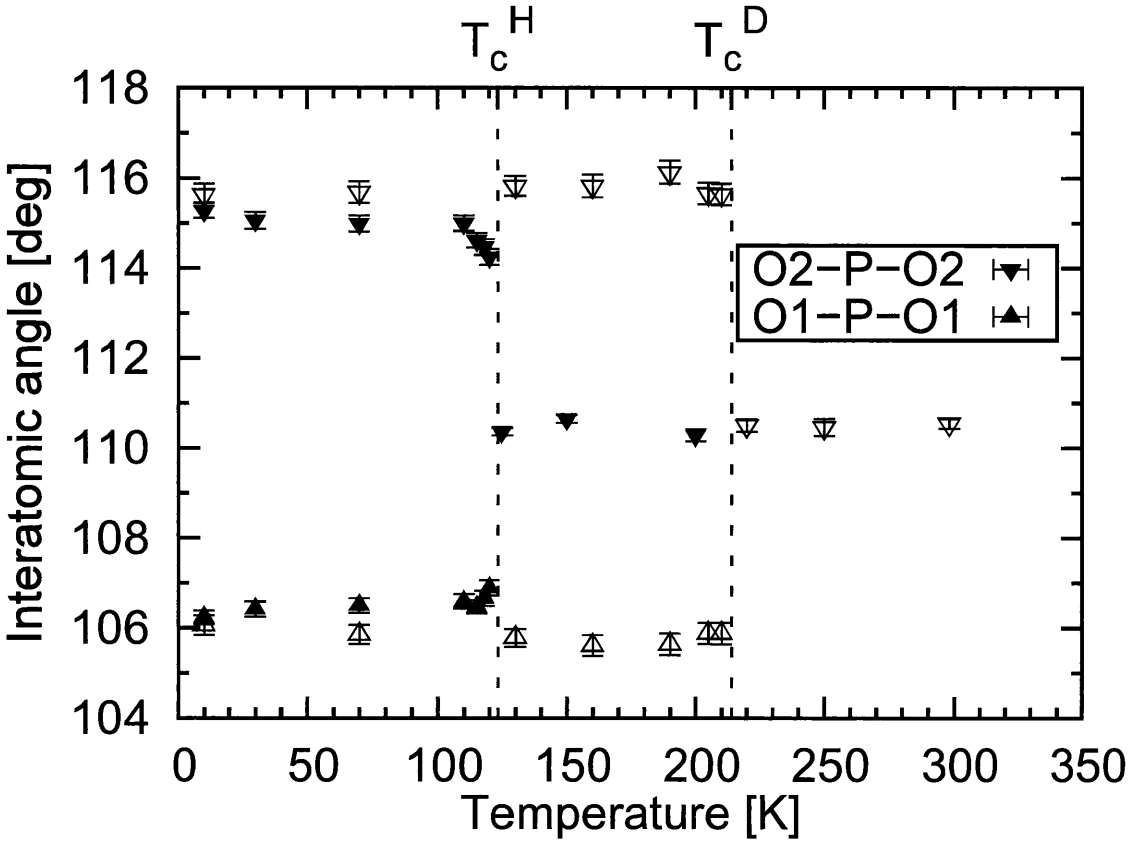

Figure 3.6 Temperature dependences of the interatomic angles, O2–P–O2 and O1–P–O1 in both KDP (solid symbols) and DKDP (open symbols).

the values of both ferroelectric and paraelectric phase in KDP and DKDP are almost in accordance.

The deformation of the PO_4 tetrahedron in the ferroelectric phase means the following: i) the O1–O1′ distance decreases by *ca.* 0.01 Å, ii) the O2–O2′ distance increases by *ca.* 0.01 Å, and iii) the P atom shifts along the z-axis relatively to the z-parameters of O atoms (getting away from O1 and approaching O2), while iv) the O1–O2 distance increases slightly. The successive change in i)–iii) is considered to be caused by the ordering of the hydrogen atom (*i.e.*, H/D approaches O1), and is well known as the Cochran mode. (Refer Fig. 3.10.) [17] The shifts of potassium and phosphorus ions (*i.e.*, atoms) along the polar axis (c-axis) mainly cause the spontaneous polarization of KDP/DKDP. On the other hand, The hydrogen atoms (*i.e.*, the protons/deuterons) in the hydrogen bond with the oxygen atoms moves almost within the ab-plane perpendicular to the polar axis of the unit cell, and the oxygen atoms show almost negligible shifts. All the displacements of atoms are strongly and inseparably relevant to each other. The deformed PO_4 tetrahedron has C_2 symmetry in the ferroelectric phase; however, the tetrahedron is S_4 in the paraelectric phase.

Next let the author mention the position of H/D. In the ferroelectric phase, the H

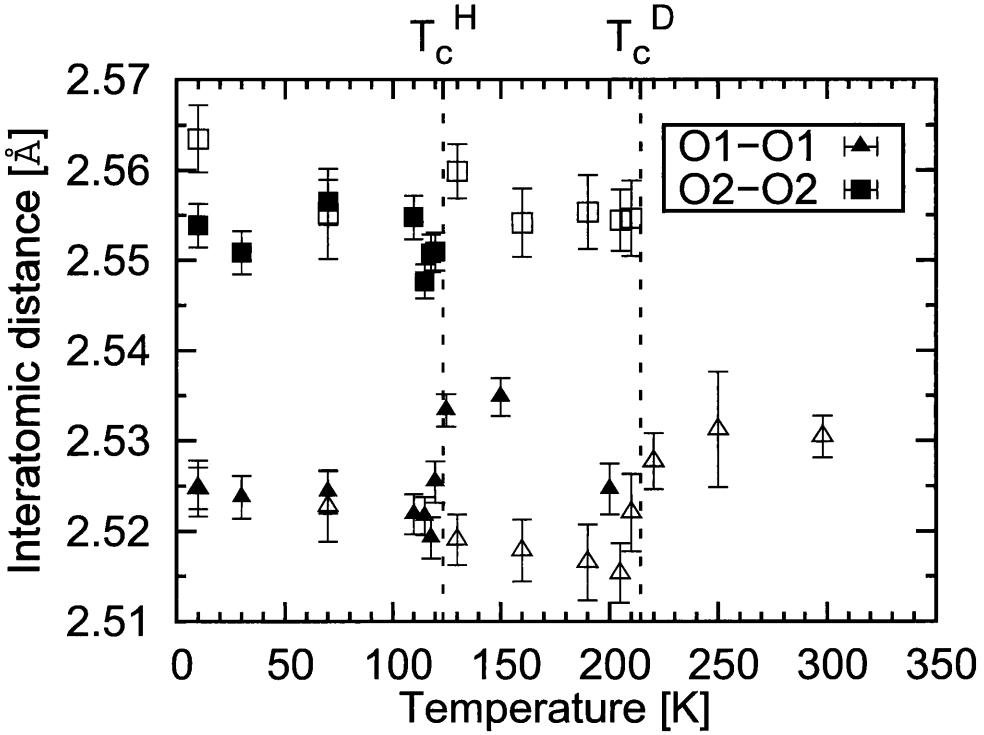

Figure 3.7 Temperature dependences of the interatomic distances, O1–O1 and O2–O2. The solid and open symbols denote the values of KDP and DKDP, respectively.

atom is at the distances r and r' from the acceptor O1 and the donor O2, respectively. Above T_c, r and r' mean the distances from one of the two disordered positions to the hydrogen-bonded oxygen position. Figure 3.11 shows the temperature dependences of the distances r (left ordinate) and r' (right ordinate). It is apparent that values of r and r' are not identical for KDP (solid symbols) and DKDP (open symbols). Although the large e.s.d. (estimated standard deviation) due to the noticeable thermal vibration of protons in KDP may not be negligible, r increases (r' decreases) with decreasing temperature; the same tendency was also reported previously. [39] Just below T_c of KDP, r and r' show gradual changes. On the other hand, the r and r' of DKDP change stepwise at T_c, and r coincides with the previously reported data indicated by the dotted line. The r of DKDP is smaller than that of KDP even in the ferroelectric phase.

Figure 3.12 shows the temperature dependences of the interatomic distances R_{O-O} (left ordinate) and δ (right ordinate) for the hydrogen bond in both KDP (solid symbols) and DKDP (open symbols). R_{O-O} and δ indicate the distances between two oxygen atoms as the donor and acceptor and between two positions at which hydrogen occupies with one-half probability in the paraelectric phase, respectively. [39, 40, 43]

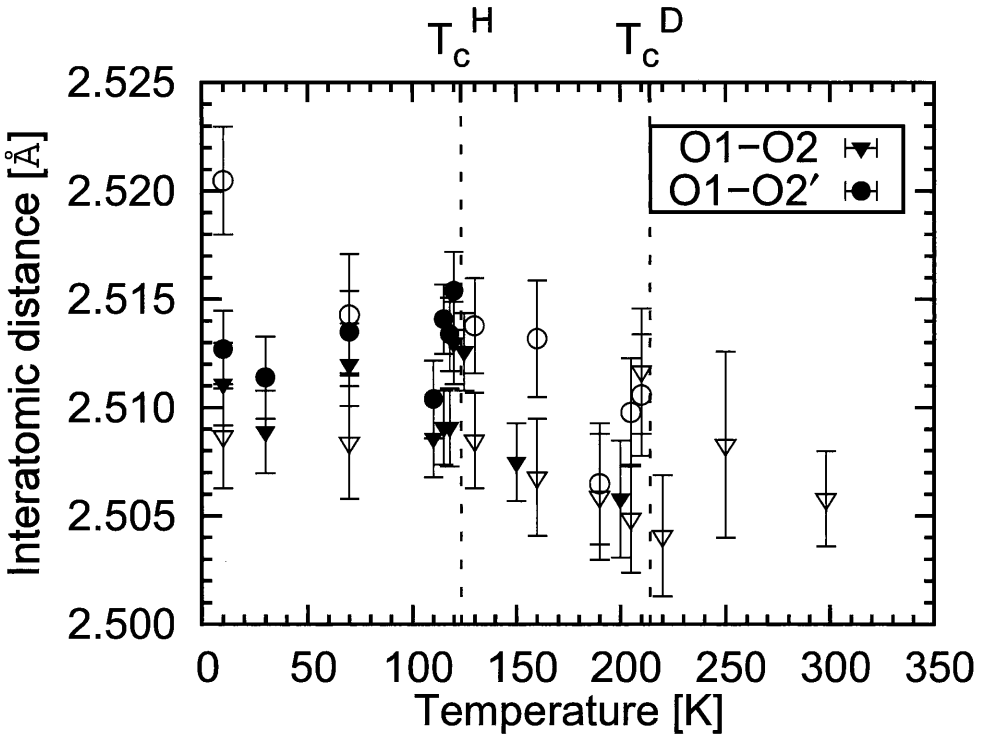

Figure 3.8 Temperature dependences of the interatomic distances, O1–O2 and O1–O2′. The solid and open symbols denote the values of KDP and DKDP, respectively.

The behaviors of R_{O-O} in the vicinities of the transition temperatures are also remarkable. For KDP, R_{O-O} in the ferroelectric phase is *ca.* 2.503 Å, and decreases as it approaches T_c. Just above T_c, R_{O-O} is *ca.* 2.483 Å , and then increases gradually with a temperature rise in the paraelectric phase. On the other hand, R_{O-O} for DKDP remains almost constant within the e.s.d.'s in each phase; a small discontinuous change can be detected at the transition point.

The disordered hydrogen in the paraelectric phase can be represented by the split-atom method, in which each atom occupies two sites with equal probability. The split parameter δ of KDP depends on temperature slightly, and it is *ca.* 0.30 Å just above T_c. On the other hand, δ = 0.45 Å of DKDP is almost temperature-independent. These values of δ are almost in agreement with those previously reported by Nelmes *et al.* [39]

Although the difference in R_{O-O} is *ca.* 0.04 Å, the difference in δ between both crystals is remarkably large, amounting to *ca.* 0.1 Å. This difference in δ between KDP and DKDP seems to arise mainly from the dissimilar behaviors of proton and deuteron in the hydrogen bond. Since R_{O-O} does not differ markedly, it can be assumed that protons and deuterons exist in approximately equivalent potentials of

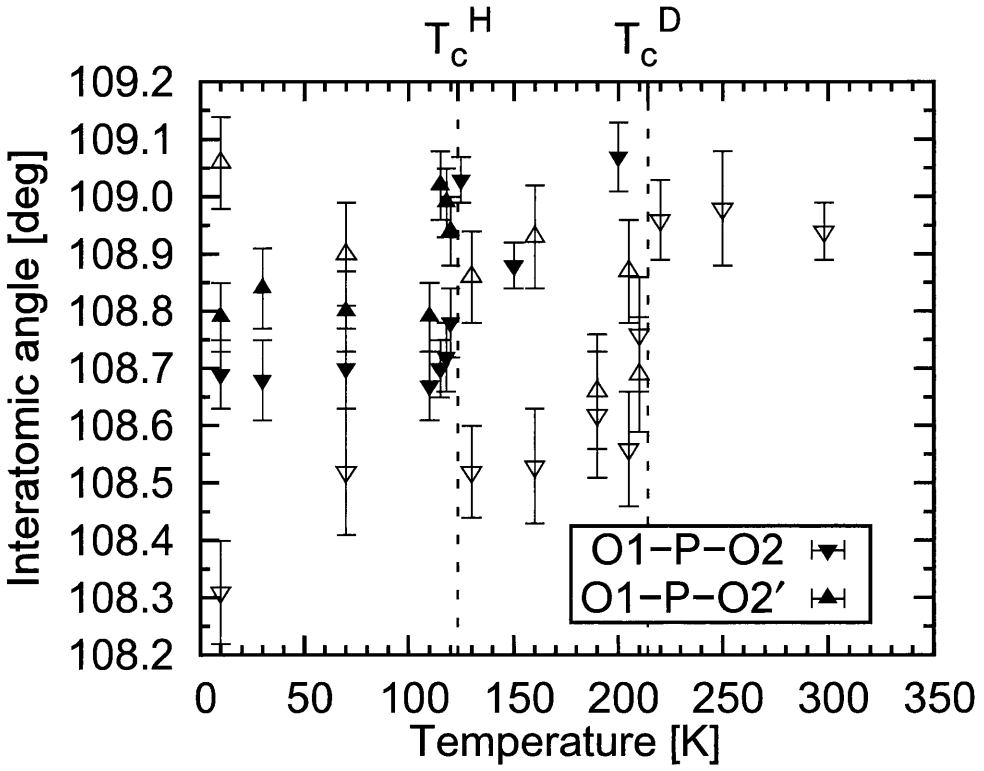

Figure 3.9 Temperature dependences of the interatomic angles, O1–P–O2 and O1–P–O2′ in both KDP and DKDP. The solid and open symbols denote the values of KDP and DKDP, respectively.

the hydrogen bonds. Since the proton is a lighter particle than the deuteron, the zero-point energy is higher and the density distribution of protons lies farther from oxygen atoms, which induces a smaller separation of δ for KDP than for DKDP.

Figs. 3.13–3.18 show temperature dependences of other interatomic distances and angles relevant to the hydrogen atom or the hydrogen-bond. If the readers are interested in them, please check them.

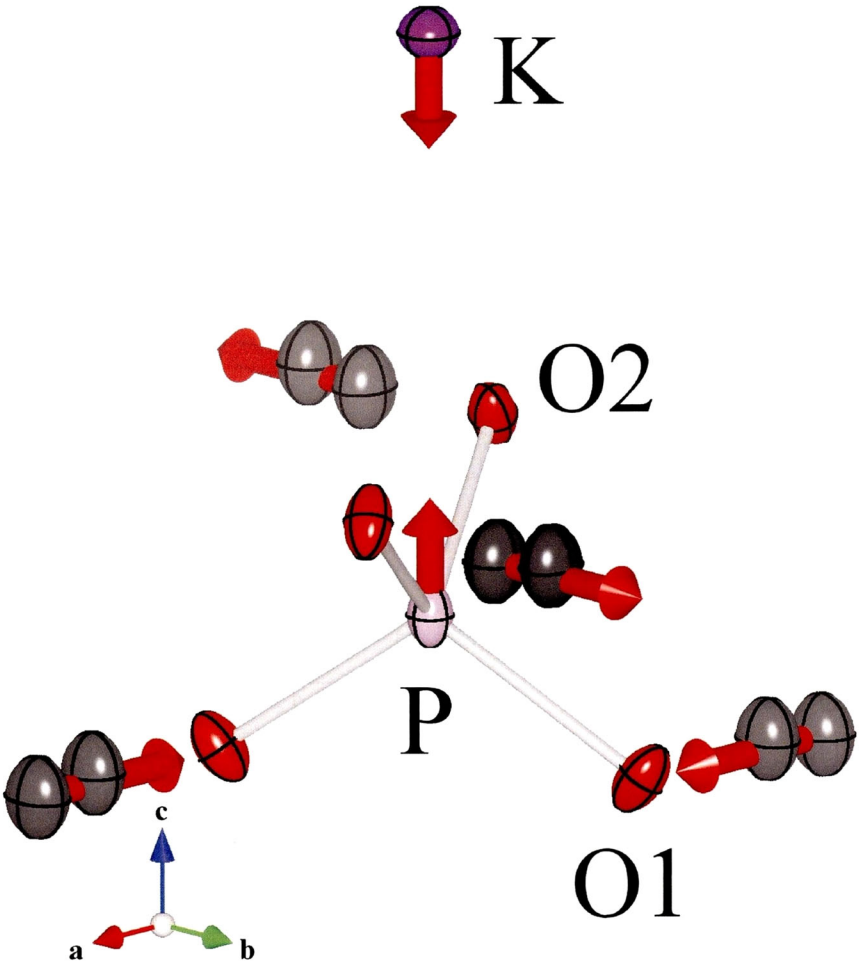

Figure 3.10 Schematic view of the Cochran mode, in which some and successive atomic displacements are involved, and indicated with the red arrows. [17]

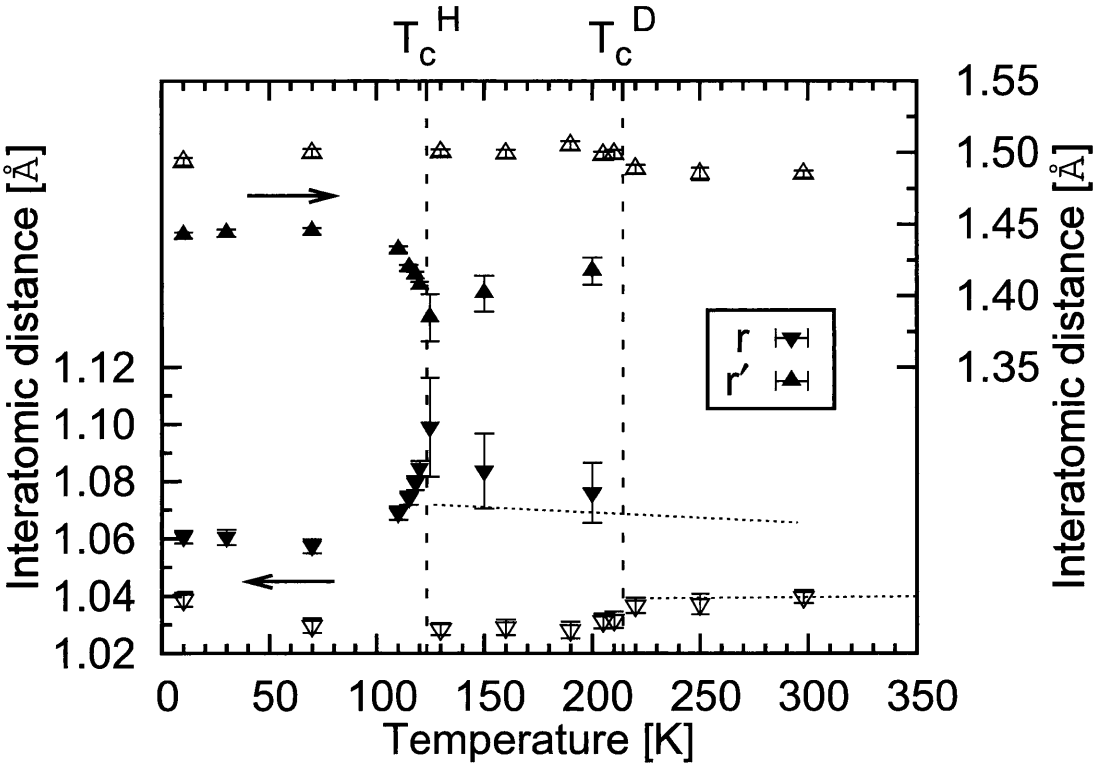

Figure 3.11 Temperature dependences of the interatomic distances r (left ordinate) and r' (right ordinate) between oxygen and hydrogen. The solid and open symbols denote the values of KDP and DKDP, respectively. Here, r and r' are defined as the distances of the O–H/D bond and the H/D$\cdots$O bond, respectively. The dotted lines indicate the reported values in the paraelectric phase. [39]

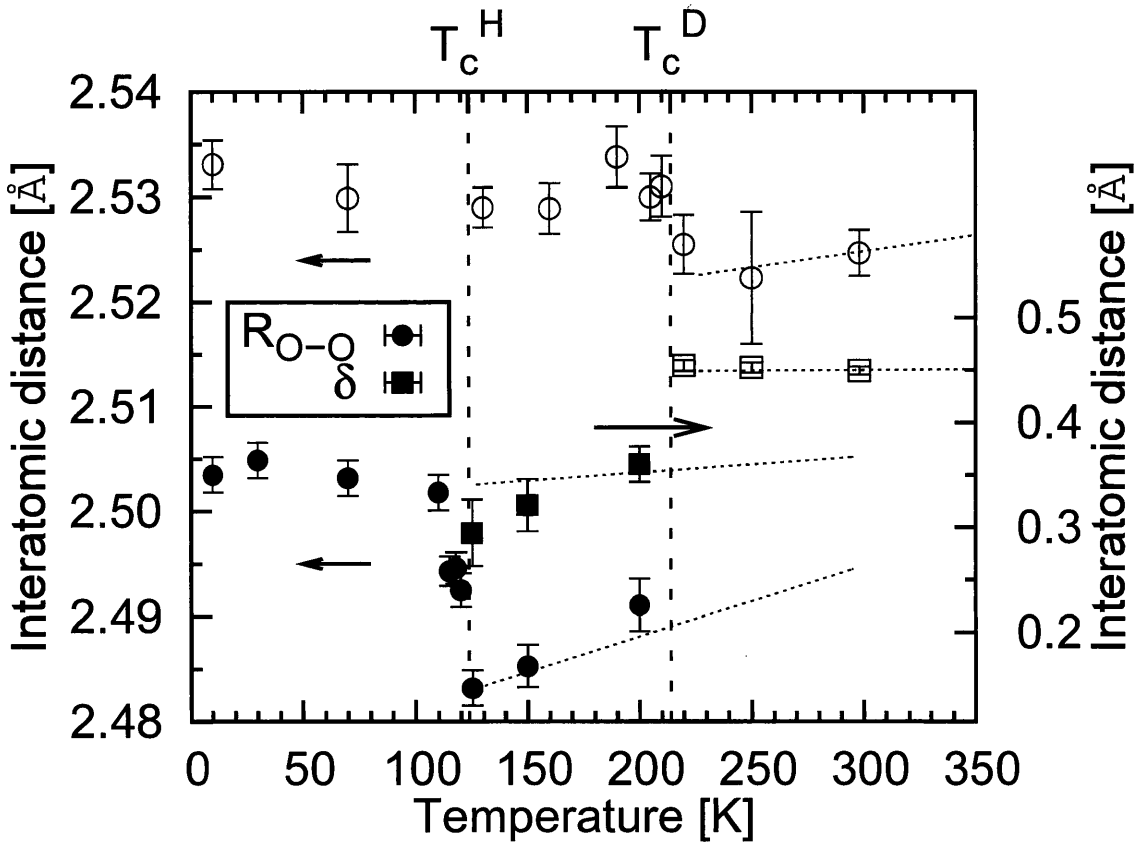

Figure 3.12 Temperature dependences of the interatomic distances R_{O-O} (left ordinate) and δ (right ordinate) for the hydrogen bond in both KDP (solid symbols) and DKDP (open symbols). The dotted lines indicate previously reported data. [39]

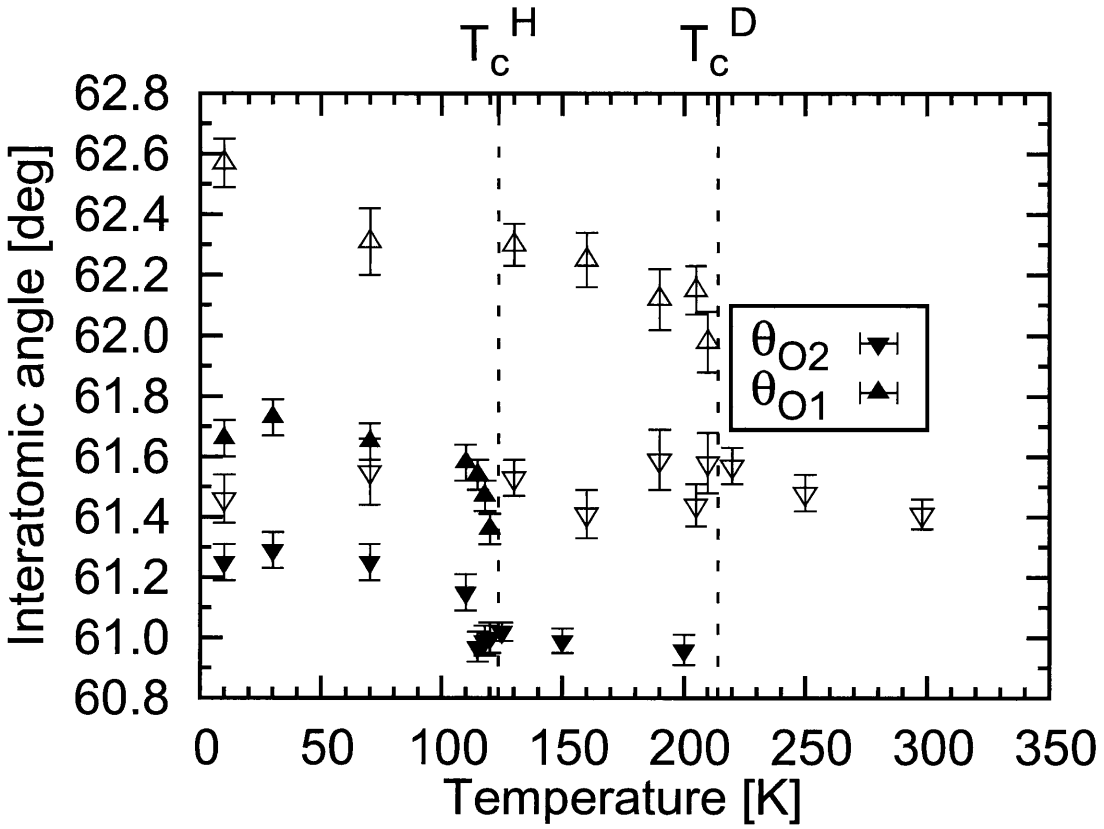

Figure 3.13 Temperature dependences of the angles θ_{O1} and θ_{O2} in both KDP and DKDP. The solid and open symbols denote the values of KDP and DKDP, respectively. θ denotes rotation angle of PO_4 anion about c-axis. (Refer Fig 1.10.) [39,40,43,82,83] θ_{O1} and θ_{O2} are crystallographically independent of each other in the ferroelectric phase, and then these two angles coincides in paraelectric phase, since the symmetry of PO_4 tetrahedron changes from C_2 in the ferroelectric into S_4 in the paraelectric phase. θ_{O1} and θ_{O2} in the ferroelectric phases are calculated from the position of the PO_4 tetrahedra on polar 2-fold axis'.. It is apparent that the value of θ in KDP is smaller than that in DKDP in paraelectric phase, which corresponds to smaller interatomic distance between two oxygen atoms as donar-acceptor of the hydrogen bond, R_{O-O}, in paraelectric phase of KDP than that of DKDP.

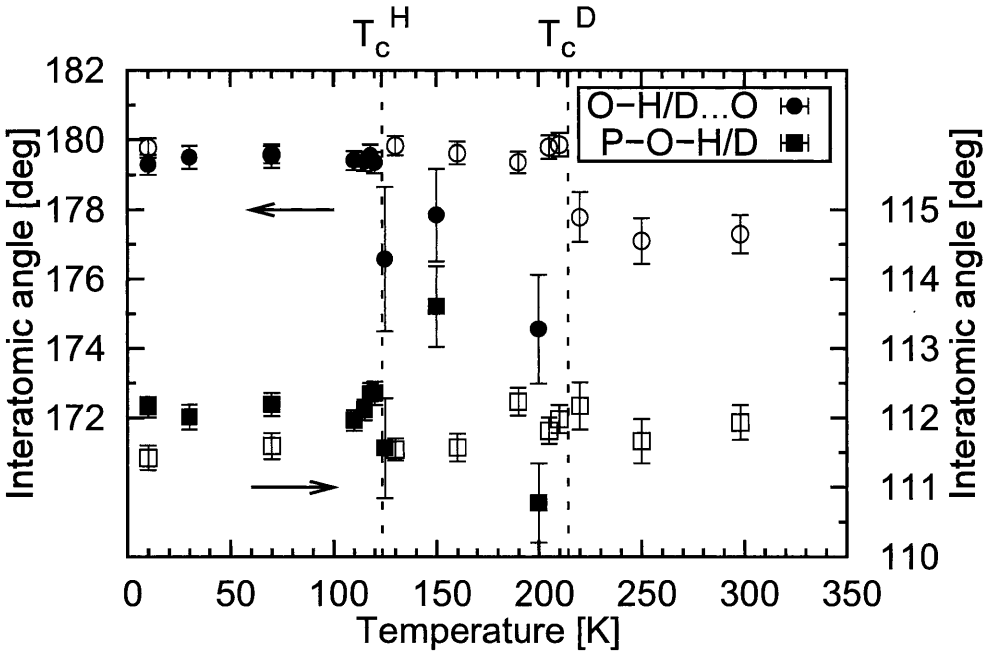

Figure 3.14 Temperature dependences of the interatomic angles, O–H/D···O (left ordinate) and P–O–H/D (right ordinate) in both KDP and DKDP. The solid and open symbols denote the values of KDP and DKDP, respectively. No remarkable difference about both interatomic angles can be recognized in KDP and DKDP. Interatomic angles about O–H/D···O and P–O–H/D are of *ca.* 179° and 112° in both phases. The hydrogen bond between two oxygen atoms of PO_4 anions in KDP and DKDP is approximately linear.

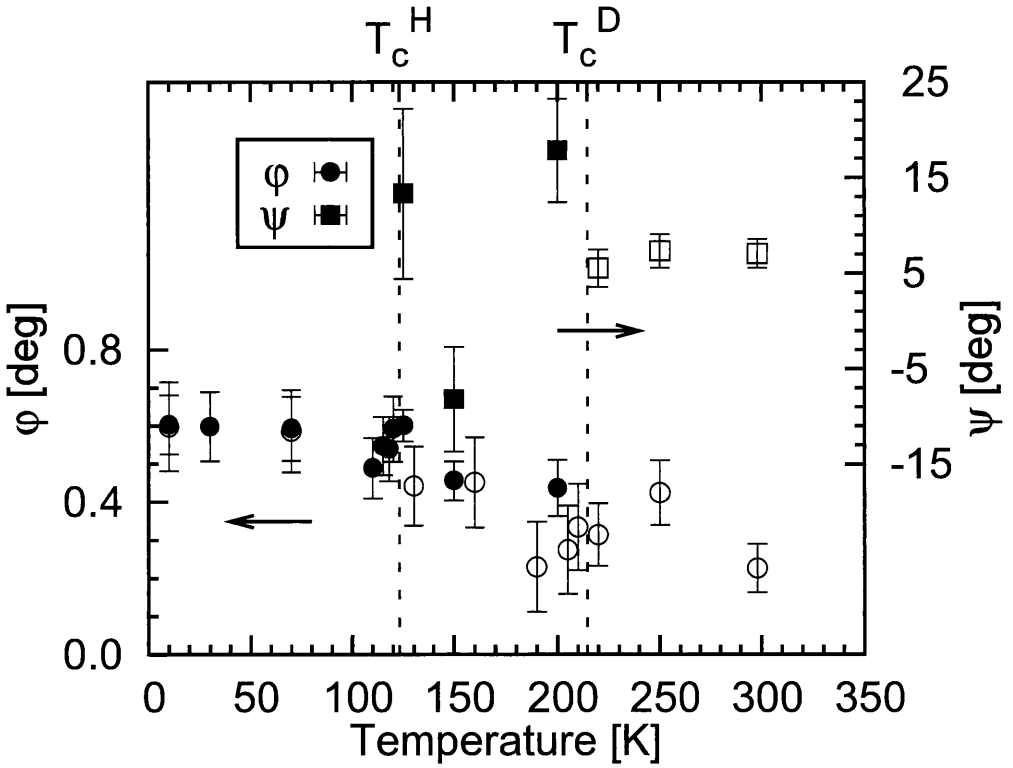

Figure 3.15 Temperature dependences of the angles φ (left ordinate) and ψ (right ordinate), the angles related with hydrogen-bond in both KDP and DKDP. The solid and open symbols denote the values of KDP and DKDP, respectively. The angles φ and ψ mean the arguments of lines formed by two oxygen atoms as donar-acceptor in the hydrogen bond and two splitting hydrogen/deuterium atoms with a half occupancy from ab plane, respectively. (Refer Appendix A.1.) [39,40,43,82,83] ψ cannot be calculated in ferroelectric phase for disappearance of two-fold symmetry as like about $(x, 1/4, 1/8)$. φ and ψ are of *ca.* 0.4° and 5°, respectively. No remarkable variation and difference of φ and ψ can be recognized in KDP and DKDP with temperature variation. Especially, negligible temperature dependence of φ indicates that atomic shift along ferroelectric c-axis between two oxygen atoms as donar-acceptor of the hydrogen bond is negligible in both ferroelectric and paraelectric phases.

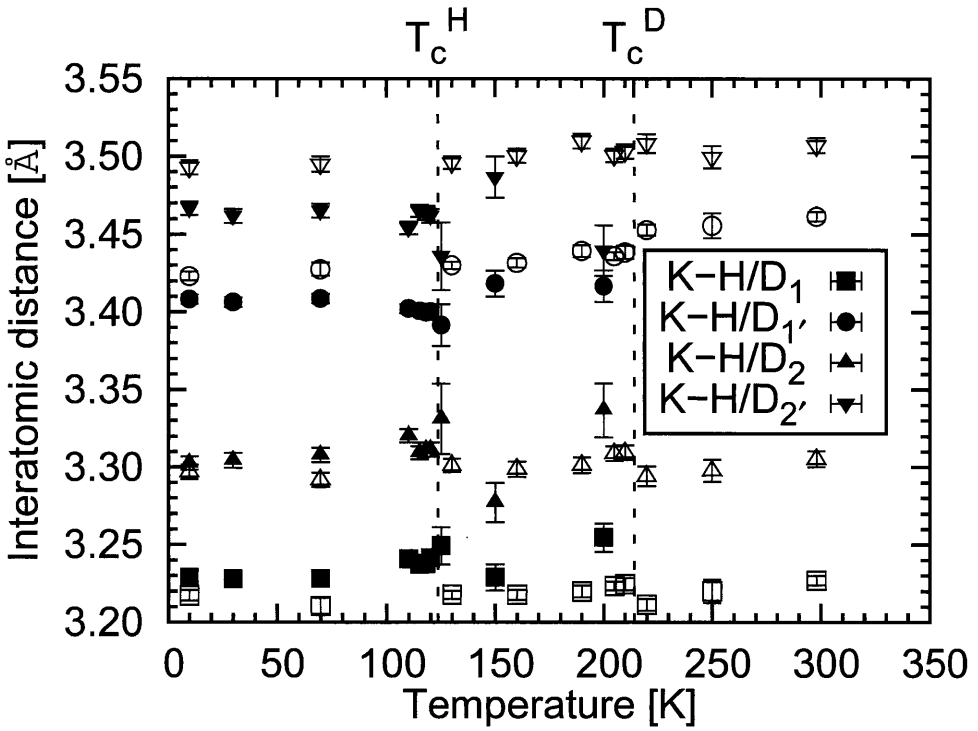

Figure 3.16 Temperature dependences of the interatomic distances, K–H/D_1, K–H/$D_{1'}$, K–H/D_2, and K–H/$D_{2'}$. The solid and open symbols denote the values of KDP and DKDP, respectively. These four interatomic distances in ferroelectric phase remain as four interatomic distances even in paraelectric phase, because they are crystallographically independent of each other. Strictly, K–H/D_1, K–H/$D_{1'}$, K–H/D_2, and K–H/$D_{2'}$ indicate K–H/D^i, K–H/D^d, K–H/D^e, and K–H/D in the ferroelectric phase of KDP and DKDP, respectively; the superscript i denotes symmetry coordinate, $x - 1/2, y, z + 1/2$.

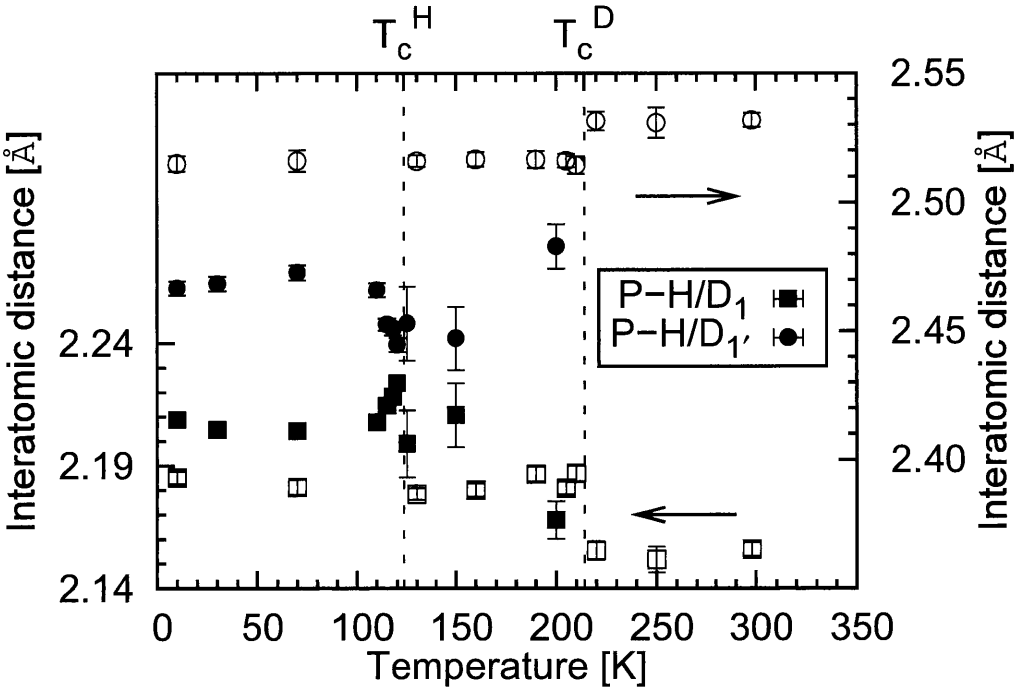

Figure 3.17 Temperature dependences of the interatomic distances, P–H/D_1 (left ordinate) and P–H/$D_{1'}$ (right ordinate) in both KDP and DKDP. The solid and open symbols denote the values of KDP and DKDP, respectively. Strictly, P–H/D_1 and P–H/$D_{1'}$ in the legend indicate P–H/D^d and P–H/D in the ferroelectric phase of KDP and DKDP, respectively. In addition to recognition of Curie point increase up to *ca.* 100 K between KDP and DKDP, the differences between KDP and DKDP in these two interatomic distances are small.

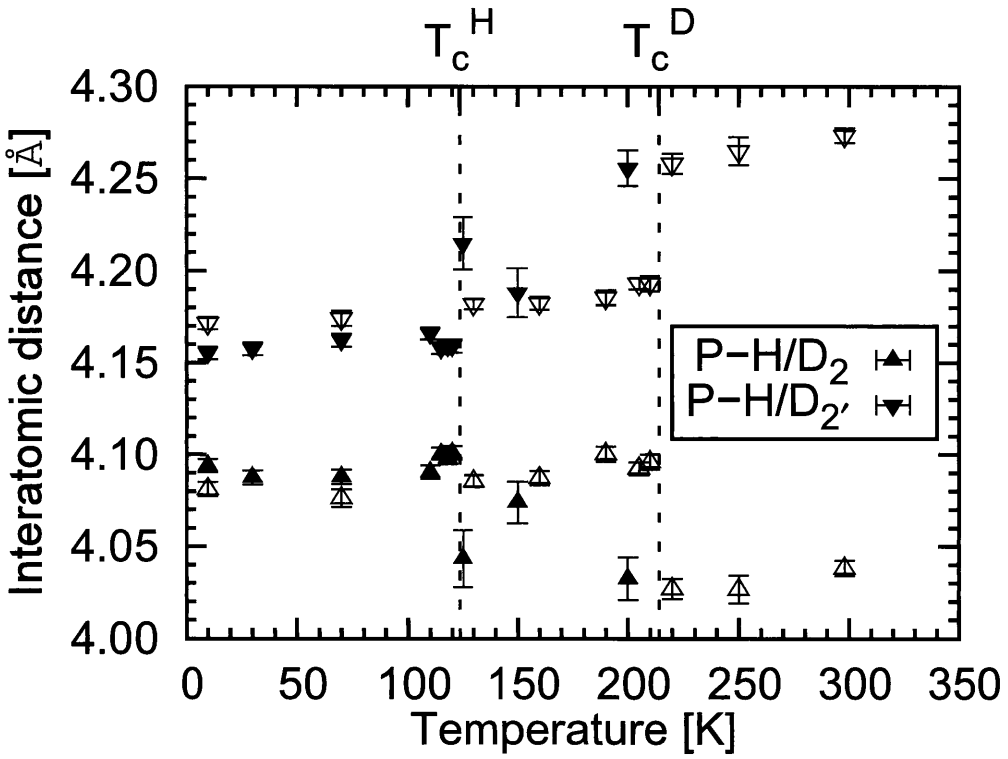

Figure 3.18 Temperature dependences of the interatomic distances, P–H/D_2 and P–H/$D_{2'}$ in both KDP (solid symbols) and DKDP (open symbols). Strictly, P–H/D_2 and P–H/$D_{2'}$ in the legend indicate P–H/D^j and P–H/D^d in the ferroelectric phase of KDP and DKDP, respectively; the superscripts j denotes symmetry operation, $x-1/2, y, z-1/2$. In addition to recognition of Curie point increase up to *ca.* 100 K between KDP and DKDP, the differences between KDP and DKDP in these two interatomic distances are small.

3.3 Positional shifts and spontaneous polarization along c-axis

The potassium and phosphorus atoms displace in the opposite direction along the polar c-axis after structural phase transition into the ferroelectric phase. Figure 3.19 shows the temperature dependences of the atomic shifts along the polar c-axis in both KDP (solid symbols) and DKDP (open symbols). The positional shifts of all the atoms in the unit cell are directly calculated as relative displacements in the center-of-gravity coordinate system.

The center of gravity of the unit cell in the ferroelectric phase coincides with that of the paraelectric phase. (Refer Appendix A.2.) To keep the center of gravity of the unit cell, the atomic displacement of the phosphorus atom is made larger than that of the potassium atom because of the difference in the atomic mass. The displacements of the potassium and phosphorus atoms are *ca.* −0.05 and +0.065 Å, respectively. In

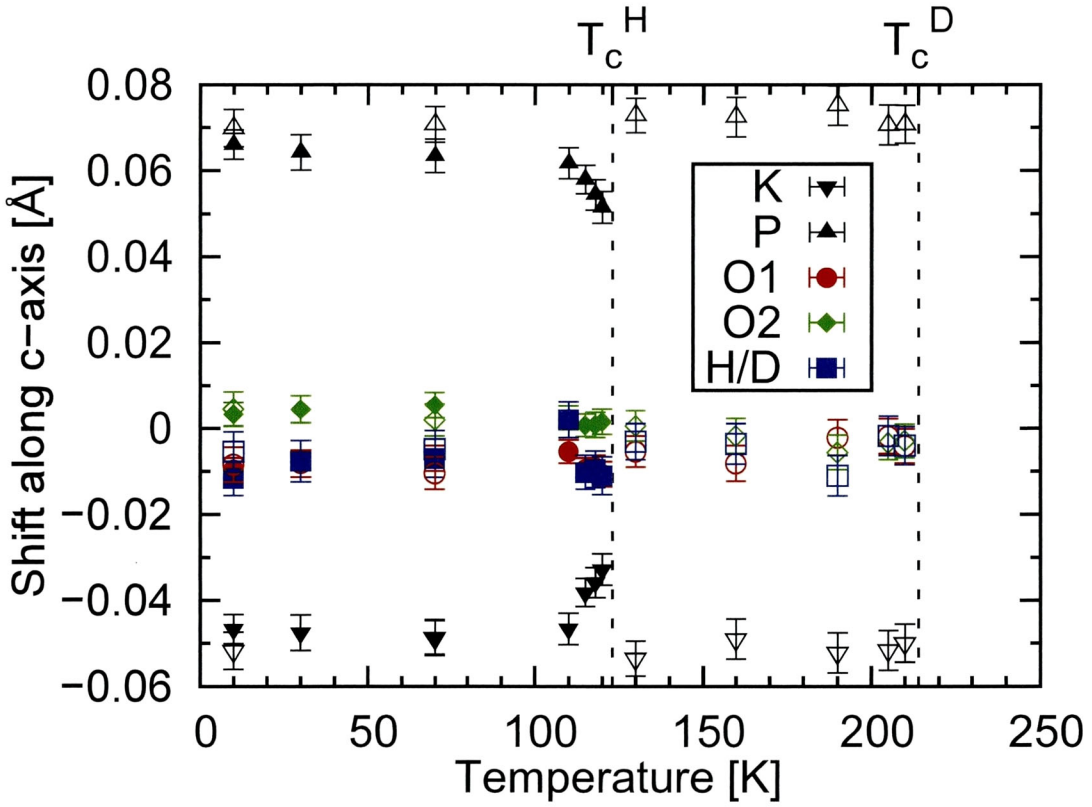

Figure 3.19 Temperature dependences of the atomic shifts along the polar c-axis in the ferroelectric phases of both KDP (solid symbols) and DKDP (open symbols). The positional shifts are calculated as relative displacements in the center-of-gravity coordinate system.

KDP, these two atoms shift gradually with decreasing temperature, which is different from that observed in DKDP, where the atomic positions are almost constant in the whole ferroelectric phase. The displacements of the potassium and phosphorus atoms in DKDP are larger than those in KDP. On the other hand, the displacements along the c-axis of the oxygen and hydrogen/deuterium atoms are overwhelmingly smaller than those of the potassium and phosphorus atoms.

From the atomic shifts along the c-axis, we can estimate the polarization. Let us adopt the point-charge method, and assign $+e$, $+5e$, $-2e$, and $+e$ as charges of the potassium, phosphorus, oxygen, and hydrogen/deuterium atoms, respectively. (Refer Appendix A.3.) The contribution of each atom is calculated using the displacement given in Fig. 3.19. The temperature dependences of the calculated components of P_s are shown in Fig. 3.20 for KDP (solid symbols) and DKDP (open symbols). The contribution of the distortion of the O_4 frame of the PO_4 tetrahedron is not so large. The dominant contributions are the displacements of the phosphorus and potassium atoms along the c-axis. If the phosphorus atom shifts in the positive direction, then

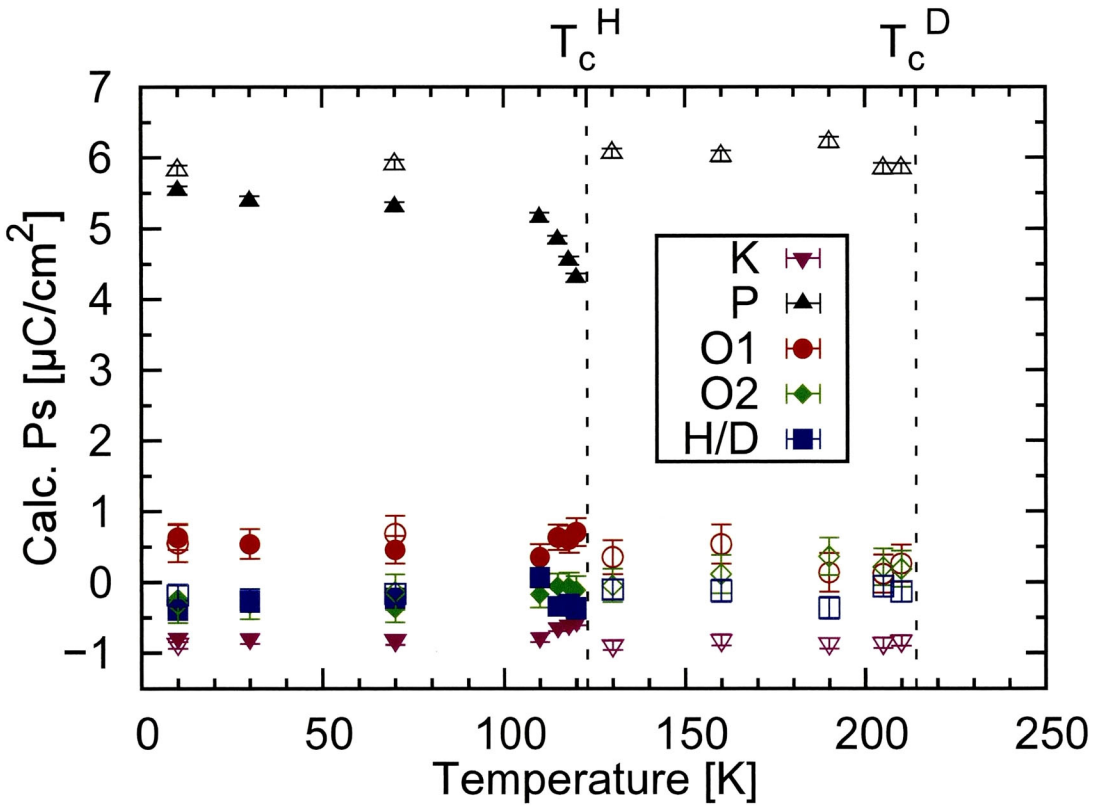

Figure 3.20 Temperature dependences of the calculated atomic contributions to polarization along the polar c-axis in the ferroelectric phases of both KDP (solid symbols) and DKDP (open symbols) by the point-charge method. $+e$, $+5e$, $-2e$, and $+e$ are assigned as charges of the K, P, O, and H/D atoms, respectively.

the potassium atom shifts in the negative direction. The contribution of the phosphorus atom is overwhelmingly larger than that of the potassium atom because the charge of the phosphorus atom is five times larger than that of the potassium atom. Consequently, positive spontaneous polarization appears along the c-axis.

The calculated polarizations are compared with the experimental values of KDP and DKDP (deuterium replacement ratio of 98 %) reported by Samara, [84] in Fig. 3.21. At around T_c, the calculated values are in agreement with the reported ones, which indicates that the point-charge method is well applicable to the study of both KDP and DKDP. In particular, the calculated values in the vicinity of the paraelectric-ferroelectric phase transition in KDP show a gradual change, which is in good agreement with the experimental result. The experimental values reported by Samara and the values calculated by the author indicate that the spontaneous polarization of DKDP is *ca.* 1.2 times larger than that of KDP. This is mainly due to the displace-

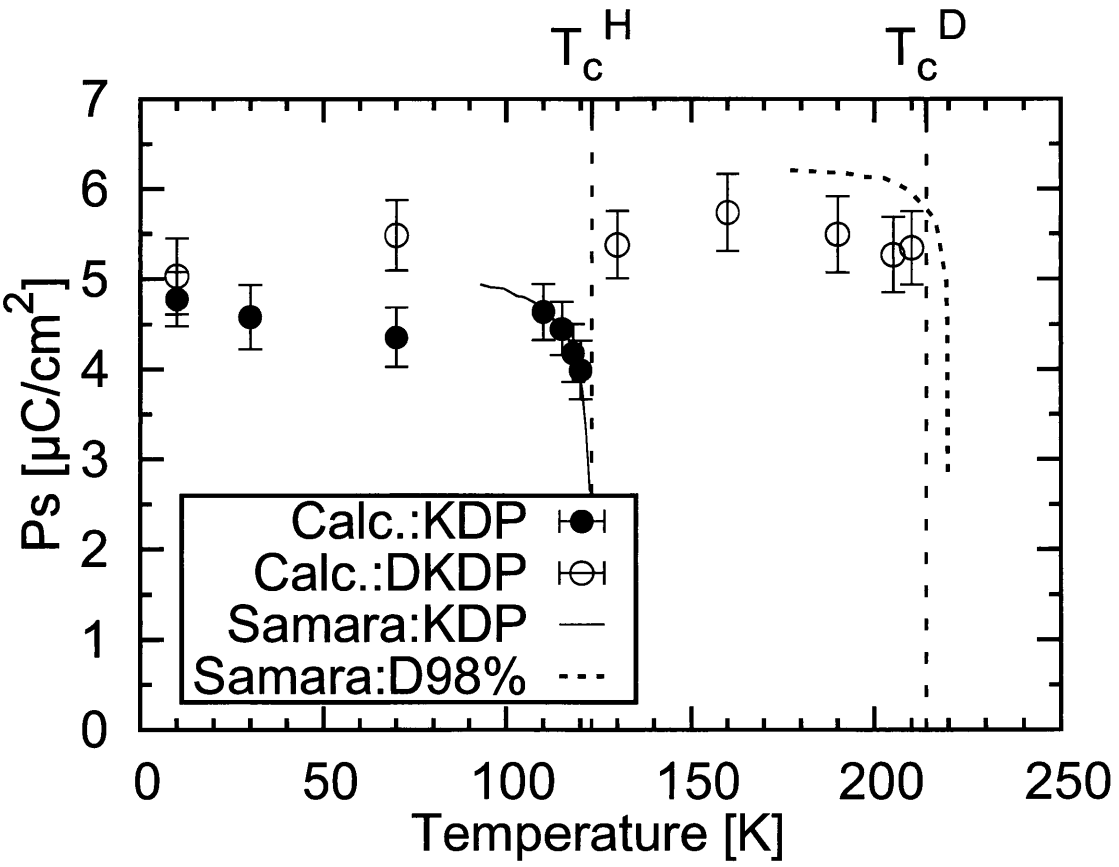

Figure 3.21 Temperature dependences of the calculated spontaneous polarization, P_s, along the polar c-axis in the ferroelectric phases of both KDP (solid symbols) and DKDP (open symbols) by the point-charge method. The solid and broken lines show the experimental values of KDP and DKDP (deuterium replacement ratio of 98 %), respectively, reported by Samara [84].

ment of the phosphorus atom, which is discussed in chapter 4.

Here, the author notes the effect of the applied DC bias field. By referring to the X-ray dilatometric study under a DC bias field, [85] the field strength in present study is considered to shift T_c slightly, and to be insufficient to induce a qualitative change in the phase transition.

3.4 Atomic displacement parameter U_{jk}

The temperature dependences of U_{33}'s for KDP are shown in Fig. 3.22. It is apparent that the U_{33} of the hydrogen atom is larger than those of the other atoms because of the low mass of hydrogen. On the other hand, the potassium, phosphorus, and oxygen atoms show much smaller U_{33}'s than the hydrogen atom. Although some

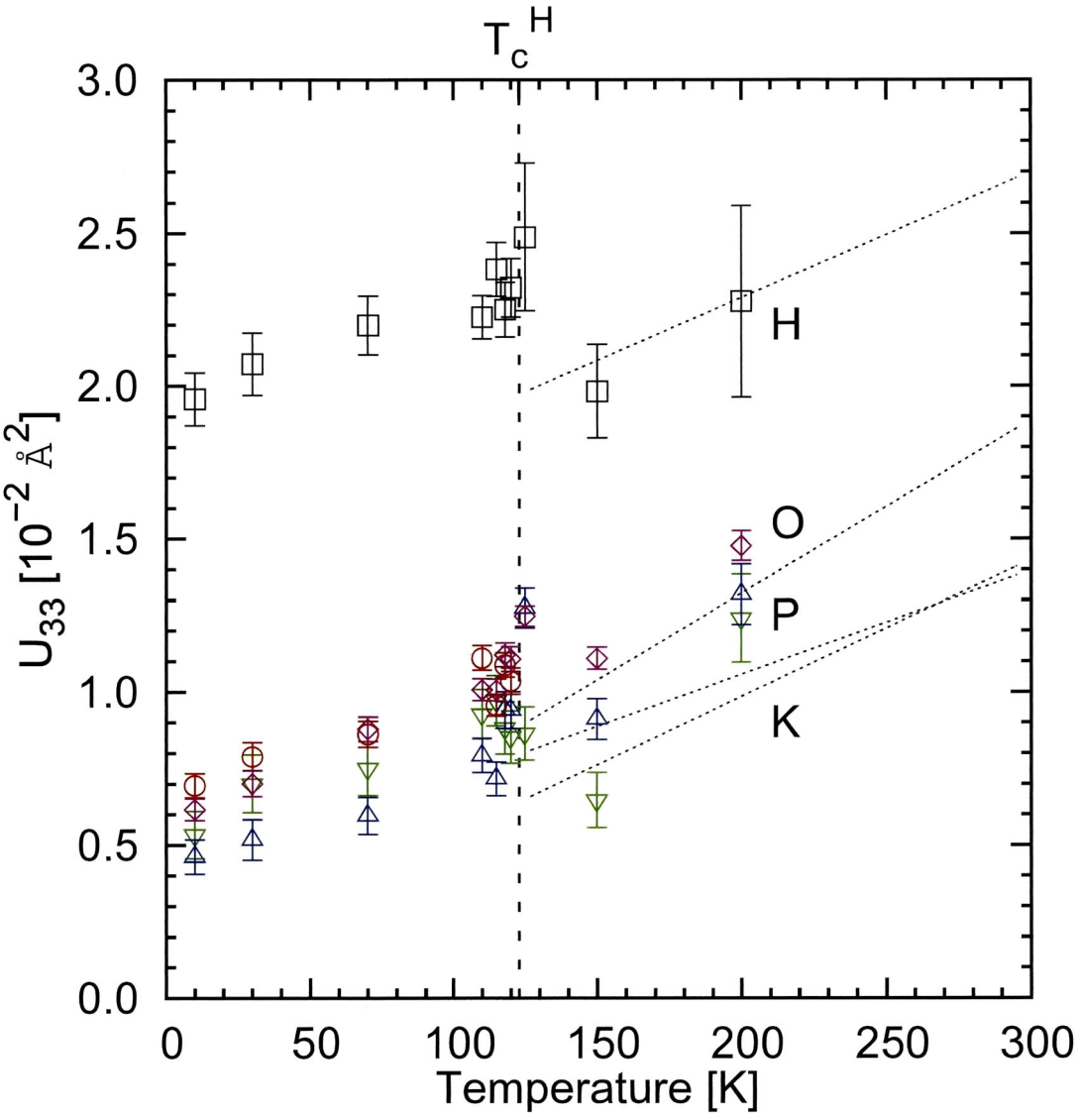

Figure 3.22 Temperature dependences of the atomic displacement parameters, U_{33}'s, of KDP. The symbols ▽, △, ○, ◇, and □ denote the values of the K, P, O1, O2, and H atoms, respectively. The O1 atom becomes equivalent to the O2 atom in the paraelectric phase. The dotted lines denote the interpolated temperature dependences from the values at 295 and 127 K reported by Nelmes *et al.* [39] The error bars indicate e.s.d.'s.

scattering of data may be observed in the paraelectric phase, the temperature dependences are essentially in agreement with the previous report by Nelmes *et al.* [39] It should be noted that the U_{33}'s of heavy atoms show no noticeable changes through the paraelectric-ferroelectric phase transition. These values decrease monotonically with decreasing temperature.

Figure 3.23 shows the temperature dependences of the anisotropic atomic displacement parameters, U_{33}'s, of all the atoms in both the ferroelectric and paraelectric

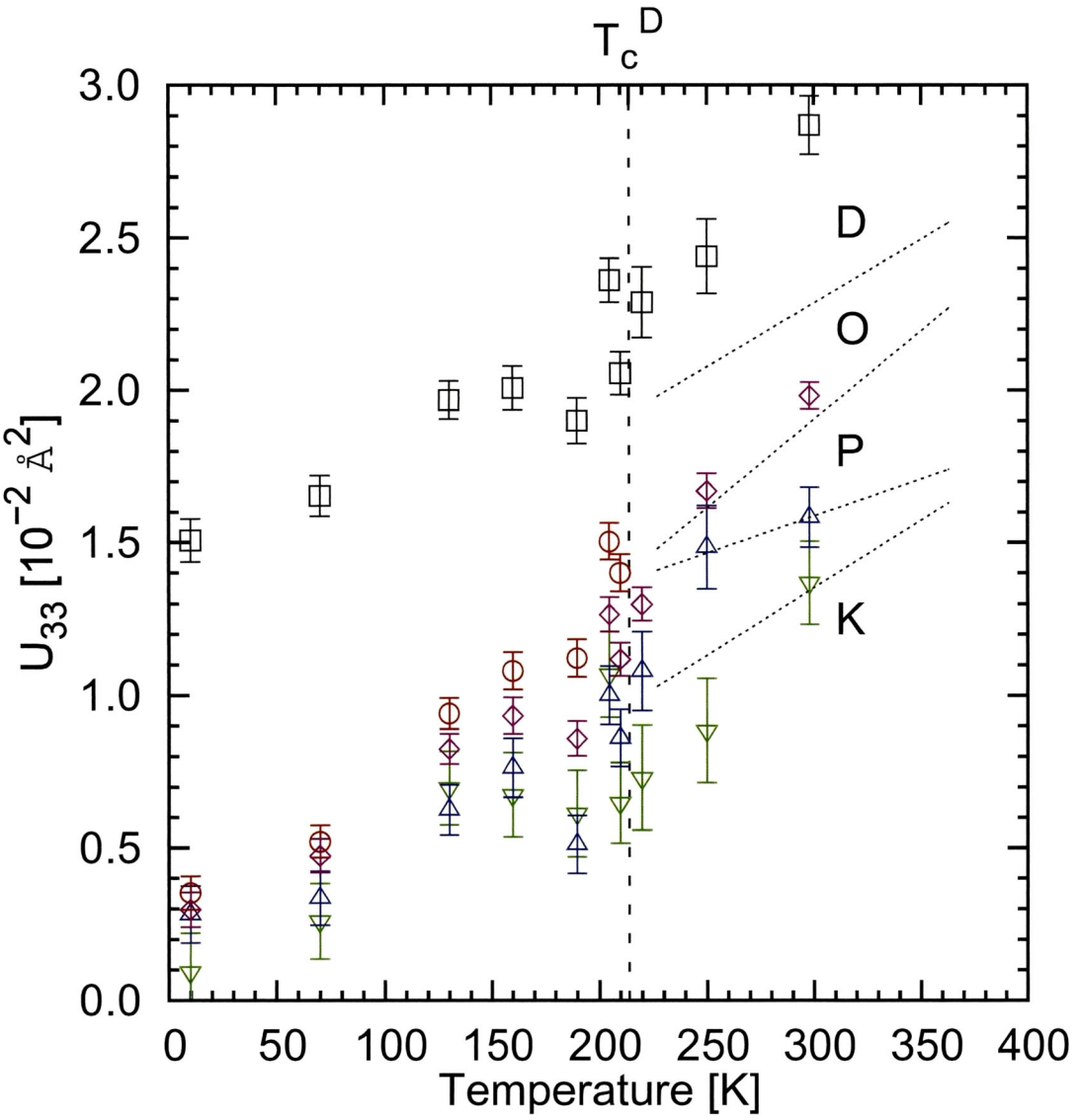

Figure 3.23 Temperature dependences of the anisotropic atomic displacement parameters U_{33}'s of all the atoms in both the ferroelectric and paraelectric phases of DKDP. The symbols ▽, △, ○, ◇, and □ denote the values of the K, P, O1, O2, and D atoms, respectively. The O1 atom becomes crystallographically equivalent to the O2 atom in the paraelectric phase. The dotted lines denote the interpolated data at 363 and 227 K reported by Nelmes *et al.* [39].

phases of DKDP. In the paraelectric phase, the temperature dependences are in good agreement with those shown by dotted lines [39]. Similarly to that observed in KDP, the potassium, phosphorus, and oxygen atoms show much smaller U_{33}'s than the deuterium atom. It should be noted that the U_{33}'s of all the atoms show no noticeable changes throughout the paraelectric-ferroelectric phase transition. Only the U_{33} of the phosphorus atom may change rapidly at T_c, although the data scattering prevents the author from drawing a decisive conclusion.

Here, the author mentions the temperature dependences of U_{11} and U_{22} shown in Figs. 3.24–3.27. In the paraelectric phase, U_{11} and U_{22} decrease monotonically with decreasing temperature. As for the relative magnitude, $U_{11}^{\mathrm{P}} < U_{11,22}^{\mathrm{O}} < U_{11}^{\mathrm{K}} < U_{11,22}^{\mathrm{H/D}}$, where the superscripts indicate the atoms. Since $U_{33}^{\mathrm{K}} < U_{33}^{\mathrm{P}} < U_{33}^{\mathrm{O}} < U_{33}^{\mathrm{H/D}}$, as shown in Figs. 3.22 and 3.23, the nuclear distribution of K is planular within the xy-plane, while that of P is elongated along the z-axis. The ratios of $\sqrt{U_{11}/U_{33}}$ at T_c are *ca.* 1.2, 0.73, and 0.78 for K, P, and O, respectively. These values are almost in agreement with the previous reports. [39, 43] Within the ferroelectric phase, the temperature variations of U_{11} and U_{22} are small and the values are almost continuous to the paraelectric ones.

For reference, the author presents the temperature dependences of U_{eq} shown in Figs. 3.28–3.29. We may confirm the relation, $U_{\mathrm{eq}}^{\mathrm{P}} < U_{\mathrm{eq}}^{\mathrm{O}} < U_{\mathrm{eq}}^{\mathrm{K}} < U_{\mathrm{eq}}^{\mathrm{H/D}}$.

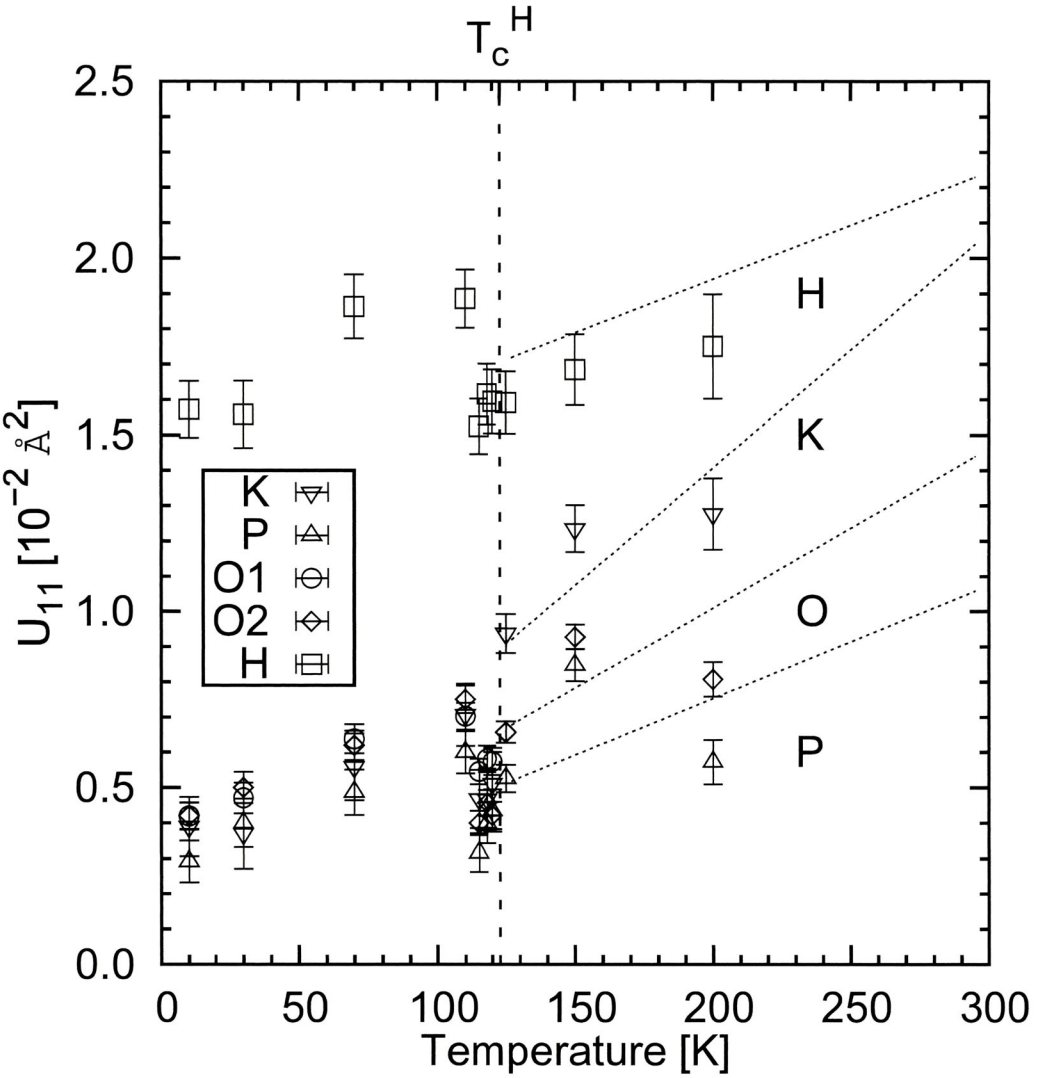

Figure 3.24 Temperature dependences of the anisotropic atomic displacement parameters, U_{11}'s, of all the atoms in both the ferroelectric and paraelectric phases of KDP. (Refer Appendix A.4.) The symbols, $\bigtriangledown$, $\bigtriangleup$, $\bigcirc$, $\diamond$, and $\square$ denote the values of K, P, O1, O2, and H atoms, respectively. In the ferroelectric phase, the $\langle 1\bar{1}0 \rangle$ direction of the unit cell is parallel to the tetragonal a-axis. The O1 atom become crystallographically equivalent with O2 atom in the paraelectric phase. The open symbols denote the values in this study, and the dotted lines denote the interpolated temperature dependences from the values at 295 and 127 K reported by Nelmes *et al.* [39]. It should be noted that U_{11} of hydrogen atom is one part of the split hydrogen atom.

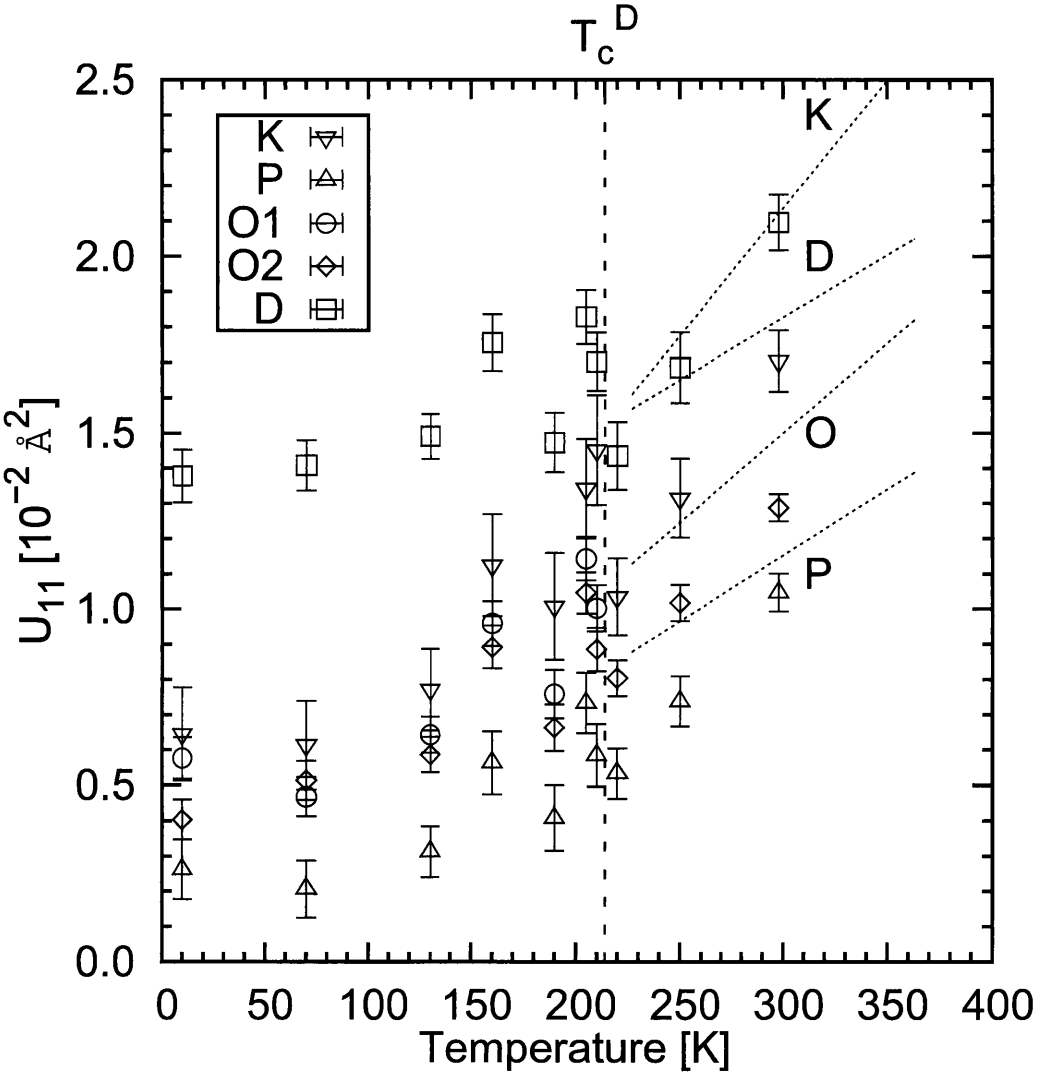

Figure 3.25 Temperature dependences of the anisotropic atomic displacement parameters, U_{11}'s, of all the atoms in both the ferroelectric and paraelectric phases of DKDP. (Refer Appendix A.4.) The symbols, ▽, △, ○, ◇, and □ denote the values of K, P, O1, O2, and D atoms, respectively. The O1 atom become crystallographically equivalent with O2 atom in the paraelectric phase. The open symbols denote the values in this study, and the dotted lines denote the interpolated data at 363 and 227 K reported by Nelmes *et al.* [39].

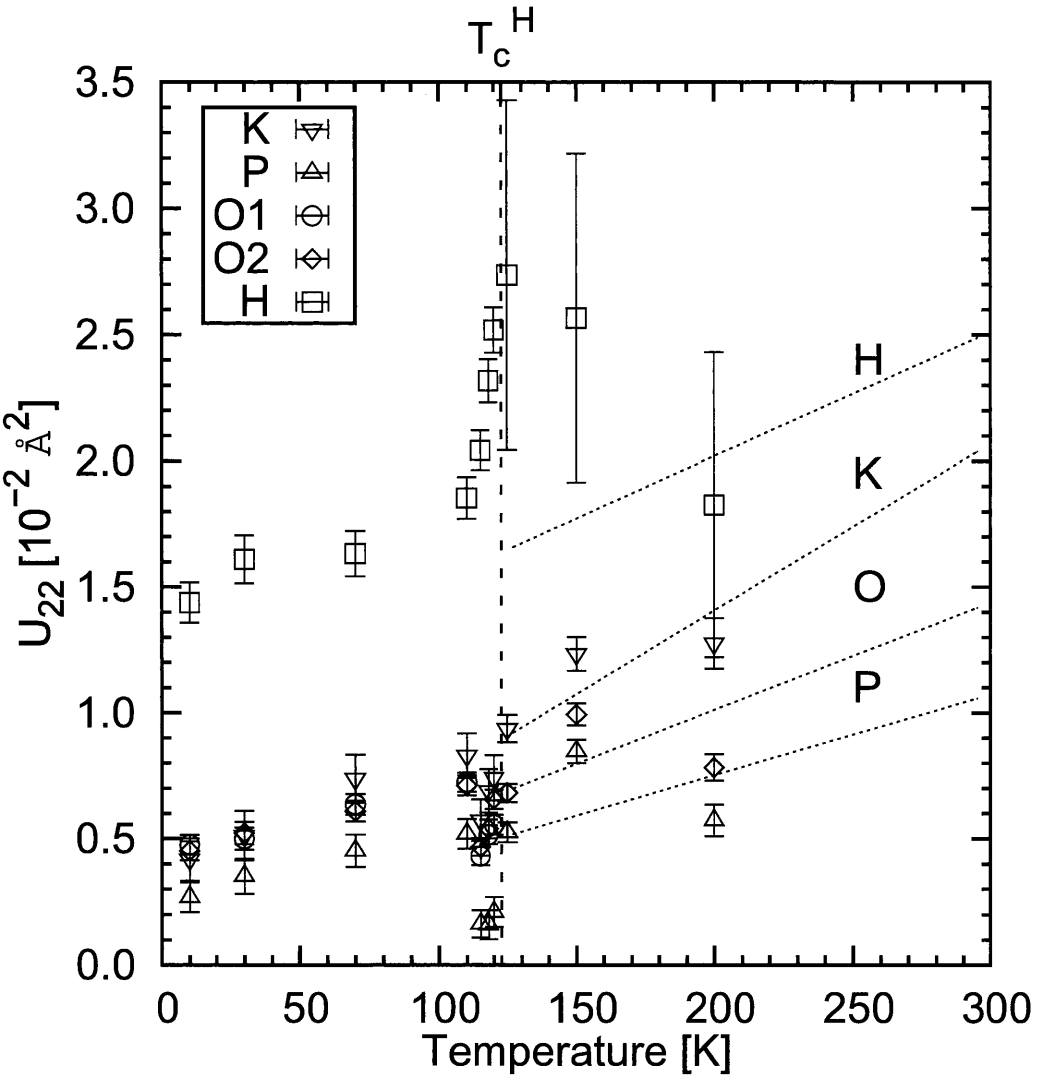

Figure 3.26 Temperature dependences of the anisotropic atomic displacement parameters, U_{22}'s, of all the atoms in both the ferroelectric and paraelectric phases of KDP. (Refer Appendix A.4.) The symbols, ▽, △, ○, ◇, and □ denote the values of K, P, O1, O2, and H atoms, respectively. The O1 atom become crystallographically equivalent with O2 atom in the paraelectric phase. The open symbols denote the values in this study, and the dotted lines denote the interpolated temperature dependences from the values at 295 and 127 K reported by Nelmes *et al.* [39]. The values in the ferroelectric phase are presented as converted values onto the paraelectric tetragonal lattice approximately; the ferroelectric orthorhombic lattice rotates *ca.* 45° to the paraelectric tetragonal one about those *c*-axes. The prominent e.s.d.'s (estimated standard deviations) of hydrogen atom in the paraelectric phase of KDP must be noticed.

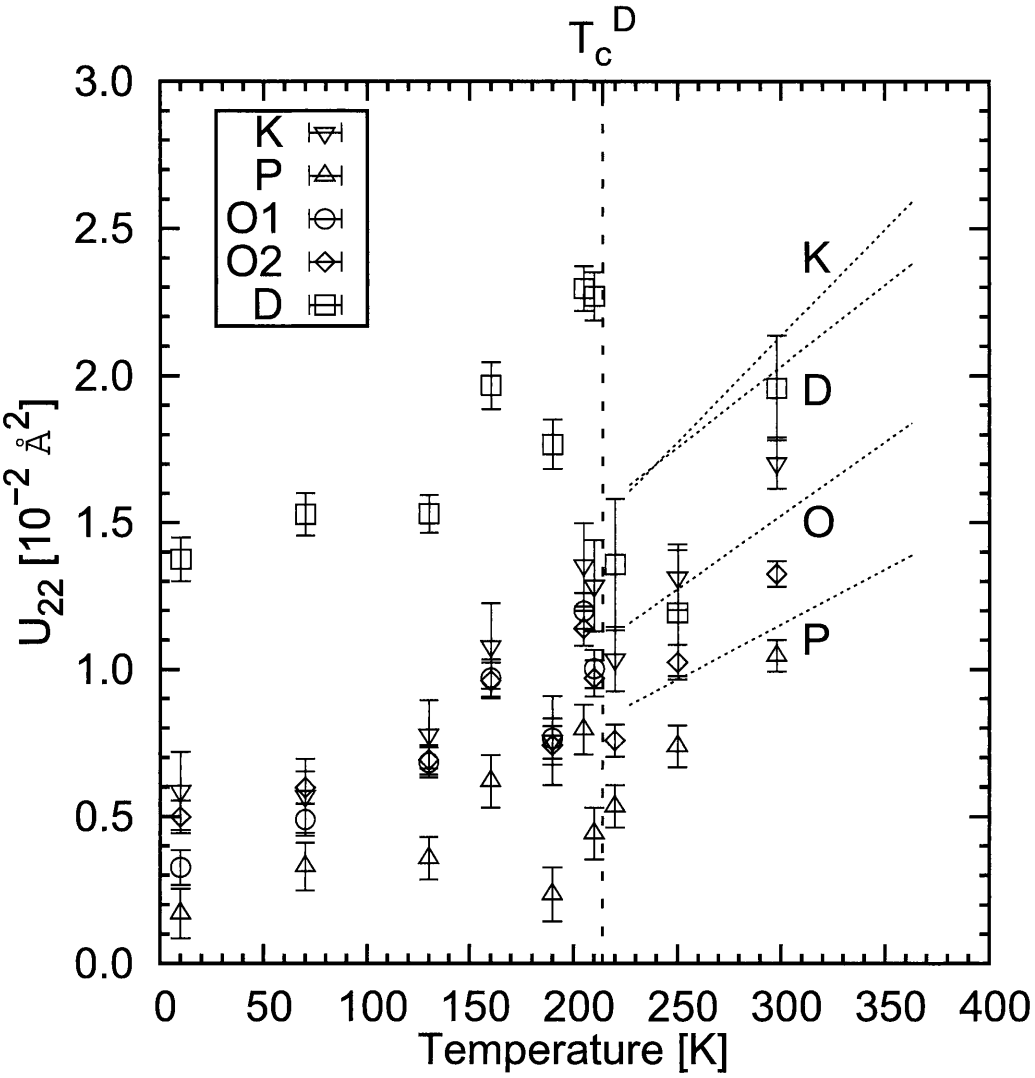

Figure 3.27 Temperature dependences of the anisotropic atomic displacement parameters, U_{22}'s, of all the atoms in both the ferroelectric and paraelectric phases of DKDP. (Refer Appendix A.4.) The symbols, $\triangledown$, $\triangle$, $\bigcirc$, $\diamond$, and $\square$ denote the values of K, P, O1, O2, and D atoms, respectively. The O1 atom become crystallographically equivalent with O2 atom in the paraelectric phase. The open symbols denote the values in this study, and the dotted lines denote the interpolated data at 363 and 227 K reported by Nelmes *et al.* [39].

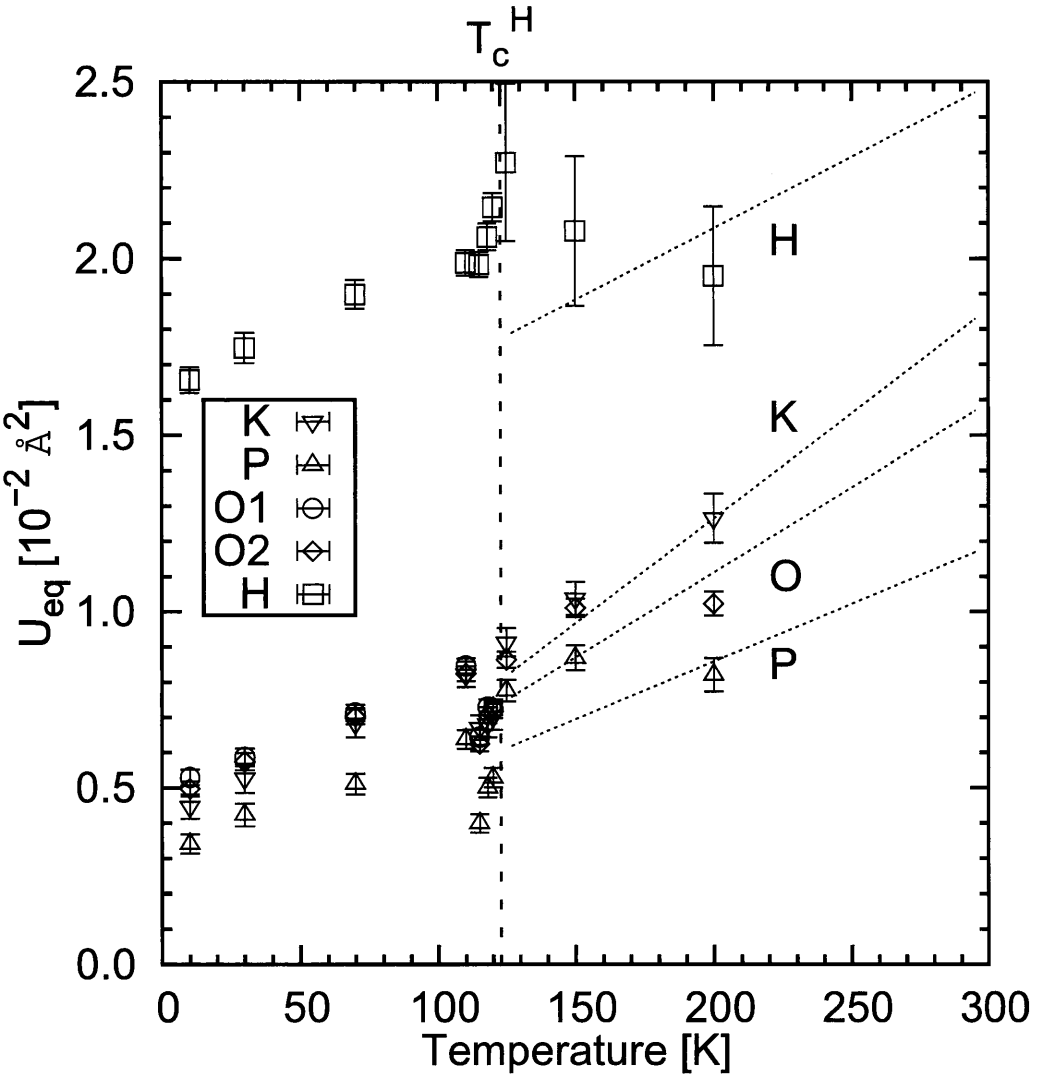

Figure 3.28 Temperature dependences of the isotropic atomic displacement parameters, U_{eq}'s, of all the atoms in both the ferroelectric and paraelectric phases of KDP. The symbols, $\bigtriangledown$, $\bigtriangleup$, $\bigcirc$, $\diamond$, and $\square$ denote the values of K, P, O1, O2, and H atoms, respectively. The O1 atom become crystallographically equivalent with O2 atom in the paraelectric phase. The open symbols denote the values in this study, and the dotted lines denote the interpolated temperature dependences from the values at 295 and 127 K reported by Nelmes *et al.* [39]. It is apparent that U_{eq} of hydrogen atom displays larger value than those of other atoms. The prominent e.s.d.'s (estimated standard deviations) of hydrogen atom in the paraelectric phase of KDP must be noticed. It is considered as its dominant reason that the least-square fittings are somewhat insufficient only for hydrogen atom in the paraelectric phase of KDP.

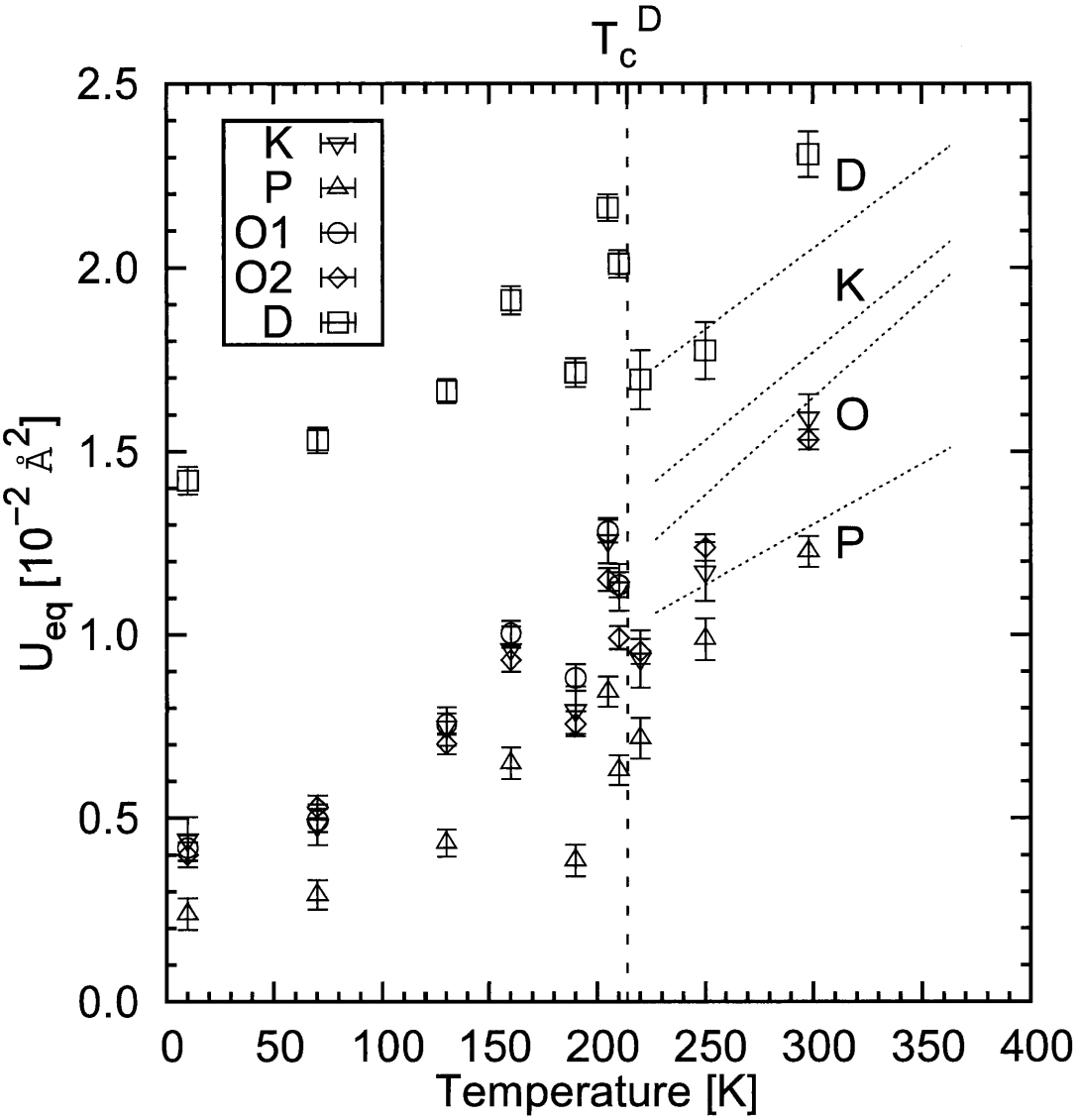

Figure 3.29 Temperature dependences of the isotropic atomic displacement parameters, U_{eq}'s, of all the atoms in both the ferroelectric and paraelectric phases of DKDP. The symbols, $\bigtriangledown$, $\bigtriangleup$, $\bigcirc$, $\diamond$, and $\square$ denote the values of K, P, O1, O2, and D atoms, respectively. The O1 atom become crystallographically equivalent with O2 atom in the paraelectric phase. The open symbols denote the values in this study, and the dotted lines denote the interpolated data at 363 and 227 K reported by Nelmes *et al.* [39]. It is apparent that U_{eq} of deuterium atom displays larger value than those of other atoms.

Chapter 4

Discussion

科学者になるには自然を恋人としなければならない。自然はやはりその恋人にのみ真心を打ち明けるものである。

科学の歴史はある意味では錯覚と失策の歴史である。偉大なる迂愚者の頭の悪い能率の悪い仕事の歴史である。

失敗をこわがる人は科学者にはなれない。科学もやはり頭の悪い命知らずの死骸の山の上に築かれた殿堂であり、血の川のほとりに咲いた花園である。

— 寺田寅彦, '科学者とあたま' より

Scientist or investigator must be the worst work in the world. They encourage themselves because other people in the world do not but need them to create any and real sakes for the world.

Scientist or investigator must be the worst work in the world. The author thinks so...

Somebody, however, likes the work in the world. The authur likes the work, too...

In the previous chapter, the interatomic distances and angles are explained in the figures. At low temperatures, the structures of KDP and DKDP are almost the same except for the cell parameter a. The parameter a of DKDP is 0.5 % (0.05 Å) larger than KDP, which reflects the difference in the hydrogen-bonded O1–O2 distance $R_{\mathrm{O-O}}$; the distance of DKDP is *ca.* 0.03 Å longer than that of KDP. The magnitudes and temperature dependences of the atomic displacements along the polar axis perpendicular to hydrogen bonds are almost the same in both crystals. Another difference is the bond distance between O and H/D; in KDP O1–H, $r_{\mathrm{H}} = 1.06$ Å, while in DKDP O1–D, $r_{\mathrm{D}} = 1.03$ Å in the ferroelectric phase. Even if a proton and a deuteron are within the same local potential, the zero-point energy depends on the particle mass. Therefore, the average position of a deuteron will be closer to O1 than that of a

proton, which is in agreement with the above-mentioned result.

Here, the author comments on the 'precursor' temperature dependence of δ in KDP. As shown in Fig. 3.12, δ decreases with decreasing temperature in the paraelectric phase. If it was a precursor effect of the ferroelectric transition, δ would increase on approaching T_c since r_H decreases after the ferroelectric transition, as shown in Fig. 3.11. The parameter δ reflects the shape of the nuclear density, as determined by the split-atom method. The nuclear density will be given by the superposition of two wave functions of the ground and first-excited states. [38] Since the energy gap is large enough in KDP, the weight of the upper energy level decreases rapidly with decreasing temperature, so that δ decreases at lower temperatures. On the other hand, the energy gap is so small in DKDP that the δ of deuterons may not change with temperature.

Some authors claimed that the difference in R_{O-O} causes an isotope effect on the transition temperature (geometrical isotope effect). However, they could not explain why R_{O-O} differs. [21–26]

We consider that the more rapid motion of protons than of deuterons bonds the two oxygen atoms more strongly, so that the geometrical isotope effect itself may be caused by the tunneling motion of protons. As a consequence of the short R_{O-O}, the δ of KDP is smaller than that of DKDP, and the localization of protons is prevented down to low temperatures. Under hydrostatic pressure, a small R_{O-O} turns the double-minimum potential for protons/deuterons into a single-minimum type; finally, the transition temperatures disappear. (Refer Appendix A.5.) [74]

If hydrogen localizes by O1 below T_c, then the tetragonal PO_4^{3-} (site symmetry of S_4) changes into $H_2PO_4^-$ (site symmetry of C_2), in which P shifts toward the O2 side and induces a dipole moment along the c-axis. Simultaneously, the K^+ ion shifts to P. The deformation of the $D_2PO_4^-$ molecule is similar to that of $H_2PO_4^-$, except for the small difference in bond length between O1–D and O1–H. The deformation of the molecule is considered to be induced by a change of chemical bonding. First-principles calculations have shown that some amount of electron charge is redistributed during the transition. [73] Although neutron structural analysis can only determine the nuclear positions, the difference between r_H and r_D surely affects the amount of the spontaneous shift of P in the ferroelectric phase.

Some researchers claimed that the phosphate molecule was a disordered $H_2PO_4^-$ cluster even in the paraelectric phase. [27–34] If this is real, then the atomic displacement parameter U_{33}^{para} of P or K in the paraelectric phase can be expressed using U_{33}^{ferro} in the ferroelectric phase as [86]

$$U_{33}^{\text{para}} = d^2 + U_{33}^{\text{ferro}}, \tag{4.0.1}$$

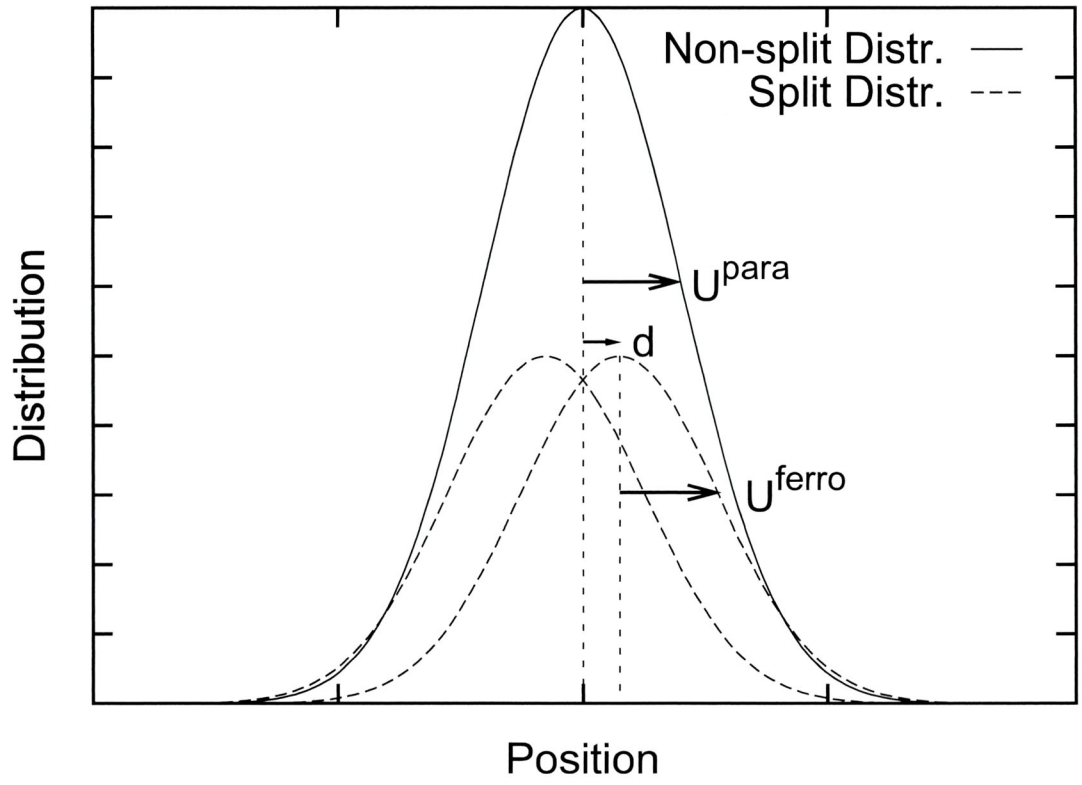

Figure 4.1 Schematic view of relational expression about nuclear density distributions before and after the ferroelectric transition, $U^{\mathrm{para}} = d^2 + U^{\mathrm{ferro}}$. If disordered state is true in the paraelectric phase, the double Gaussian curve (split distribution) will be approximately expressed by the single Gaussian curve (non split distribution), although its expression would be imperfect with finite d.

where $2d$ is the assigned split distance of P or K. (Refer Fig. 4.1.)

Usually, the split distance is determined by structural analysis while assuming split atoms in the disordered phase. However, such analysis failed in both KDP and DKDP in the author's determination. The least-squares calculations converged in $d = 0$; no splitting for K, P nor O. Here, we may estimate d from the spontaneous displacements in the ferroelectric phase. As shown in Table 4.1, the atomic displacement parameter U_{33} of K is small in the paraelectric phase; therefore, eq. (4.0.1) does not hold at all. The U_{33}'s of O1 and O2 decrease smoothly through T_{c}, and do not obey eq. (4.0.1). Moreover, the oxygen atoms remain at almost the same z's from the center of gravity, throughout the phase transition.

It has been noted that the U_{33} of P is larger than U_{11} in the paraelectric phase, which is reconfirmed in the author's analyses. However, it changes smoothly at T_{c} in KDP, which does not support a finite d in the paraelectric phase. On the other hand, the U_{33} of P may decrease abruptly below T_{c} in the case of DKDP. From

eq. (4.0.1), d is estimated at *ca.* 0.014 Å, which is much smaller than the spontaneous displacement of *ca.* 0.07 Å. Therefore, we cannot conclude that the distorted $H_2PO_4^-$ cluster exists in the paraelectric phase from a structural point of view. It should be noted that eq. (4.0.1) holds if the transition mechanism is an order-disordered one, and the reverse is not true. Even if the transition mechanism is displacive, an atomic displacement parameter sometimes decreases steeply below T_c. [86]

From the figures in the last chapter, the structural change at T_c is discontinuous and is accompanied by a jump. Only in KDP, can a gradual change be recognized just below T_c. This may be related to the residual double peaks of proton density in the ferroelectric phase, as reported by Nelmes *et al.* [42] With decreasing temperature below T_c, the proton density changes gradually into the ground-state wave function form, so that the distortion of the PO_4 tetrahedron and the shift of the K atom approach the values at 0 K. In DKDP, the deuteron may behave as a more classical particle, and its nuclear density does not indicate a quasi-double-peak below T_c.

Table 4.1 Atomic displacement parameters U_{33}'s [Å^2] of KDP and DKDP above and below T_c. The split distances d's [Å] are assigned using the displacements in the ferroelectric phase. The calculated U_{33}^{Para} is given by eq. (4.0.1) in the text.

KDP				
Atom	d	U_{33}(120 K)	U_{33}^{Para}	U_{33}(150 K)
K	0.032 8	0.008 53	0.009 61	0.006 47
P	0.051 5	0.009 41	0.012 1	0.009 12

DKDP				
Atom	d	U_{33}(210 K)	U_{33}^{Para}	U_{33}(220 K)
K	0.050 0	0.006 48	0.008 98	0.007 30
P	0.070 7	0.008 61	0.013 6	0.010 8

Chapter 5

Conclusions

Learn from yesterday, live for today, hope for tomorrow. The important thing is not to stop questioning.
— Albert Einstein, in 'LIFE' (2 May 1955)

This is a story of a student of a doctoral course in a country university. He had another and original study theme of hydrogen-bond-type ferroelectric, however it was unsuccessful in his doctoral course life. He obtained another theme as alternative study theme, which is the study of KDP/DKDP. The 'mountain' of KDP/DKDP was too high and too steep for the student to climb. Although he frustrated once, he made it through. Consequently, he acquired precious and invaluable knowledge for the hydrogen bonds for ferroelectrics.

IT MUST HELP HIM IN FUTURE!

In this report, the author has refined the atomic parameters in both the paraelectric and ferroelectric phases, in order to elucidate the isotope effect of the structural difference between KDP and DKDP. The structures have been analyzed using neutron diffraction data from single crystals at ten temperatures down to 10 K. The temperature dependences of the parameters have been discussed not from two or three temperature points but from ten data points in a wide temperature range. Here, we summarize the structural changes at the ferroelectric transition and the differences between KDP and DKDP.

(i) The refined structural parameters are in agreement with the previous results, in general. Protons/deuterons are in disorder in the paraelectric phase, while the potassium and phosphorus atoms are not in disorder in both KDP and DKDP, from the crystallographic viewpoints. In the ferroelectric phases, the

displacements of the potassium and phosphorus atoms along c-axis arise in connection with the ordering of protons/deuterons. These characteristics are essentially the same as the previous reports. [39–44]

(ii) In DKDP, the atomic coordinates show no remarkable temperature dependence except for the stepwise change during the ferroelectric transition. On the other hand, the 'precursor' behavior in the paraelectric phase and the continuous changes of the atomic coordinates just below T_c are confirmed in KDP.

(iii) The displacements of nuclei accompanied by the phase transition are considered in keeping a common center of gravity of the unit cell in both KDP and DKDP. In the ferroelectric phase, the potassium and phosphorus nuclei display remarkable displacements, and the oxygen and hydrogen nuclei tiny shifts along the polar axis in comparison with those in the paraelectric phase. The antiparallel displacements of the potassium and phosphorus atoms keep the center of gravity of the unit cell throughout the phase transition.

(iv) The spontaneous polarizations along the c-axis are calculated from the structural parameters by the point-charge method (K:$+e$, P:$+5e$, O:$-2e$, and H/D:$+e$). The calculated magnitudes of the spontaneous polarization are in agreement with the previous values measured directly. The contribution of the atoms to the polarization mainly consists of one associated with the displacement of the phosphorus atom with a large valence charge. The experimental spontaneous polarization of DKDP is *ca.* 1.2 times larger than that of KDP, as reported previously, and this difference arises from the slightly larger displacement of the phosphorus atom in DKDP than in KDP.

(v) In KDP, the atomic shifts along the c-axis indicate gradual increases with decreasing temperature just below T_c. This character is consequently associated with the temperature dependence of the spontaneous polarization.

(vi) Except for the temperature dependence just below T_c in KDP, no remarkable change is found in the crystal structure below the liquid-nitrogen temperature. At very low temperatures, the thermal contraction of the cell affects the magnitude of the displacements, *i.e.*, the spontaneous polarizations, although the decreases are small.

(vii) All the atomic distances and angles are examined in both KDP and DKDP. From the result, remarkable differences are confirmed in the geometrical parameters relevant to the hydrogen bonds (O–H$\cdots$O bond), while no significant difference is confirmed in the other parameters.

(viii) The separation distance between equilibrium sites of the hydrogen atom, δ, is *ca.* 0.13 Å longer in DKDP than in KDP, and the distance between two oxygen atoms of the hydrogen bond, R_{O-O}, has a difference of *ca.* 0.04 Å

between KDP and DKDP. These two are reconfirmed in the author's study, and the author additionally found that deuteron has a smaller distance from the acceptor oxygen atom; the distance r_D is *ca.* 0.04 Å shorter than r_H in both the paraelectric and ferroelectric phases. r_D depends slightly on temperature, while r_H strongly.

Even if the proton and deuteron are located at the same potential, the remarkable difference should appear in their reciprocating motions between two equilibrium positions because of their mass. Consequently, it generates a difference in the strength of the hydrogen bond; if a proton vibrates more frequently, it makes the distance R_{O-O} shorter. Therefore, the isotope effect for KDP and DKDP can be explained as a result of such a mass effect. Additionally, the difference between the behaviors of proton and deuteron is found to definitely increase the difference of the spontaneous polarizations; a heavy deuteron attaches closer to the acceptor O1, and the electron charge transfer from O1 to D takes place, so that the shift of the phosphorus atom can become larger.

Our structural analyses support a scenario in which the differences of the hydrogen mass and the potentials associated with different distances between the two oxygen atoms cause the differences in the transition temperature, the spontaneous polarization, and the vanishing of the ferroelectric phases at different critical pressures in KDP and DKDP. Namely, 'tunneling' hydrogen is the key to understanding the phase transition of KDP-type ferroelectrics, although 'tunneling' may be a dynamical disorder without quantum coherency. Finally, a disordered or distorted $H_2PO_4^-$ cluster in the paraelectric phase has not been established from the structural point of view. [75]

References

[1] K. Momma and F. Izumi. VESTA: a three-dimensional visualization system for electronic and structural analysis. *J. Appl. Crystallogr.*, Vol. 41, pp. 653–658, 2008.

[2] G. Busch and P. Scherrer. Eine neue seignette-elektrische Substanz. *Naturwissenschaften*, Vol. 23, p. 737, 1935.

[3] G. Busch and P. Scherrer. A new seignette-electric substance. *Ferroelectrics*, Vol. 71, pp. 15–16, 1987.

[4] G. Busch. (title unknown). *Helv. Phys. Acta*, Vol. 11, p. 269, 1938.

[5] G. Busch. New seignette-electrics. *Ferroelectrics*, Vol. 71, pp. 17–24, 1987.

[6] J. C. Slater. Theory of the transition in KH_2PO_4. *J. Chem. Phys.*, Vol. 9, pp. 16–33, 1941.

[7] Tatsuki Miyoshi, Hironobu Kasano, and Hiroyuki Mashiyama. Rotational displacement of IO_4 tetrahedron in the phase II of pyridinium periodate. *Ferroelectrics*, Vol. 346, pp. 130–135, 2007.

[8] W. Bantle and P. Scherrer. Anomaly of the specific heat of potassium dihydrogen phosphate at the upper Curie point. *Nature*, Vol. 143, p. 980, 1939.

[9] W. Bantle and P. Scherrer. (title unknown). *Helv. Phys. Acta*, Vol. 14, p. 146, 1941.

[10] B. Zwicker and P. Scherrer. (title unknown). *Helv. Phys. Acta*, Vol. 17, p. 346, 1944.

[11] G. E. Bacon and R. S. Pease. A neutron diffraction study of potassium dihydrogen phosphate by fourier synthesis. *Proc. R. Soc. London, Ser. A*, Vol. 220, pp. 397–421, 1953.

[12] G. E. Bacon and R. S. Pease. A neutron-diffraction study of the ferroelectric transition of potassium dihydrogen phosphate. *Proc. R. Soc. London, Ser. A*, Vol. 230, pp. 359–381, 1955.

[13] R. Blinc. On the isotopic effects in the ferroelectric behaviour of crystals with short hydrogen bonds. *J. Phys. Chem. Solids*, Vol. 13, pp. 204–211, 1960.

[14] P. G. de Gennes. Collective motions of hydrogen bonds. *Solid State Commun.*,

Vol. 1, pp. 132–137, 1963.

[15] Masaharu Tokunaga and Takeo Matsubara. Theory of ferroelectric phase transition in KH_2PO_4 type crystals. *Prog. Theor. Phys.*, Vol. 35, pp. 581–599, 1966.

[16] Kenji K. Kobayashi. Dynamical theory of the phase transition in KH_2PO_4-type ferroelectric crystals. *J. Phys. Soc. Jpn.*, Vol. 24, pp. 497–508, 1968.

[17] W. Cochran. Dynamical, scattering and dielectric properties of ferroelectric crystals. *Adv. Phys.*, Vol. 18, pp. 157–192, 1969.

[18] Masaharu Tokunaga. Models of the phase transition in KDP type ferroelectrics. *Ferroelectrics*, Vol. 1, pp. 195–206, 1970.

[19] Masaharu Tokunaga and Takeo Matsubara. Review on tunneling model for KH_2PO_4. *Ferroelectrics*, Vol. 72, pp. 175–191, 1987.

[20] Eiko Matsushita and Takeo Matsubara. Note on isotope effect in hydrogen bonded crystals. *Prog. Theor. Phys.*, Vol. 67, pp. 1–19, 1982.

[21] M. Ichikawa. The O–H *vs* O$\cdots$O distance correlation, the geometric isotope effect in OHO bonds, and its application to symmetric bonds. *Acta Crystallogr., Sect. B*, Vol. 34, pp. 2074–2080, 1978.

[22] M. Ichikawa. Correlation between two isotope effects in hydrogen-bonded crystals. transition temperature and separation of two equilibrium sites. *Chem. Phy. Lett.*, Vol. 79, pp. 583–587, 1981.

[23] M. Ichikawa. A comparison between predicted and measured structural parameters in symmetric hydrogen bonds. *J. Cryst. Mol. Struct.*, Vol. 11, pp. 167–172, 1981.

[24] M. Ichikawa, K. Motida, and N. Yamada. Negative evidence for a proton-tunneling mechanism in the phase transition of KH_2PO-type crystals. *Phys. Rev. B*, Vol. 36, pp. 874–876, 1987.

[25] Mizuhiko Ichikawa. Comparison among pressure, temperature and deuteration effects on the crystal structure in KH_2PO and squaric acid. *J. Phys. Soc. Jpn*, Vol. 56, pp. 3748–3749, 1987.

[26] M. Ichikawa, D. Amasaki, T. Gustafsson, and I. Olovsson. Structural parameters determining the transition temperature of tetragonal KH_2PO-type crystals. *Phys. Rev. B*, Vol. 64, p. 100101, 2001.

[27] Yasunori Tominaga, Masaru Kasahara, Masaharu Tokunaga, Hisako Urabe, and Itaru Tatsuzaki. Raman spectra of low-lying longitudinal mode in $KDP_{1-x}DKDP_x$ mixed crystals. *Ferroelectrics*, Vol. 44, pp. 265–269, 1983.

[28] Y. Tominaga, M. Kasahara, H. Urabe, and I. Tatsuzaki. Raman spectra of low-lying longitudinal mode of KH_2PO_4 and KD_2PO_4 in ferroelectric phase. *Solid State Commun.*, Vol. 47, pp. 835–837, 1983.

[29] Y. Tominaga, H. Urabe, and M. Tokunaga. Internal modes and local symmetry of PO_4 tetrahedrons in KH_2PO_4 by Raman scattering. *Solid State Commun.*, Vol. 48, pp. 265–267, 1983.

[30] Yasunori Tominaga. Study on ferroelectric phase transition of KH_2PO_4 by Raman scattering — objection to the proton tunneling model. *Ferroelectrics*, Vol. 52, pp. 91–100, 1983.

[31] I. Takenaka, Y. Tominaga, S. Endo, and M. Kobayashi. High pressure Raman scattering and local distortion of PO_4 in paraelectric KH_2PO_4. *Solid State Commun.*, Vol. 84, pp. 931–933, 1992.

[32] Yasunori Tominaga, Akane Agui, and Shiku Shin. Low-frequency modes of KDP-type crystals and transition mechanism. *Ferroelectrics*, Vol. 152, pp. 397–401, 1994.

[33] Yasunori Tominaga, Yoshimi Kawahata, and Yuko Amo. Hydrogen modes in KDP/DKDP mixed crystals. *Solid State Commun.*, Vol. 125, pp. 419–422, 2003.

[34] Yoshimi Kawahata and Yasunori Tominaga. Dynamical mechanism of ferroelectric phase transition in KDP/DKDP mixed crystals and distortion of PO_4 tetrahedron. *Solid State Commun.*, Vol. 145, pp. 218–222, 2008.

[35] M. C. Lawrence and G. N. Robertson. The temperature and pressure dependence of the proton tunnelling frequency in KDP. *J. Phys. C: Solid State Phys.*, Vol. 13, pp. L1053–L886, 1980.

[36] H. Sugimoto and S. Ikeda. Isotope effects in hydrogen-bonded crystal KH_2PO_4. *Phys. Rev. Lett.*, Vol. 67, pp. 1306–1309, 1991.

[37] Chieko Totsuji and Takeo Matsubara. A simple model for ferroelectrics and antiferroelectrics with isolated hydrogen bonds. *J. Phys. Soc. Jpn.*, Vol. 63, pp. 2760–2768, 1994.

[38] H. Mashiyama. Proton potential and a tunneling model for KDP. *J. Korean Phys. Soc.*, Vol. 46, pp. 63–68, 2005.

[39] R. J. Nelmes, G. M. Meyer, and J. E. Tibballs. The crystal structure of tetragonal KH_2PO_4 and KD_2PO_4 as a function of temperature. *J. Phys. C: Solid State Phys.*, Vol. 15, pp. 59–75, 1982.

[40] J. E. Tibballs, R. J. Nelmes, and G. J. McIntyre. The crystal structure of tetragonal KH_2PO_4 and KD_2PO_4 as a function of temperature and pressure. *J. Phys. C: Solid State Phys.*, Vol. 15, pp. 37–58, 1982.

[41] W. F. Kuhs, R. J. Nelmes, and J. E. Tibballs. The proton distribution in KDP above T_c. *J. Phys. C: Solid State Phys.*, Vol. 16, pp. L1029–L1032, 1983.

[42] R. J. Nelmes, W. F. Kuhs, C. J. Howard, J. E. Tibballs, and T. W. Ryan. Structural ordering below T_c in KDP and DKDP. *J. Phys. C: Solid State Phys.*, Vol. 18, pp. L711–L716, 1985.

[43] Z. Tun, R. J. Nelmes, W. F. Kuhs, and R. F. D. Stansfield. A high-resolution neutron-diffraction study of the effects of deuteration on the crystal structure of KH_2PO_4. *J. Phys. C: Solid State Phys.*, Vol. 21, pp. 245–258, 1988.

[44] R. J. Nelmes. On the structural evidence for a direct proton tunneling effect in the KH_2PO_4-type transition. *J. Phys. C: Solid State Phys.*, Vol. 21, pp. L881–L886, 1988.

[45] J. West. (title unknown). *Z. Kristallogr.*, Vol. 74, pp. 306–332, 1930.

[46] J. West. A quantitative X-ray analysis of the structure of potassium dihydrogen phosphate (KH_2PO_4). *Ferroelectrics*, Vol. 71, pp. 1–9, 1987.

[47] A. R. Ubbelohde and I. Woodward. Structure and thermal properties associated with some hydrogen bonds in crystals. *Proc. R. Soc. London, Ser. A*, Vol. 188, pp. 358–371, 1947.

[48] Benjamin Chalmers Frazer and Ray Pepinsky. Structural changes in the ferroelectric transition of KH_2PO_4. *Phys. Rev.*, Vol. 85, pp. 479–480, 1952.

[49] Benjamin Chalmers Frazer and Ray Pepinsky. A X-ray analysis of the ferroelectric transition in KH_2PO_4. *Acta Crystallogr.*, Vol. 6, pp. 273–285, 1953.

[50] R. S. Pease and G. E. Bacon. Ferroelectric structure of potassium dihydrogen phosphate. *Nature*, Vol. 173, p. 443, 1954.

[51] Jun-ichi Nakano, Yoichi Shiozaki, and Eiji Nakamura. X-ray structural study of KD_2PO_4 at room temperature. *J. Phys. Soc. Jpn.*, Vol. 34, p. 1423, 1973.

[52] J. Nakano, Y. Shiozaki, and E. Nakamura. X-ray structural study of KD_2PO_4. *Ferroelectrics*, Vol. 8, pp. 483–484, 1974.

[53] Tadao Hayashide and Yukio Noda. Electron distribution of hydrogen and deuteron in KH_2PO_4 and KD_2PO_4. *J. Phys. Soc. Jpn.*, Vol. 66, pp. 270–271, 1996.

[54] Kazuyuki Itoh and Makoto Uchimoto. Forty crystal structure analyses of KH_2PO_4 in the paraelectric phase. *Ferroelectrics*, Vol. 217, pp. 155–162, 1998.

[55] V. R. Eiriksson, K. D. Rouse, and R. J. Nelmes. The crystal structure of the paraelectric phase of $K(D_{0.88}H_{0.12})_2PO_4$. *Ferroelectrics*, Vol. 8, p. 485, 1974.

[56] R. J. Nelmes and K. D. Rouse. Structural studies of the system KH_2PO_4-KD_2PO_4. *Ferroelectrics*, Vol. 8, p. 487, 1974.

[57] N. S. J. Kennedy, R. J. Nelmes, F. R. Thornley, and K. D. Rouse. Recent structural studies of the KH_2PO_4-KD_2PO_4 system. *Ferroelectrics*, Vol. 14, pp. 591–593, 1976.

[58] R. J. Nelmes, W. F. Kuhs, C. J. Howard, J. E. Tibballs, and T. W. Ryan. Structural evidence for centre-of-mass motion in the ferroelectric fluctuation of KDP and DKDP. *J. Phys. C: Solid State Phys.*, Vol. 18, pp. L1023–L1030, 1985.

[59] M. I. McMahon, R. J. Nelmes, R. O. Piltz, and W. F. Kuhs. Possible disorder of the P atom in KD_2PO_4. *Europhys. Lett.*, Vol. 13, pp. 143–148, 1990.

[60] Susumu Ikeda, Kaoru Shibata, Yusuke Nakai, and Peter W. Stephens. Incoherent neutron scattering measurements on KDP. *J. Phys. Soc. Jpn.*, Vol. 61, pp. 2619–2623, 1992.

[61] H. Umebayashi, B. C. Frazer, and G. Shirane. Effect of hydrostatic pressure on the ferroelectric curie temperatures of KH_2PO_4 and KD_2PO_4. *Solid State Commun.*, Vol. 5, pp. 591–594, 1967.

[62] E. Hegenbarth and S. Ullwer. The shifting of the transition temperature of KH_2PO_4 crystals by hydrostatic pressure. *Cryogenics*, Vol. 7, pp. 306–307, 1967.

[63] G. A. Samara. Pressure dependence of the ferroelectric properties of KD_2PO_4. *Phys. Lett.*, Vol. 25A, pp. 664–666, 1967.

[64] J. Skalyo, Jr., B. C. Frazer, G. Shirane, and W. B. Daniels. The pressure dependence of the transition temperature in KDP and ADP. *J. Phys. Chem. Solids*, Vol. 30, pp. 2045–2051, 1969.

[65] G. A. Samara. Vanishing of the ferroelectric and antiferroelectric states in KH_2PO_4-type crystals at high pressure. *Phys. Rev. Lett.*, Vol. 27, pp. 103–106, 1971.

[66] George A. Samara. Vanishing of the ferroelectricity in displacive and hydrogen-bond ferroelectrics at high pressure. *Ferroelectrics*, Vol. 7, pp. 221–224, 1974.

[67] G. A. Samara. Pressure dependence of the static dielectric properties of $K(H_{1-x}D_x)_2PO_4$ and RbH_2PO_4. *Ferroelectrics*, Vol. 22, pp. 925–936, 1979.

[68] S. Endo, T. Chino, S. Tsuboi, and K. Koto. Pressure-induced transition of the hydrogen bond in the ferroelectric compounds KH_2PO_4 and KD_2PO_4. *Nature*, Vol. 340, p. 452, 1989.

[69] S. Endo, T. Sawada, T. Tsukawake, Y. Kobayashi, M. Ishizuka, K. Deguchi, and M. Tokunaga. Vanishing of the ferroelectric state with a finite curie constant in the hydrogen-bond crystal KD_2PO_4 at high pressure. *Solid State Commun.*, Vol. 112, pp. 655–660, 1999.

[70] Shoichi Endo, Takuya Sawada, Takashi Tsukawake, Yuki Kobayashi, and Mamoru Ishizuka. Vanishing of ferroelectric phase transition in DKDP and KDP at high pressure. *J. Korean Phys. Soc.*, Vol. 35, pp. S1380–S1383, 1999.

[71] Shoichi Endo, Kiyoshi Deguchi, and Masaharu Tokunaga. Quantum paraelectricity in KD_2PO and KH_2PO under high pressure. *Phys. Rev. Lett.*, Vol. 88, p. 035503, 2002.

[72] G. F. Reiter, J. Mayers, and P. Platzman. Direct observation of tunneling in KDP using neutron compton scattering. *Phys. Rev. Lett.*, Vol. 89, p. 135505,

2002.

[73] S. Koval, J. Kohanoff, J. Lasave, G. Colizzi, and R. L. Migoni. First-principles study of ferroelectricity and isotope effects in H-bonded KH_2PO_4 crystals. *Phys. Rev. B*, Vol. 71, p. 184102, 2005.

[74] Serges E. Mkam Tchouobiap and H. Mashiyama. Quasiharmonic approximation for a double Morse-type local potential model: Application to a KH_2PO_4-type phase diagram. *Phys. Rev. B*, Vol. 76, p. 014101, 2007.

[75] Tatsuki Miyoshi, Hiroyuki Mashiyama, Takanao Asahi, Hiroyuki Kimura, and Yukio Noda. Single-crystal neutron structural analyses of potassium dihydrogen phosphate and potassium dideuterium phosphate. *J. Phys. Soc. Jpn.*, Vol. 80, No. 4, pp. 04xxxx–04xxxxx, 2011.

[76] Yukio Noda, Hiroyuki Kimura, Ryoji Kiyanagi, Akiko Kojima, Yukio Morii, Nobuaki Minakawa, and Naohisa Takesue. Aspects of the neutron 4-circle diffractometer FONDER and the bent Si monochrometer. *Proc. 1st. Int. Symp. Advanced Science Research (ASR-2000) "Advances in Neutron Scattering Research", J. Phys. Soc. Jpn. Suppl. A*, Vol. 70, pp. 456–458, 2001.

[77] K. N. Trueblood, H.-B. Bŭrgi, H. Burzlaff, J. D. Dunitz, C. M. Gramaccioli, H. H. Schulz, U. Shmueli, and S. C. Abrahams. Atomic displacement parameter nomenclature. Report of a subcommittee on atomic displacement parameter nomenclature. *Acta Crystallogr., Sect. A*, Vol. 52, pp. 770–781, 1996.

[78] Profile Check, DABEXN, and RADIELN can be obtained *via* `http://www.tagen.tohoku.ac.jp/labo/noda/FONDER/FONDER.html`.

[79] P. Coppens, T. N. Guru Row, P. Leung, E. D. Stevens, P. J. Becker, and Y. W. Yang. Net atomic charges and molecular dipole moments from spherical-atom X-ray refinements, and the relation between atomic charge and shape. *Acta Crystallogr., Sect. A*, Vol. 35, pp. 63–72, 1979.

[80] G. M. Sheldrick. a short history of *SHELX*. *Acta Crystallogr., Sect. A*, Vol. 64, pp. 112–122, 2008.

[81] L. J. Farrugia. *WinGX* suite for small-molecule single-crystal crystallography. *J. Appl. Crystallogr.*, Vol. 32, p. 837, 1999.

[82] R. Nelmes. Structural studies of KDP and the KDP-type transition by neutron and x-ray diffraction: 1970–1985. *Ferroelectrics*, Vol. 71, pp. 87–123, 1987.

[83] R. Nelmes. A compilation of accurate structural parameters for KDP and DKDP, and a users' guide to their crystal structures. *Ferroelectrics*, Vol. 71, pp. 125–141, 1987.

[84] G. A. Samara. The effects of deuteration on the static ferroelectric properties of KH_2PO_4 (KDP). *Ferroelectrics*, Vol. 5, pp. 25–37, 1973.

[85] Y. Uesu, T. Tanaka, and J. Kobayashi. X-Ray dilatometric study of the phase

transition of the important ferroelectrics KH_2PO_4 and KD_2PO_4. *Ferroelectrics*, Vol. 7, pp. 247–249, 1974.

[86] Kazuyuki Itoh. An atomic order parameter in disordered crystals undergoing structural phase transitions and its determination by the crystal structure analysis. *J. Phys. Soc. Jpn.*, Vol. 53, pp. 2049–2053, 1984.

[87] W. Bantle. (title unknown). *Helv. Phys. Acta*, Vol. 15, p. 373, 1942.

[88] H. J. Bleif, R. A. Cowley, and R. J. Nelmes. The ferroelectric fluctuation in KD_2PO_4. *J. Phys. C: Solid State Phys.*, Vol. 15, pp. L201–L206, 1982.

[89] R. Blinc and S. Svetina. Low-frequency hydrogen modes in KH_2PO_4 type ferroelectrics crystals. *Phys. Lett.*, Vol. 15, pp. 119–120, 1965.

[90] R. Blinc, S. Svetina, and B. Žekš. On the vanishing of ferroelectricity in KH_2PO_4 at high pressures. *Solid State Commun.*, Vol. 10, pp. 387–389, 1972.

[91] R. Blinc, J. Seliger, R. Osredkar, and T. Prelesnik. Double resonance study of the ^{18}O quadrupole coupling in paraelectric and ferroelectric KH_2PO_4. *Chem. Phys. Lett.*, Vol. 23, pp. 486–488, 1973.

[92] R. Blinc, V. SMOLEJ, B. Žekš, I. Levstek, and B. Lavrenčič. Dynamical susceptibility of KH_2PO_4 type ferroelectrics below t_c. *Ferroelectrics*, Vol. 7, pp. 203–204, 1974.

[93] R. Blinc and B. Žekš. On the pressure dependence of the ferroelectric curie temperature of KH_2PO_4 and KD_2PO_4. *Phys. Lett.*, Vol. 26A, pp. 468–469, 1968.

[94] R. Brout, K. A. Müller, and H. Thomas. Tunnelling and collective excitations in a microscopic model of ferroelectricity. *Solid State Commun.*, Vol. 4, pp. 507–510, 1966.

[95] Georg Busch. How I discovered the ferroelectric properties of KH_2PO_4. *Ferroelectrics*, Vol. 71, pp. 43–47, 1987.

[96] A. Bussmann-Holder and K. H. Michel. Bond geometry and phase transition mechanism of H-bonded ferroelectrics. *Phys. Rev. Lett.*, Vol. 80, pp. 2173–2176, 1998.

[97] M. Chabin and F. Gilletta. Polarization and dielectric constant of KDP-type crystals. *Ferroelectrics*, Vol. 15, pp. 149–154, 1977.

[98] R. A. Cowley, H. J. Bleif, S. R. Andrews, and R. J. Nelmes. Ferroelectric fluctuations in KDP and DKDP. *Physica*, Vol. 120B, pp. 267–269, 1983.

[99] M. de Quervain. (title unknown). *Helv. Phys. Acta*, Vol. 17, p. 509, 1944.

[100] D. H. W. Dickson and A. R. Ubbelohde. The hydrogen bond in crystals. VIII. the isotope effect in KH_2AsO_4. *Acta Crystallogr.*, Vol. 3, pp. 6–9, 1950.

[101] R. M. Hill and S. K. Ichiki. Paraelectric response of KD_2PO_4. *Phys. Rev.*, Vol. 130, pp. 150–151, 1963.

[102] R. M. Hill and S. K. Ichiki. High-frequency behavior of hydrogen-bonded ferroelectrics: Triglycine sulphate and KD_2PO_4. *Phys. Rev.*, Vol. 132, pp. 1603–1608, 1963.

[103] S. Ikeda, Y. Noda, H. Sugimoto, and Y. Yamada. Incoherent neutron scattering from KDP. *Ferroelectrics*, Vol. 156, pp. 291–296, 1994.

[104] S. Ikeda and Y. Yamada. Phase transition in hydrogen-bonded ferroelectric compounds - quantum fluctuations versus thermal fluctuations. *Physica*, Vol. 213B, pp. 652–657, 1995.

[105] F. Jona and G. Shirane. *Ferroelectric crystals. (The Macmillan Company, New York)*, Vol. Chap. 3, p. 93, 1962.

[106] I. P. Kaminow. Microwave dielectric properties of $NH_4H_2PO_4$, KH_2AsO_4, and partially deuterated KH_2PO_4. *Phys. Rev.*, Vol. 138, pp. A1539–A1543, 1965.

[107] I. P. Kaminow and T. C. Damen. Temperature dependence of the ferroelectric mode in KH_2PO_4. *Phys. Rev. Lett*, Vol. 20, pp. 1105–1108, 1968.

[108] J. Kano and T. Yagi. Dynamic property of the initial process in the dielectric relaxation phenomenon in KH_2PO_4. *Ferroelectrics*, Vol. 333, pp. 41–46, 2006.

[109] Toshio Kikuta, Akira Onodera, Toshihiko Takama, Masahisa Fujita, and Haruyasu Yamashita. Molecular motion of PO_4 in KDP at ferroelectric phase transition. *Ferroelectrics*, Vol. 170, pp. 17–22, 1995.

[110] J. A. Krumhansl. Sorting chikens from eggs. *Nature*, Vol. 348, p. 286, 1990.

[111] B. Lavrenčič, I. Levstek, B. Žekš, R. Blinc, and D. Hadži. Laser Raman study of quasi-spin wave hydrogen tunneling modes in KH_2PO_4 and KD_2PO_4. *Chem. Phys. Lett.*, Vol. 5, pp. 441–444, 1970.

[112] M. C. Lawrence and G. N. Robertson. Estimating the proton potential in KDP from infrared and crystallographic data. *Ferroelectrics*, Vol. 34, pp. 179–186, 1981.

[113] Henri A. Levy, S. W. Peterson, and S. H. Simonsen. Neutron diffraction study of the ferroelectric modification of potassium dihydrogen phosphate. *Phys. Rev.*, Vol. 93, pp. 1120–1121, 1954.

[114] G. M. Loiacono, J. F. Balascio, and W. Osborne. Effect of deuteration on the ferroelectric transition temperature and the distribution coefficient of deuterium in KD_2PO_4. *Appl. Phys. Lett.*, Vol. 24, pp. 455–456, 1974.

[115] G. M. Loiacono. Crystal growth of KH_2PO_4. *Ferroelectrics*, Vol. 71, pp. 49–60, 1987.

[116] Hiroyuki Mashiyama, Serges E. Mkam Tchouobiap, and Tatsuki Miyoshi. Quantum effects of phase transitions in ferroelectric crystals—experiments and models. *Ferroelectrics*, Vol. 378, pp. 163–168, 2009.

[117] M. Mathew and W. Wong-Ng. Crystal structure of a new monoclinic

from of potassium dihydrogen phosphate containing orthophosphacidium ion, $[H_4PO_4]^{+1}$. *J. Solid State Chem.*, Vol. 114, pp. 219–223, 1995.

[118] Takeo Matsubara and Eiko Matsushita. Further comment on isotope effect in hydrogen bonded crystals. *Prog. Theor. Phys.*, Vol. 71, pp. 209–211, 1984.

[119] B. T. Matthias. Phase transition of $ND_4D_2PO_4$. *Phys. Rev.*, Vol. 85, pp. 141–141, 1951.

[120] R. J. Mayer and J. L. Bjorkstam. Dielectric properties of KD_2PO_4. *J. Phys. Chem. Solids*, Vol. 23, pp. 619–620, 1961.

[121] Dalibor Merunka and Boris Rakvin. Displacive and order–disorder behavior of KDP-type ferroelectrics on the local scale. *Solid State Commun.*, Vol. 129, pp. 375–377, 2004.

[122] R. J. Nelmes, N. S. J. Kennedy, E. Baharie, and A. W. Hewat. The structure of KH_2PO_4 and KD_2PO_4 at high pressure ($\sim$ 20 kbar) in relation to the effect of pressure on T_C. *Ferroelectrics*, Vol. 21, pp. 439–440, 1978.

[123] Yukio Noda, Hironobu Maeda, Hikaru Terauchi, Hirofumi Kasatani, Kenichiro Ogura, Kazuya Kamon, Takashi Umeki, Yasuhiro Yoneda, Satoshi Murakami, and Yoshihiro Kuroiwa. Local distortion of AsO_4 and PO_4 molecules in KDP-family crystals. *Proc. 7th Int. Conf. X-Ray Absorption Fine Structure, Kobe, 1992, Jpn. J. Appl. Phys.*, Vol. 32, pp. Suppl. 32–2 pp. 740–742, 1993.

[124] Christer E. Nordman and William N. Lipscomb. Note on the hydrogen-deuterium isotope effect in crystals. *J. Chem. Phys.*, Vol. 19, pp. 1422–1422, 1951.

[125] P. S. Peercy. Observation of an underdamped "soft" mode in potassium dihydrogen phosphate. *Phys. Rev. Lett.*, Vol. 31, pp. 379–382, 1973.

[126] P. S. Peercy. Measurement of the "soft" mode and coupled modes in the paraelectric and ferroelectric phases of KH_2PO_4 at high pressure. *Phys. Rev. B*, Vol. 12, pp. 2725–2740, 1975.

[127] I. Pelah, I. Lefkowitz, W. Kley, and E. Tunkelo. Observations of hydrogen vibration frequencies in phosphates by means of inelastic scattering of cold neutrons. *Phys. Rev. Lett.*, Vol. 2, pp. 94–95, 1959.

[128] S. W. Peterson, Henri A. Levy, and S. H. Simonsen. Neutron diffraction study of tetragonal potassium dihydrogen phosphate. *J. Chem. Phys.*, Vol. 21, pp. 2084–2085, 1953.

[129] Ronald L. Reese, I. J. Fritz, and H. Z. Cummins. Simultaneous observation of the soft ferroelectric and acoustic modes of KD_2PO_4. *Solid State Commun.*, Vol. 9, pp. 327–330, 1971.

[130] G. Reiter, A. Shukla, P. M. Platzman, and J. Mayers. Deuteron momentum distribution in KD_2PO_4. *New J. Phys.*, Vol. 10, p. 013016, 2008.

[131] Rafael Rodriguez-Clemente and Sabino Veintemillas. KDP (KH_2PO_4) growth from boiling solutions. *Ferroelectrics*, Vol. 56, pp. 1045–1048, 1984.

[132] G. A. Samara. Pressure and temperature dependence of the ferroelectric properties of deuterated Rochelle salt. *J. Phys. Chem. Solids*, Vol. 29, pp. 870–873, 1968.

[133] Hajime Shibata, Yuhji Tsujimi, Tomoyuki Hikita, and Takuro Ikeda. Light scattering study of effect of hydrostatic-pressure on the ferroelectric relaxational mode in KH_2PO_4. *J. Phys. Soc. Jpn.*, Vol. 55, pp. 2543–2546, 1986.

[134] Takeshi SHIGENARI and Yasunari TAKAGI. Raman spectrum of "ferroelectric mode" in a KDP crystal. *J. Phys. Soc. Jpn.*, Vol. 31, pp. 312–312, 1971.

[135] T. R. Sliker and S. R. Burlage. Some dielectric and optical properties of KD_2PO_4. *J. Appl. Phys*, Vol. 34, pp. 1837–1840, 1963.

[136] Gert Steulmann. Die Dielektrizitatskonstanten einer Anzahl von Kaliumsalzen und Alkalihalogeniden. *Z. Physik*, Vol. 77, pp. 114–116, 1932.

[137] Gert Steulmann. The dielectric constants of some potassium salts and alkali halides. *Ferroelectrics*, Vol. 71, pp. 11–13, 1987.

[138] B. A. Strukov, V. G. Vaks, A. Baddur, V. I. Zinenko, and V.A. Koptsik. Experimental and theoretical study of phase transition in KH_2PO_4 (KDP)-type crystals. *Ferroelectrics*, Vol. 7, pp. 195–197, 1974.

[139] Yutaka Takagi. Theory of the transition in KH_2PO_4. (I). *J. Phys. Soc. Jpn.*, Vol. 3, pp. 271–272, 1948.

[140] Y. Tominaga and T. Nakamura. Raman scattering spectra of B_2-polariton and B_2(LO) modes in paraelectric KDP. *Solid State Commun.*, Vol. 27, pp. 1375–1377, 1978.

[141] Yasunori Tominaga and Hisako Urabe. Low-lying B_2(LO) Raman spectra in paraelectric KH_2PO_4. *J. Phys. Soc. Jpn.*, Vol. 50, pp. 3841–3842, 1981.

[142] Y. Tominaga and H. Urabe. Central component of $y(xy)x$ Raman spectra in paraelectric KH_2PO_4. *Solid State Commun.*, Vol. 41, pp. 561–564, 1982.

[143] Chieko Totsuji and Takeo Matsubara. Theory of phase transition induced by deuteration of hydrogen bond. *J. Korean Phys Soc.*, Vol. 32, pp. S50–S52, 1998.

[144] Chieko Totsuji and Takeo Matsubara. Deuteration induced phase transition in hydrogen bond. *Solid State Commun.*, Vol. 105, pp. 731–733, 1998.

[145] Chieko Totsuji and Takeo Matsubara. Thermodynamics of a model system for isolates hydrogen bonds. *Solid State Commun.*, Vol. 107, pp. 741–744, 1998.

[146] Chieko Totsuji and Takeo Matsubara. Phase transitions in hydrogen-bonded materials. *J. Korean Phys Soc.*, Vol. 35, pp. S1339–S1342, 1999.

[147] A. R. Ubbelhode. Structure and thermal properties associated with some hydrogen bonds in crystals III. Further examples of the isotope effect. *Proc. R.*

Soc. London, Ser. A, Vol. 173, pp. 417–427, 1939.

[148] E. Wiener and I. Pelah. Indication of low frequency hydrogen modes in KH_2PO_4 from infrared measurements. *Phys. Lett.*, Vol. 13, pp. 206–207, 1964.

[149] Toshirou Yagi. Breakdown of the soft-mode model of KDP — low-frequency Raman spectroscopy under high pressure. *Ferroelectrics*, Vol. 152, pp. 409–414, 1994.

[150] Qing Zhang, F. Chen, Nicholas Kioussis, S. G. Demos, and H. B. Radousky. *Ab initio* study of the electronic and structural properties of the ferroelectric transition in KH_2PO_4. *Phys. Rev. B*, Vol. 65, p. 024108, 2001.

[151] I. S. Zheludev, V. V. Gladkii, E. V. Sidnenko, and V. K. Magataev. Dielectric nonlinearity and phase transition in KH_2PO_4-type crystals. *Ferroelectrics*, Vol. 7, pp. 567–568, 1974.

[152] Michael N. Burnett and Carroll K. Johnson. ORTEP-III: Oak Ridge Thermal Ellipsoid Plot Program for Crystal Structure Illustrations. *Oak Ridge National Laboratory Report*, pp. ORNL–6895, 1996.

[153] 桜井敏雄 (Tosio Sakurai). X 線結晶解析 (X-RAY ANALYSIS OF CRYSTAL STRUCTURE). 裳華房 (SYÔKABÔ), 2006.

[154] 桜井敏雄 (Tosio Sakurai). X 線結晶解析の手引き (HANDBOOK OF X-RAY ANALYSIS OF CRYSTAL STRUCTURE). 裳華房 (SYÔKABÔ), 2004.

Appendix

A.1 Interatomic angles, φ_{para}, φ_{ferro}, and ψ, and their propagations of the errors

Here, the author presents the calculation process for interatomic angles, φ_{para}, φ_{ferro}, and ψ, and their propagations of the errors in both KDP and DKDP. They are previously referred by Nelmes, Kuhs, and other workers. For O atom in H bond only in paraelectric phase, it is defined by

$$\varphi_{\text{para}} \equiv \arctan\left\{-\frac{c\left(z_{\text{O}}-\frac{1}{8}\right)}{b\left(y_{\text{O}}-\frac{1}{4}\right)}\right\}, \tag{A.1.1}$$

and in ferroelectric phase as

$$\varphi_{\text{ferro}} \equiv \arctan\left[-\frac{c\left(\frac{1}{4}+z_{\text{O1}}-z_{\text{O2}}\right)}{\left\{a^2\left(\frac{1}{4}+x_{\text{O1}}-x_{\text{O2}}\right)^2+b^2\left(-\frac{1}{4}+y_{\text{O1}}+y_{\text{O2}}\right)^2\right\}^{1/2}}\right]. \tag{A.1.2}$$

And it is for H/D atom in H bond only in paraelectric phase as,

$$\psi \equiv \arctan\left\{\frac{c\left(z_{\text{H/D}}-\frac{1}{8}\right)}{b\left(y_{\text{H/D}}-\frac{1}{4}\right)}\right\}. \tag{A.1.3}$$

The calculation of φ_{para} does require the coordinate of only one oxygen atom of unit cell content in paraelectric phase. On the other hand, φ_{ferro} can be calculated from the coordinates of two oxygen atoms (O_1 and O_2) in the ferroelectric phase, the later of which has the translated coordinate of $(x_{O_2}-1/4, -y_{O_2}+1/4, z_{O_2}-1/4)$ as a general equivalent position. Besides, ψ for H/D atom in splitting state can be calculated only in the paraelectric phase, but the calculation of ψ is impossible and nonsense in ferroelectric phase.

For easy expressions, let us rewrite φ_{para}, φ_{ferro}, and ψ as follows:

$$\alpha \equiv -\frac{c\,(z_{\text{O}} - 1/8)}{b\,(y_{\text{O}} - 1/4)} \quad \text{or} \quad \frac{c\,(z_{\text{H/D}} - 1/8)}{b\,(y_{\text{H/D}} - 1/4)}, \tag{A.1.4}$$

$$\begin{aligned}\beta &\equiv -\frac{c\,(1/4 + z_{\text{O1}} - z_{\text{O2}})}{\left\{a^2\,(1/4 + x_{\text{O1}} - x_{\text{O2}})^2 + b^2\,(-1/4 + y_{\text{O1}} + y_{\text{O2}})^2\right\}^{1/2}} \\ &= -\frac{c\,(1/4 + z_{\text{O1}} - z_{\text{O2}})}{\gamma^{1/2}},\end{aligned} \tag{A.1.5}$$

$$\gamma \equiv a^2\,(1/4 + x_{\text{O1}} - x_{\text{O2}})^2 + b^2\,(-1/4 + y_{\text{O1}} + y_{\text{O2}})^2, \tag{A.1.6}$$

$$\varphi_{\text{para}} = \arctan\alpha, \tag{A.1.7}$$

$$\varphi_{\text{ferro}} = \arctan\beta, \tag{A.1.8}$$

$$\psi = \arctan\alpha. \tag{A.1.9}$$

By using of above α, β, and γ, We can obtain the propagations of the errors for φ_{para}, φ_{ferro}, and ψ as following expressions.

Firstly, about $\mu_{\varphi_{\text{para}}}$ is shown as follows:

$$\mu^2_{\varphi_{\text{para}}} = \left\{\left(\frac{\partial\varphi_{\text{para}}}{\partial b}\right)^2\mu_b^2 + \left(\frac{\partial\varphi_{\text{para}}}{\partial c}\right)^2\mu_c^2 + \left(\frac{\partial\varphi_{\text{para}}}{\partial y_{\text{O}}}\right)^2\mu^2_{y_{\text{O}}} + \left(\frac{\partial\varphi_{\text{para}}}{\partial z_{\text{O}}}\right)^2\mu^2_{z_{\text{O}}}\right\}, \tag{A.1.10}$$

$$\frac{\partial\varphi_{\text{para}}}{\partial b} = \frac{\alpha}{1+\alpha^2}\left(-\frac{1}{b}\right), \tag{A.1.11}$$

$$\frac{\partial\varphi_{\text{para}}}{\partial c} = \frac{\alpha}{1+\alpha^2}\left(\frac{1}{c}\right), \tag{A.1.12}$$

$$\frac{\partial\varphi_{\text{para}}}{\partial y_{\text{O}}} = \frac{\alpha}{1+\alpha^2}\left(-\frac{1}{y_{\text{O}} - 1/4}\right), \tag{A.1.13}$$

$$\frac{\partial\varphi_{\text{para}}}{\partial z_{\text{O}}} = \frac{\alpha}{1+\alpha^2}\left(\frac{1}{z_{\text{O}} - 1/8}\right), \tag{A.1.14}$$

$$\mu_{\varphi_{\text{para}}} = \frac{|\alpha|}{1+\alpha^2}\left\{\left(\frac{\mu_b}{b}\right)^2 + \left(\frac{\mu_c}{c}\right)^2 + \left(\frac{\mu_{y_{\text{O}}}}{y_{\text{O}} - 1/4}\right)^2 + \left(\frac{\mu_{z_{\text{O}}}}{z_{\text{O}} - 1/8}\right)^2\right\}^{1/2}. \tag{A.1.15}$$

In the same way, μ_ψ can be calculated as below.

$$\mu_\psi^2 = \left\{ \left(\frac{\partial\psi}{\partial b}\right)^2 \mu_b^2 + \left(\frac{\partial\psi}{\partial c}\right)^2 \mu_c^2 + \left(\frac{\partial\psi}{\partial y_{\mathrm{H/D}}}\right)^2 \mu_{y_{\mathrm{H/D}}}^2 + \left(\frac{\partial\psi}{\partial z_{\mathrm{H/D}}}\right)^2 \mu_{z_{\mathrm{H/D}}}^2 \right\}, \tag{A.1.16}$$

$$\frac{\partial\psi}{\partial b} = \frac{\alpha}{1+\alpha^2}\left(-\frac{1}{b}\right), \tag{A.1.17}$$

$$\frac{\partial\psi}{\partial c} = \frac{\alpha}{1+\alpha^2}\left(\frac{1}{c}\right), \tag{A.1.18}$$

$$\frac{\partial\psi}{\partial y_{\mathrm{H/D}}} = \frac{\alpha}{1+\alpha^2}\left(-\frac{1}{y_{\mathrm{H/D}} - 1/4}\right), \tag{A.1.19}$$

$$\frac{\partial\psi}{\partial z_{\mathrm{H/D}}} = \frac{\alpha}{1+\alpha^2}\left(\frac{1}{z_{\mathrm{H/D}} - 1/8}\right), \tag{A.1.20}$$

$$\mu_\psi = \frac{|\alpha|}{1+\alpha^2}\left\{\left(\frac{\mu_b}{b}\right)^2 + \left(\frac{\mu_c}{c}\right)^2 + \left(\frac{\mu_{y_{\mathrm{H/D}}}}{y_{\mathrm{H/D}} - 1/4}\right)^2 + \left(\frac{\mu_{z_{\mathrm{H/D}}}}{z_{\mathrm{H/D}} - 1/8}\right)^2\right\}^{1/2}. \tag{A.1.21}$$

Finally, $\mu_{\varphi_{\text{ferro}}}$ is shown below.

$$\mu^2_{\varphi_{\text{ferro}}} = \left\{ \left(\frac{\partial\varphi_{\text{ferro}}}{\partial a}\right)^2 \mu_a^2 + \left(\frac{\partial\varphi_{\text{ferro}}}{\partial b}\right)^2 \mu_b^2 + \left(\frac{\partial\varphi_{\text{ferro}}}{\partial c}\right)^2 \mu_c^2 + \left(\frac{\partial\varphi_{\text{ferro}}}{\partial x_{\text{O1}}}\right)^2 \mu^2_{x_{\text{O1}}} + \left(\frac{\partial\varphi_{\text{ferro}}}{\partial x_{\text{O2}}}\right)^2 \mu^2_{x_{\text{O2}}} + \left(\frac{\partial\varphi_{\text{ferro}}}{\partial y_{\text{O1}}}\right)^2 \mu^2_{y_{\text{O1}}} + \left(\frac{\partial\varphi_{\text{ferro}}}{\partial y_{\text{O2}}}\right)^2 \mu^2_{y_{\text{O2}}} + \left(\frac{\partial\varphi_{\text{ferro}}}{\partial z_{\text{O1}}}\right)^2 \mu^2_{z_{\text{O1}}} + \left(\frac{\partial\varphi_{\text{ferro}}}{\partial z_{\text{O2}}}\right)^2 \mu^2_{z_{\text{O2}}} \right\}, \tag{A.1.22}$$

$$\frac{\partial\varphi_{\text{ferro}}}{\partial a} = \frac{\beta}{1+\beta^2}\left(-\frac{a}{\gamma}\right)\left(\frac{1}{4} + x_{\text{O1}} - x_{\text{O2}}\right)^2, \tag{A.1.23}$$

$$\frac{\partial\varphi_{\text{ferro}}}{\partial b} = \frac{\beta}{1+\beta^2}\left(-\frac{b}{\gamma}\right)\left(-\frac{1}{4} + y_{\text{O1}} + y_{\text{O2}}\right)^2, \tag{A.1.24}$$

$$\frac{\partial\varphi_{\text{ferro}}}{\partial c} = \frac{\beta}{1+\beta^2}\left(\frac{1}{c}\right), \tag{A.1.25}$$

$$\frac{\partial\varphi_{\text{ferro}}}{\partial x_{\text{O1}}} = \frac{\beta}{1+\beta^2}\left(-\frac{a^2}{\gamma}\right)\left(\frac{1}{4} + x_{\text{O1}} - x_{\text{O2}}\right), \tag{A.1.26}$$

$$\frac{\partial\varphi_{\text{ferro}}}{\partial x_{\text{O2}}} = \frac{\beta}{1+\beta^2}\left(\frac{a^2}{\gamma}\right)\left(\frac{1}{4} + x_{\text{O1}} - x_{\text{O2}}\right), \tag{A.1.27}$$

$$\frac{\partial\varphi_{\text{ferro}}}{\partial y_{\text{O1}}} = \frac{\beta}{1+\beta^2}\left(-\frac{b^2}{\gamma}\right)\left(-\frac{1}{4} + y_{\text{O1}} + y_{\text{O2}}\right), \tag{A.1.28}$$

$$\frac{\partial\varphi_{\text{ferro}}}{\partial y_{\text{O2}}} = \frac{\beta}{1+\beta^2}\left(-\frac{b^2}{\gamma}\right)\left(-\frac{1}{4} + y_{\text{O1}} + y_{\text{O2}}\right), \tag{A.1.29}$$

$$\frac{\partial\varphi_{\text{ferro}}}{\partial z_{\text{O1}}} = \frac{\beta}{1+\beta^2}\left(\frac{1}{1/4 + z_{\text{O1}} - z_{\text{O2}}}\right), \tag{A.1.30}$$

$$\frac{\partial\varphi_{\text{ferro}}}{\partial z_{\text{O2}}} = \frac{\beta}{1+\beta^2}\left(-\frac{1}{1/4 + z_{\text{O1}} - z_{\text{O2}}}\right), \tag{A.1.31}$$

$$\mu_{\varphi_{\text{ferro}}} = \frac{|\beta|}{1+\beta^2}\left[\frac{1}{\gamma^2}\left\{a^2\left(1/4 + x_{\text{O1}} - x_{\text{O2}}\right)^4 \mu_a^2 + b^2\left(-1/4 + y_{\text{O1}} + y_{\text{O2}}\right)^4 \mu_b^2 + a^4\left(1/4 + x_{\text{O1}} - x_{\text{O2}}\right)^2\left(\mu^2_{x_{\text{O1}}} + \mu^2_{x_{\text{O2}}}\right) + b^4\left(-1/4 + y_{\text{O1}} + y_{\text{O2}}\right)^2\left(\mu^2_{y_{\text{O1}}} + \mu^2_{y_{\text{O2}}}\right)\right\} + \left(\frac{\mu_c}{c}\right)^2 + \frac{\mu^2_{z_{\text{O1}}} + \mu^2_{z_{\text{O2}}}}{\left(1/4 + z_{\text{O1}} - z_{\text{O2}}\right)^2}\right]^{1/2}. \tag{A.1.32}$$

A.2 Center of mass of KDP/DKDP

Here, let us consider center of mass of KDP/DKDP in idea of fractional coordinate.

$$\begin{aligned} m_{\mathrm{all}} z_{\mathrm{g}} &= m_{\mathrm{K}} \left[\frac{1}{2} z_{\mathrm{K}} + \frac{1}{2} \left(z_{\mathrm{K}} - 1 \right) \right] + m_{\mathrm{P}} z_{\mathrm{P}} \\ &\quad + m_{\mathrm{O}} \left(2 z_{\mathrm{O}_1} + 2 z_{\mathrm{O}_2} \right) + m_{\mathrm{H/D}} \left[2 \frac{1}{2} z_{\mathrm{H/D}} + 2 \frac{1}{2} \left(z_{\mathrm{H/D}} - 0.25 \right) \right] \\ &= m_{\mathrm{K}} \left(z_{\mathrm{K}} - 0.5 \right) + m_{\mathrm{P}} z_{\mathrm{P}} + m_{\mathrm{O}} \left(2 z_{\mathrm{O}_1} + 2 z_{\mathrm{O}_2} \right) + m_{\mathrm{H/D}} \left(2 z_{\mathrm{H/D}} - 0.25 \right), \end{aligned} \tag{A.2.1}$$

where m_{K}, m_{P}, m_{O}, $m_{\mathrm{H/D}}$ are atomic/ionic masses of $39.098\,3/N_{\mathrm{A}}$, $30.973\,762/N_{\mathrm{A}}$, $15.999\,4/N_{\mathrm{A}}$, and $(1+R_{\mathrm{d}})/N_{\mathrm{A}}$, respectively, in which N_{A} and R_{d} represent Avogadro's constant and deuterium replacement rate, respectively. Therefore,

$$z_{\mathrm{g}} = \frac{1}{m_{\mathrm{all}}} \left[m_{\mathrm{K}} \left(z_{\mathrm{K}} - 0.5 \right) + m_{\mathrm{P}} z_{\mathrm{P}} + m_{\mathrm{O}} \left(2 z_{\mathrm{O}_1} + 2 z_{\mathrm{O}_2} \right) + m_{\mathrm{H/D}} \left(2 z_{\mathrm{H/D}} - 0.25 \right) \right], \tag{A.2.2}$$

$$m_{\mathrm{all}} \equiv m_{\mathrm{K}} + m_{\mathrm{P}} + 4 m_{\mathrm{O}} + 2 m_{\mathrm{H/D}}. \tag{A.2.3}$$

For the propagation of error,

$$Y = f\left(X_1, X_2, X_3, \cdots \right), \tag{A.2.4}$$

$$\mu_Y^2 = \left(\frac{\partial f}{\partial X_1} \right)^2 \mu_{X_1}^2 + \left(\frac{\partial f}{\partial X_2} \right)^2 \mu_{X_2}^2 + \cdots, \tag{A.2.5}$$

$$\begin{aligned} \mu_{z_{\mathrm{g}}}^2 &= \left(\frac{\partial z_{\mathrm{g}}}{\partial z_{\mathrm{K}}} \right)^2 \mu_{z_{\mathrm{K}}}^2 + \left(\frac{\partial z_{\mathrm{g}}}{\partial z_{\mathrm{P}}} \right)^2 \mu_{z_{\mathrm{P}}}^2 \\ &\quad + \left(\frac{\partial z_{\mathrm{g}}}{\partial z_{\mathrm{O}_1}} \right)^2 \mu_{z_{\mathrm{O}_1}}^2 + \left(\frac{\partial z_{\mathrm{g}}}{\partial z_{\mathrm{O}_2}} \right)^2 \mu_{z_{\mathrm{O}_2}}^2 + \left(\frac{\partial z_{\mathrm{g}}}{\partial z_{\mathrm{H/D}}} \right)^2 \mu_{z_{\mathrm{H/D}}}^2, \end{aligned} \tag{A.2.6}$$

$$\mu_{z_{\mathrm{g}}}^2 = \left(\frac{1}{m_{\mathrm{all}}} \right)^2 \left[m_{\mathrm{K}}^2 \mu_{z_{\mathrm{K}}}^2 + m_{\mathrm{P}}^2 \mu_{z_{\mathrm{P}}}^2 + 4 m_{\mathrm{O}}^2 \left(\mu_{z_{\mathrm{O}_1}}^2 + \mu_{z_{\mathrm{O}_2}}^2 \right) + 4 m_{\mathrm{H/D}}^2 \mu_{z_{\mathrm{H/D}}}^2 \right], \tag{A.2.7}$$

$$\mu_{z_{\mathrm{g}}} = \frac{1}{m_{\mathrm{all}}} \left[m_{\mathrm{K}}^2 \mu_{z_{\mathrm{K}}}^2 + m_{\mathrm{P}}^2 \mu_{z_{\mathrm{P}}}^2 + 4 m_{\mathrm{O}}^2 \left(\mu_{z_{\mathrm{O}_1}}^2 + \mu_{z_{\mathrm{O}_2}}^2 \right) + 4 m_{\mathrm{H/D}}^2 \mu_{z_{\mathrm{H/D}}}^2 \right]^{1/2}. \tag{A.2.8}$$

Moreover,

$$z_i' \equiv z_i + z_{\mathrm{g}}, \tag{A.2.9}$$

$$\mu_{z_i'}^2 = \mu_{z_i}^2 + \mu_{z_{\mathrm{g}}}^2, \tag{A.2.10}$$

$$\mu_{z_i'} = \left(\mu_{z_i}^2 + \mu_{z_{\mathrm{g}}}^2 \right)^{1/2}. \tag{A.2.11}$$

We can convert these calculations into ones of real space (*e.g.*, in Å, nm and etc.).

$$\begin{aligned} c_{\mathrm{g}} &\equiv c z_{\mathrm{g}} \\ &= \frac{c}{m_{\mathrm{all}}} \left[m_{\mathrm{K}} \left(z_{\mathrm{K}} - 0.5 \right) + m_{\mathrm{P}} z_{\mathrm{P}} + m_{\mathrm{O}} \left(2 z_{\mathrm{O}_1} + 2 z_{\mathrm{O}_2} \right) + m_{\mathrm{H/D}} \left(2 z_{\mathrm{H/D}} - 0.25 \right) \right], \end{aligned} \tag{A.2.12}$$

$$\begin{aligned} \mu_{c_{\mathrm{g}}}^2 &= \left(\frac{1}{m_{\mathrm{all}}} \right)^2 \left[m_{\mathrm{K}} \left(z_{\mathrm{K}} - 0.5 \right) + m_{\mathrm{P}} z_{\mathrm{P}} + m_{\mathrm{O}} \left(2 z_{\mathrm{O}_1} + 2 z_{\mathrm{O}_2} \right) \right. \\ &\qquad \left. + m_{\mathrm{H/D}} \left(2 z_{\mathrm{H/D}} - 0.25 \right) \right]^2 \mu_c^2 \\ &\quad + \left(\frac{c}{m_{\mathrm{all}}} \right)^2 \left[m_{\mathrm{K}}^2 \mu_{z_{\mathrm{K}}}^2 + m_{\mathrm{P}}^2 \mu_{z_{\mathrm{P}}}^2 + 4 m_{\mathrm{O}}^2 \left(\mu_{z_{\mathrm{O}_1}}^2 + \mu_{z_{\mathrm{O}_2}}^2 \right) + 4 m_{\mathrm{H/D}}^2 \mu_{z_{\mathrm{H/D}}}^2 \right] \\ &= z_{\mathrm{g}}^2 \mu_c^2 + c^2 \mu_{z_{\mathrm{g}}}^2 \\ &= c_{\mathrm{g}}^2 \left[\left(\frac{\mu_c}{c} \right)^2 + \left(\frac{\mu_{z_{\mathrm{g}}}}{z_{\mathrm{g}}} \right)^2 \right], \end{aligned} \tag{A.2.13}$$

$$\mu_{c_{\mathrm{g}}} = |c_{\mathrm{g}}| \left[\left(\frac{\mu_c}{c} \right)^2 + \left(\frac{\mu_{z_{\mathrm{g}}}}{z_{\mathrm{g}}} \right)^2 \right]^{1/2}. \tag{A.2.14}$$

Finally,

$$c_i' \equiv c_i + c_{\mathrm{g}}, \tag{A.2.15}$$

$$\mu_{c_i'}^2 = \mu_{c_i}^2 + \mu_{c_{\mathrm{g}}}^2, \tag{A.2.16}$$

$$\mu_{c_i'} = \left(\mu_{c_i}^2 + \mu_{c_{\mathrm{g}}}^2 \right)^{1/2}. \tag{A.2.17}$$

A.3 Propagation of the errors for calculation of spontaneous polarization

In the point-charge method, contributions of spontaneous polarization from each atom/ion in the KDP/DKDP unit cell can be written as follows:

$$\begin{aligned} P_{\mathrm{S}} &\equiv \frac{1}{V} evom\Delta l, \\ &= A\frac{\Delta l}{V} \quad (\because A \equiv evom), \end{aligned} \tag{A.3.1}$$

where V: unit cell volume in Å^3, Δl: displacement along the c-axis of each atom in Å, e: elementary charge ($1.602\,177\,33 \times 10^{-19}$ C), v: valence charge of the ion (K: $+1$, P: -1, O: -2, and H/D: $+1$), o: occupancy at a corresponding site, and m: multiplicity for the general equivalent positions in the ferroelectric phase of the space group $Fdd2$ (*i.e.*, 16).

Therefore,

$$\begin{aligned} (\mu_{P_{\mathrm{S}}})^2 &= \left(\frac{\partial P_{\mathrm{S}}}{\partial \Delta l}\right)^2 \mu_{\Delta l}^2 + \left(\frac{\partial P_{\mathrm{S}}}{\partial V}\right)^2 \mu_V^2 \\ &= A^2 \left(\frac{1}{V}\right)^2 \mu_{\Delta l}^2 + A^2 \left(\frac{-\Delta l}{V^2}\right)^2 \mu_V^2 \\ &= \left(\frac{A}{V}\right)^2 \left\{\mu_{\Delta l}^2 + \left(\frac{\Delta l}{V}\right)^2 \mu_V^2\right\} = P_{\mathrm{S}}^2 \left\{\left(\frac{\mu_{\Delta l}}{\Delta l}\right)^2 + \left(\frac{\mu_V}{V}\right)^2\right\}, \end{aligned} \tag{A.3.2}$$

$$\mu_{P_{\mathrm{S}}} = \frac{|A|}{V}\left\{\mu_{\Delta l}^2 + \left(\frac{\Delta l}{V}\right)^2 \mu_V^2\right\}^{\frac{1}{2}} = |P_{\mathrm{S}}|\left\{\left(\frac{\mu_{\Delta l}}{\Delta l}\right)^2 + \left(\frac{\mu_V}{V}\right)^2\right\}^{1/2} \tag{A.3.3}$$

Here, Δl is given as following calculation using z_{ave} and z_{g}: z_{ave} is a average coordinate z for the position of objective atom/ion in the paraelectric phase. (*e.g.*, K: 0.5, P: 0) z_{g} is the center of gravity in the ferroelectric phase of KDP/DKDP unit cell, and calculated separately for obtaining the accordance of center of gravity in both the

paraelectric and ferroelectric phases.

$$\Delta l \equiv c\left(z - z_{\mathrm{g}} - z_{\mathrm{ave}}\right), \tag{A.3.4}$$

$$\begin{aligned}\mu_{\Delta l}^2 &= \left(z - z_{\mathrm{g}} - z_{\mathrm{ave}}\right)^2 \mu_c^2 + c^2\left(\mu_z^2 + \mu_{z_{\mathrm{g}}}^2\right) \\ &= \Delta l^2 \left\{\left(\frac{\mu_c}{c}\right)^2 + \frac{\mu_z^2 + \mu_{z_{\mathrm{g}}}^2}{\left(z - z_{\mathrm{g}} - z_{\mathrm{ave}}\right)^2}\right\},\end{aligned} \tag{A.3.5}$$

$$\begin{aligned}\mu_{\Delta l} &= \left\{\left(z - z_{\mathrm{g}} - z_{\mathrm{ave}}\right)^2 \mu_c^2 + c^2\left(\mu_z^2 + \mu_{z_{\mathrm{g}}}^2\right)\right\}^{\frac{1}{2}} \\ &= |\Delta l| \left\{\left(\frac{\mu_c}{c}\right)^2 + \frac{\mu_z^2 + \mu_{z_{\mathrm{g}}}^2}{\left(z - z_{\mathrm{g}} - z_{\mathrm{ave}}\right)^2}\right\}^{1/2},\end{aligned} \tag{A.3.6}$$

$$\begin{aligned}\mu_V^2 &= (bc)^2 \mu_a^2 + (ac)^2 \mu_b^2 + (ab)^2 \mu_c^2 \\ &= V^2 \left\{\left(\frac{\mu_a}{a}\right)^2 + \left(\frac{\mu_b}{b}\right)^2 + \left(\frac{\mu_c}{c}\right)^2\right\},\end{aligned} \tag{A.3.7}$$

$$\mu_V = V\left\{\left(\frac{\mu_a}{a}\right)^2 + \left(\frac{\mu_b}{b}\right)^2 + \left(\frac{\mu_c}{c}\right)^2\right\}^{\frac{1}{2}} \tag{A.3.8}$$

$$P_{\mathrm{S,All}} \equiv P_{\mathrm{S,K}} + P_{\mathrm{S,P}} + P_{\mathrm{S,O1}} + P_{\mathrm{S,O2}} + P_{\mathrm{H/D}}, \tag{A.3.9}$$

$$\mu_{P_{\mathrm{S,All}}} = \left\{\mu_{P_{\mathrm{S,K}}}^2 + \mu_{P_{\mathrm{S,P}}}^2 + \mu_{P_{\mathrm{S,O1}}}^2 + \mu_{P_{\mathrm{S,O2}}}^2 + \mu_{P_{\mathrm{H/D}}}^2\right\}^{1/2} \tag{A.3.10}$$

A.4 Conversion from $U_{11,\mathrm{Ferro}}$ and $U_{22,\mathrm{Ferro}}$ to $U_{11,\mathrm{Para}}$ and $U_{22,\mathrm{Para}}$

In this section, we should check the conversion of the anisotropic atomic displacement parameters, U_{ij}'s, from the ferroelectric phase (space group *Fdd*2, Orthorhombic) to the paraelectric phase (space group $I\bar{4}2d$, Tetragonal) of KDP/DKDP.

Rotation angle from the ferroelectric lattice to the paraelectric lattice about the c-axis is *ca.* $-45°$.

With $\theta_\mathrm{c} \equiv -45°$,

$$\begin{aligned}
\begin{pmatrix} U_{11,\mathrm{P}} & U_{12,\mathrm{P}} \\ U_{12,\mathrm{P}} & U_{22,\mathrm{P}} \end{pmatrix} &= \begin{pmatrix} \cos\theta_\mathrm{c} & \sin\theta_\mathrm{c} \\ -\sin\theta_\mathrm{c} & \cos\theta_\mathrm{c} \end{pmatrix} \begin{pmatrix} U_{11,\mathrm{F}} & U_{12,\mathrm{F}} \\ U_{12,\mathrm{F}} & U_{22,\mathrm{F}} \end{pmatrix} \begin{pmatrix} \cos\theta_\mathrm{c} & -\sin\theta_\mathrm{c} \\ \sin\theta_\mathrm{c} & \cos\theta_\mathrm{c} \end{pmatrix} \\
&= \begin{pmatrix} \frac{1}{\sqrt{2}} & -\frac{1}{\sqrt{2}} \\ \frac{1}{\sqrt{2}} & \frac{1}{\sqrt{2}} \end{pmatrix} \begin{pmatrix} U_{11,\mathrm{F}} & U_{12,\mathrm{F}} \\ U_{12,\mathrm{F}} & U_{22,\mathrm{F}} \end{pmatrix} \begin{pmatrix} \frac{1}{\sqrt{2}} & \frac{1}{\sqrt{2}} \\ -\frac{1}{\sqrt{2}} & \frac{1}{\sqrt{2}} \end{pmatrix} \\
&= \frac{1}{2} \begin{pmatrix} 1 & -1 \\ 1 & 1 \end{pmatrix} \begin{pmatrix} U_{11,\mathrm{F}} & U_{12,\mathrm{F}} \\ U_{12,\mathrm{F}} & U_{22,\mathrm{F}} \end{pmatrix} \begin{pmatrix} 1 & 1 \\ -1 & 1 \end{pmatrix} \\
&= \frac{1}{2} \begin{pmatrix} U_{11,\mathrm{F}} - U_{12,\mathrm{F}} & U_{12,\mathrm{F}} - U_{22,\mathrm{F}} \\ U_{11,\mathrm{F}} + U_{12,\mathrm{F}} & U_{12,\mathrm{F}} + U_{22,\mathrm{F}} \end{pmatrix} \begin{pmatrix} 1 & 1 \\ -1 & 1 \end{pmatrix} \\
&= \frac{1}{2} \begin{pmatrix} U_{11,\mathrm{F}} - 2U_{12,\mathrm{F}} + U_{22,\mathrm{F}} & U_{11,\mathrm{F}} - U_{22,\mathrm{F}} \\ U_{11,\mathrm{F}} - U_{22,\mathrm{F}} & U_{11,\mathrm{F}} + 2U_{12,\mathrm{F}} + U_{22,\mathrm{F}} \end{pmatrix}.
\end{aligned} \tag{A.4.1}$$

Therefore,

$$\begin{pmatrix} U_{11,\mathrm{P}} & U_{12,\mathrm{P}} \\ U_{12,\mathrm{P}} & U_{22,\mathrm{P}} \end{pmatrix} = \frac{1}{2} \begin{pmatrix} U_{11,\mathrm{F}} - 2U_{12,\mathrm{F}} + U_{22,\mathrm{F}} & U_{11,\mathrm{F}} - U_{22,\mathrm{F}} \\ U_{11,\mathrm{F}} - U_{22,\mathrm{F}} & U_{11,\mathrm{F}} + 2U_{12,\mathrm{F}} + U_{22,\mathrm{F}} \end{pmatrix}. \tag{A.4.2}$$

About propagation of errors,

$$f(x) \equiv \frac{1}{2} \left(U_{11,\mathrm{F}} \mp 2U_{12,\mathrm{F}} + U_{22,\mathrm{F}} \right), \tag{A.4.3}$$

$$\sigma_{U_{ii,\mathrm{P}}} = \frac{1}{2} \left(\sigma^2_{U_{11,\mathrm{F}}} + 2^2 \sigma^2_{U_{12,\mathrm{F}}} + \sigma^2_{U_{22,\mathrm{F}}} \right)^{\frac{1}{2}}. \tag{A.4.4}$$

Strictly, we must treat U_{ij} (3×3 real-symmetry matrix) as follows:

$$
\begin{aligned}
&\begin{pmatrix} U_{11,\mathrm{P}} & U_{12,\mathrm{P}} & U_{13,\mathrm{P}} \\ U_{12,\mathrm{P}} & U_{22,\mathrm{P}} & U_{23,\mathrm{P}} \\ U_{13,\mathrm{P}} & U_{23,\mathrm{P}} & U_{33,\mathrm{P}} \end{pmatrix} \\
&= \begin{pmatrix} \cos\theta_{\mathrm{c}} & \sin\theta_{\mathrm{c}} & 0 \\ -\sin\theta_{\mathrm{c}} & \cos\theta_{\mathrm{c}} & 0 \\ 0 & 0 & 1 \end{pmatrix} \begin{pmatrix} U_{11,\mathrm{F}} & U_{12,\mathrm{F}} & U_{13,\mathrm{F}} \\ U_{12,\mathrm{F}} & U_{22,\mathrm{F}} & U_{23,\mathrm{F}} \\ U_{13,\mathrm{F}} & U_{23,\mathrm{F}} & U_{33,\mathrm{F}} \end{pmatrix} \begin{pmatrix} \cos\theta_{\mathrm{c}} & -\sin\theta_{\mathrm{c}} & 0 \\ \sin\theta_{\mathrm{c}} & \cos\theta_{\mathrm{c}} & 0 \\ 0 & 0 & 1 \end{pmatrix} \\
&= \begin{pmatrix} \cos\theta_{\mathrm{c}} & \sin\theta_{\mathrm{c}} & 0 \\ -\sin\theta_{\mathrm{c}} & \cos\theta_{\mathrm{c}} & 0 \\ 0 & 0 & 1 \end{pmatrix} \\
&\quad \cdot \begin{pmatrix} \cos\theta_{\mathrm{c}}U_{11,\mathrm{F}} + \sin\theta_{\mathrm{c}}U_{12,\mathrm{F}} & -\sin\theta_{\mathrm{c}}U_{11,\mathrm{F}} + \cos\theta_{\mathrm{c}}U_{12,\mathrm{F}} & U_{13,\mathrm{F}} \\ \cos\theta_{\mathrm{c}}U_{12,\mathrm{F}} + \sin\theta_{\mathrm{c}}U_{22,\mathrm{F}} & -\sin\theta_{\mathrm{c}}U_{12,\mathrm{F}} + \cos\theta_{\mathrm{c}}U_{22,\mathrm{F}} & U_{23,\mathrm{F}} \\ \cos\theta_{\mathrm{c}}U_{13,\mathrm{F}} + \sin\theta_{\mathrm{c}}U_{23,\mathrm{F}} & -\sin\theta_{\mathrm{c}}U_{13,\mathrm{F}} + \cos\theta_{\mathrm{c}}U_{23,\mathrm{F}} & U_{33,\mathrm{F}} \end{pmatrix} \\
&= \begin{pmatrix} U_{11} & U_{12} & U_{13} \\ U_{12} & U_{22} & U_{23} \\ U_{13} & U_{23} & U_{33,\mathrm{F}} \end{pmatrix}, \qquad \text{(A.4.5)}
\end{aligned}
$$

$$U_{11} = \cos^2\theta_{\mathrm{c}}U_{11,\mathrm{F}} + \sin(2\theta_{\mathrm{c}})\,U_{12,\mathrm{F}} + \sin^2\theta_{\mathrm{c}}U_{22,\mathrm{F}}, \qquad \text{(A.4.6)}$$

$$U_{22} = \sin^2\theta_{\mathrm{c}}U_{11,\mathrm{F}} - \sin(2\theta_{\mathrm{c}})\,U_{12,\mathrm{F}} + \cos^2\theta_{\mathrm{c}}U_{22,\mathrm{F}}, \qquad \text{(A.4.7)}$$

$$U_{12} = -\frac{1}{2}\sin(2\theta_{\mathrm{c}})\,U_{11,\mathrm{F}} + \left(1 - 2\sin^2\theta_{\mathrm{c}}\right)U_{12,\mathrm{F}} + \frac{1}{2}\sin(2\theta_{\mathrm{c}})\,U_{22,\mathrm{F}}, \qquad \text{(A.4.8)}$$

$$U_{13} = \cos\theta_{\mathrm{c}}U_{13,\mathrm{F}} + \sin\theta_{\mathrm{c}}U_{23,\mathrm{F}}, \qquad \text{(A.4.9)}$$

$$U_{23} = -\sin\theta_{\mathrm{c}}U_{13,\mathrm{F}} + \cos\theta_{\mathrm{c}}U_{23,\mathrm{F}}. \qquad \text{(A.4.10)}$$

The O_1 atom in ferroelectric phase is corresponding to the oxygen atom with the transformed coordinate of $(-y, x, -z)$ in paraelectric phase. When we have to treat the converted anisotropic atomic displacement parameters of $\mathrm{O}_{1,\mathrm{F}}$, we should pay careful attentions about the transformed oxygen atom in paraelectric phase as follows:

$$
\begin{aligned}
&\begin{pmatrix} 0 & -1 & 0 \\ 1 & 0 & 0 \\ 0 & 0 & -1 \end{pmatrix} \begin{pmatrix} U_{11,\mathrm{O1,P}} & U_{12,\mathrm{O1,P}} & U_{13,\mathrm{O1,P}} \\ U_{12,\mathrm{O1,P}} & U_{22,\mathrm{O1,P}} & U_{23,\mathrm{O1,P}} \\ U_{13,\mathrm{O1,P}} & U_{23,\mathrm{O1,P}} & U_{33,\mathrm{O1,P}} \end{pmatrix} \begin{pmatrix} 0 & 1 & 0 \\ -1 & 0 & 0 \\ 0 & 0 & -1 \end{pmatrix} \\
&= \begin{pmatrix} U_{22,\mathrm{O1,P}} & -U_{12,\mathrm{O1,P}} & U_{23,\mathrm{O1,P}} \\ -U_{12,\mathrm{O1,P}} & U_{11,\mathrm{O1,P}} & -U_{13,\mathrm{O1,P}} \\ U_{23,\mathrm{O1,P}} & -U_{13,\mathrm{O1,P}} & U_{33,\mathrm{O1,P}} \end{pmatrix}. \qquad \text{(A.4.11)}
\end{aligned}
$$

Therefore, we can draw the relationship between converted anisotropic atomic displacement parameters, U'_{ij}, of O_1 atom in ferroelectric phase and transformed those parameters, U_{ij}.

$$U'_{11} = U_{22}, \qquad \text{(A.4.12)}$$

$$U'_{22} = U_{11}, \qquad \text{(A.4.13)}$$

$$U'_{33} = U_{33}. \qquad \text{(A.4.14)}$$

A.5 About double-Morse Potential

The two kinds of potential model curves are well-known in the physical and chemical consideration of particles like atoms and/or molecules; Both Lennard-Jones potential and Morse potential curves are usually preferred.[A-1, A-2]

When investigating and considering a motion and/or a behavior of a particle in a sense of physics, a assumption of a potential curve for the particle should be made for any convenience on the treatment process, and it would yield usually the certain advantage for the work. Since the beginning of studying the behaviors of particles such as atoms in crystals or materials at microscopic viewpoints, two theoretical and/or analytical potential curves have been well-known, and applied for a lot of problems and works.

In general, the Lennard-Jones potential curve, $V_{\mathrm{LJ}}(x)$, are described as follows:

$$V_{\mathrm{LJ}}(x) = 4D\left[\left(\frac{\xi}{x}\right)^{12} - \left(\frac{\xi}{x}\right)^{6}\right]. \tag{A.5.1}$$

Let us consider its derivative function in order to search for its minimum of the potential curve.

$$\frac{V_{\mathrm{LJ}}(x)}{dx} = -4D\left[\frac{12}{x}\left(\frac{\xi}{x}\right)^{12} - \frac{6}{x}\left(\frac{\xi}{x}\right)^{6}\right], \tag{A.5.2}$$

$$d = 2^{1/6}\xi. \quad \because \frac{V_{\mathrm{LJ}}(d)}{dx} = -4D\left[\frac{12}{d}\left(\frac{\xi}{d}\right)^{12} - \frac{6}{d}\left(\frac{\xi}{d}\right)^{6}\right] = 0. \tag{A.5.3}$$

Using the parameter d, we can obtain a easier form of the Lennard-Jones potential curve.

$$V_{\mathrm{LJ}}(x) = 4D\left[\frac{1}{4}\left(\frac{d}{x}\right)^{12} - \frac{1}{2}\left(\frac{d}{x}\right)^{6}\right] \tag{A.5.4}$$

$$= D\left[\left(\frac{d}{x}\right)^{12} - 2\left(\frac{d}{x}\right)^{6}\right]. \tag{A.5.5}$$

As seen above, The Lennard-Jones potential curve consists of the potential depth, D, potential minimum position, d, and the two kinds of the powers of x. The unique shape of the potential curve is predominantly decided by the two and only two parameters , D and d. The potential depth D may be considered as the bond energy of the system for any cases.

On the other hand, the Morse potential curve is also used as a function with two kinds of exponential terms.

$$V_{\mathrm{M}}(x) = D\left[\exp\left(-2A\left(x-d\right)\right) - 2\exp\left(-A\left(x-d\right)\right)\right], \tag{A.5.6}$$

where D, A, and d are the potential depth, the curvature parameter, and the minimum position of the Morse potential curve, respectively. The derivative function of the Morse potential curve,

$$\begin{aligned}\frac{dV_{\mathrm{M}}(x)}{dx} &= D\left[-2A\exp\left(-2A\left(x-d\right)\right)+2A\exp\left(-A\left(x-d\right)\right)\right] \\ &= -2AD\left[\exp\left(-2A\left(x-d\right)\right)-\exp\left(-A\left(x-d\right)\right)\right], \end{aligned} \tag{A.5.7}$$

gives us the understanding of the minimum position d; the parameter d represents a position of a well in the Morse potential curve, and the curve has the only and global minimum. ($\because dV_{\mathrm{M}}(x)/dx|_{x=d} = 0$.)

For practical understanding of the Lennard-Jones and Morse potential curves, Figure A.1 shows a comparison of the two potential curves. As seen in Figure A.1, the Morse potential curves have more flexibility on calculation modeling than the Lennard-Jones potential curves for the extra parameter, A. These two kinds of the

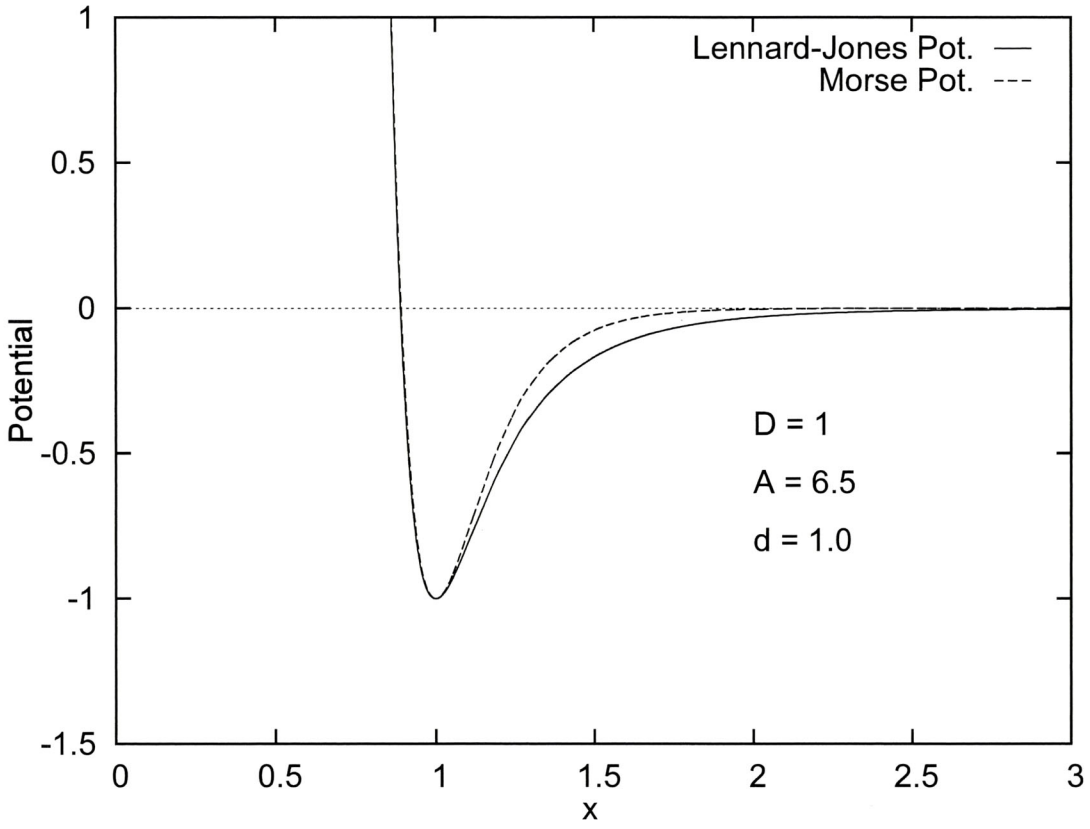

Figure A.1 Lennard-Jones and Morse potential curves with a common potential depth, D, and a common distance parameters (*i.e.*, one and only one minimum position), d. Here, the Morse potential curve has a appropriate curvature parameter, A, which is fixed by the author for likely fitting onto the Lennard-Jones potential curve. The Morse potential curves have more flexibility on calculation modeling than the Lennard-Jones potential curves for a extra parameter, A.

potential curves are convenient to express the microscopic behavior of the particles such as atom in crystals at the chemical and physical viewpoints.

The double-Morse potential curve consists of two Morse potential curves back-to-back with each other in mirror-symmetry style, as shown below.

$$\begin{aligned} V_{\mathrm{DM}}(x) &= D\left[\exp\left(-2A\left(x+d\right)\right)-2\exp\left(-A\left(x+d\right)\right)\right] \\ &\quad + D\left[\exp\left(-2A\left(-x+d\right)\right)-2\exp\left(-A\left(-x+d\right)\right)\right] \\ &= 2D\left[e^{-2Ad}\cosh\left(2Ax\right)-2e^{-Ad}\cosh\left(Ax\right)\right]. \end{aligned} \tag{A.5.8}$$

In following calculation, the existences of extremal value of $V_{\mathrm{DM}}(x)$ are checked.

$$\frac{dV_{\mathrm{DM}}(x)}{dx} = 4ADe^{-Ad}\left[e^{-Ad}\sinh\left(2Ax\right)-\sinh\left(Ax\right)\right]=0, \tag{A.5.9}$$

$$\begin{aligned} & e^{-Ad}\sinh\left(2Ax\right)-\sinh\left(Ax\right) \\ &= e^{-Ad}\frac{e^{2Ax}-e^{-2Ax}}{2}-\frac{e^{Ax}-e^{-Ax}}{2} \\ &= e^{-Ad}\frac{\left(e^{Ax}+e^{-Ax}\right)\left(e^{Ax}-e^{-Ax}\right)}{2}-\frac{e^{Ax}-e^{-Ax}}{2} \\ &= \frac{\left(e^{Ax}-e^{-Ax}\right)}{2}\left[e^{-Ad}\left(e^{Ax}+e^{-Ax}\right)-1\right]=0. \end{aligned} \tag{A.5.10}$$

Here, a trivial solution, $x_0 = 0$, is easily confirmed. Furthermore, non-trivial solution, x_{DM}, should be obtained, as shown below.

$$e^{Ax}+e^{-Ax}-e^{Ad}=0, \tag{A.5.11}$$

$$e^{2Ax}-e^{Ad}e^{Ax}+1=0, \tag{A.5.12}$$

$$e^{Ax} = \frac{e^{Ad}\pm\left(e^{2Ad}-4\right)^{1/2}}{2}, \tag{A.5.13}$$

$$x_{\mathrm{DM}} = \frac{1}{A}\ln\frac{e^{Ad}\pm\left(e^{2Ad}-4\right)^{1/2}}{2}. \tag{A.5.14}$$

It is possible for x_{DM} to be a real and multiple root, and its condition is expressed as follows:

$$e^{2Ad}-4=0, \tag{A.5.15}$$

$$2Ad=\ln 4, \tag{A.5.16}$$

$$Ad=\ln 2. \tag{A.5.17}$$

If the special condition, $Ad = \ln 2$, are hold, then $V_{\mathrm{DM}}(x)$ has only a single and global minimum at $x_0 = 0$.

Figures A.2 and A.3 show the A and d dependences on the whole shapes of double-Morse potential curves, respectively. [*1] These figure would be easy helps for beginners learning the double-Morse potential curves, and the author hopes it.

[*1] They are special demonstrations from the author for the sake of hard-working readers.

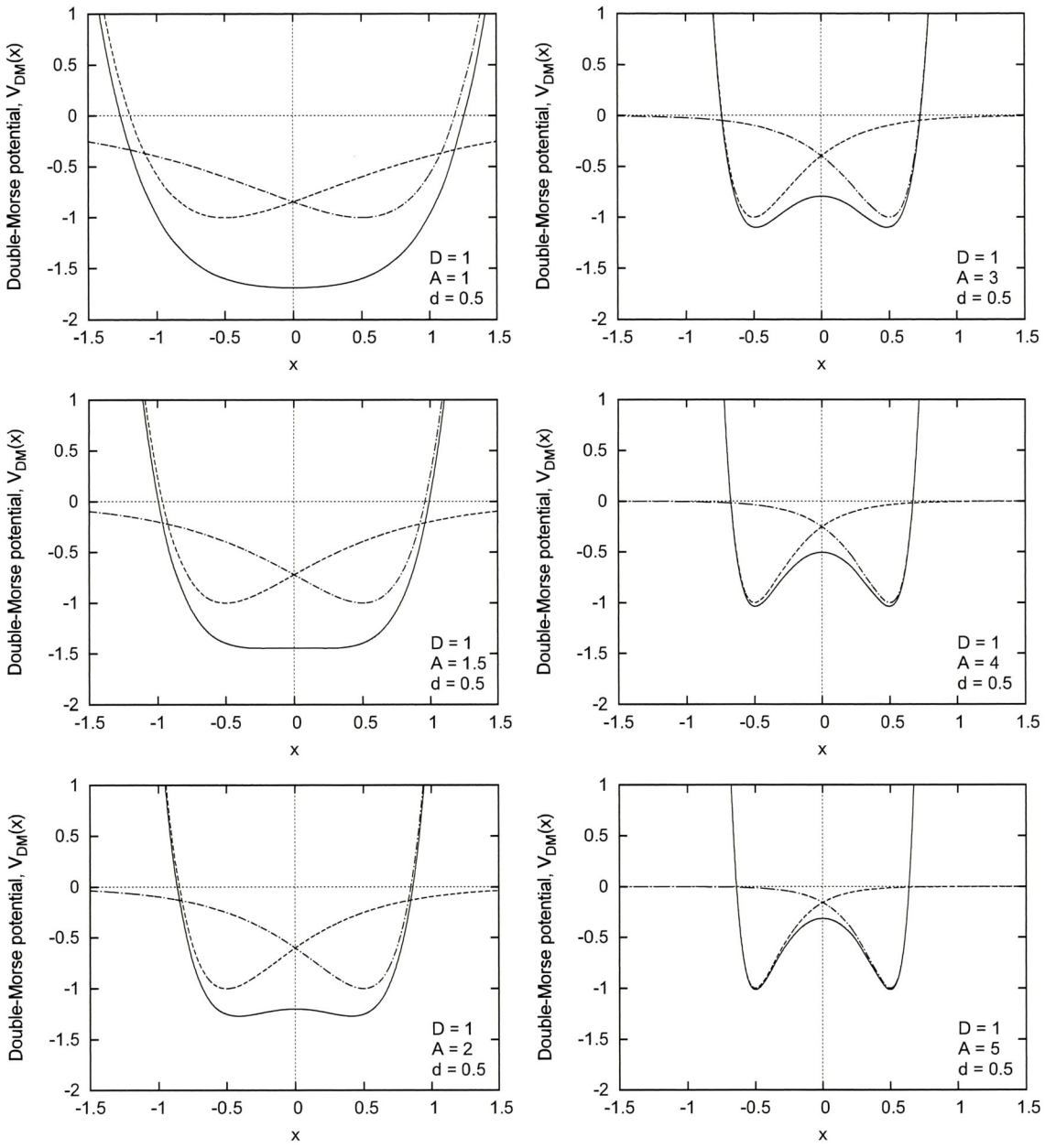

Figure A.2 Examples of double-Morse potential curves with the common potential depth, D, the various curvature parameters, $A = 1, 1.5, 2, 3, 4$, and 5, and the common distance parameter, d.

For previous reports of KDP/DKDP, the particles , *i.e.*, the protons and deuterons have been usually placed in the double-Morse potential curves. Because the protons and deuterons lie in two equilibrium sites with the equal probability in the systems, the workers have been imaged the pictures of the particles motions and behaviors in the double minimum potentials. Thus, the double-Morse potential curves are the most likely candidates of the particle potential models for KDP/DKDP. *e.g.*, Mashiyama presented a report of the behaviors of protons and deuterons in the hydrogen-bond of crystals using the double-Morse potential curves by numerical calculations, and he

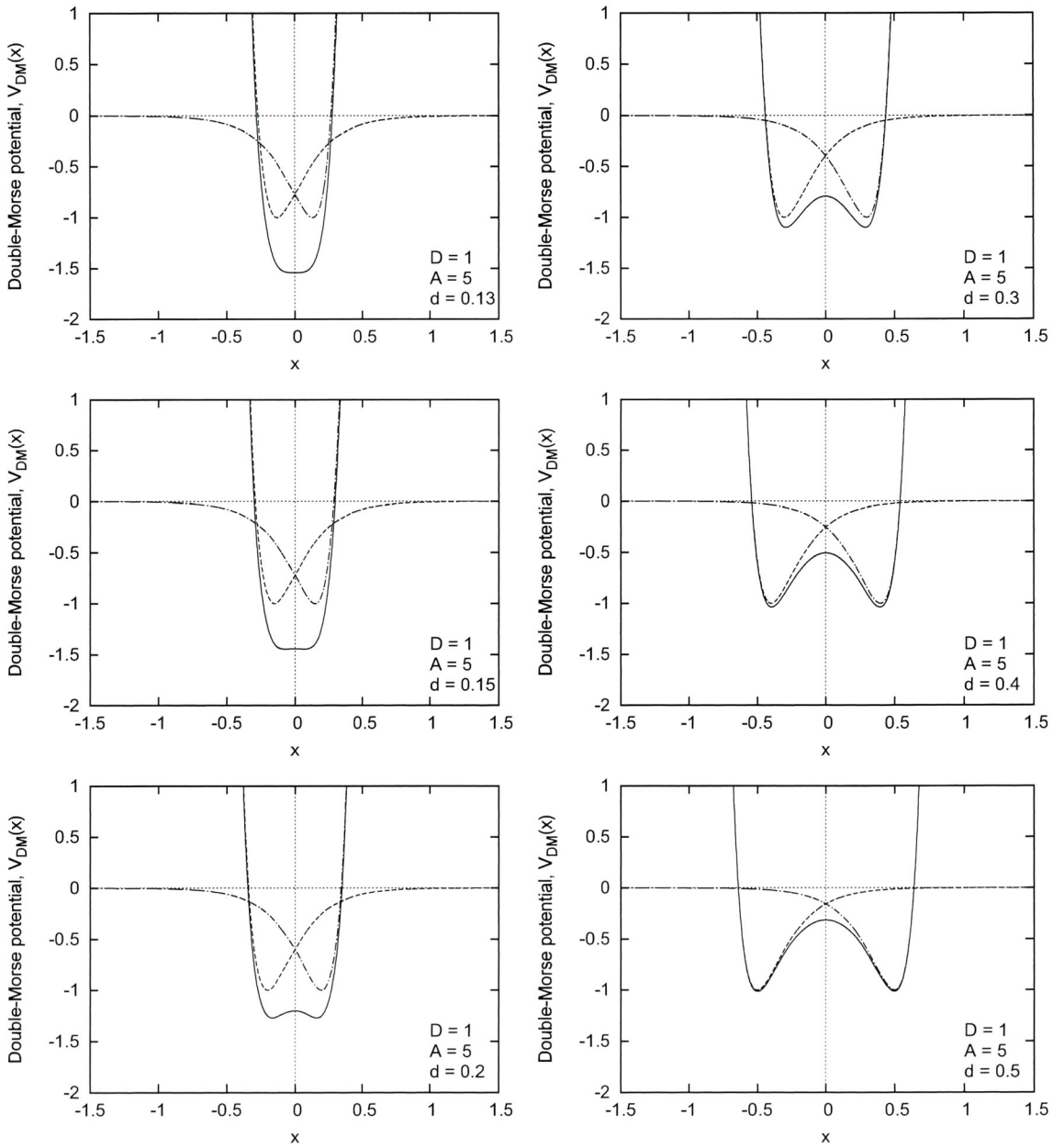

Figure A.3 Examples of double-Morse potential curves with the common potential depth, D, the common curvature parameter, A, and the various distance parameters, $d = 0.13, 0.15, 0.2, 0.3, 0.4$, and 0.5.

mentioned the deference between them. [38]

References

[A-1] J. E. Jones, On the determination of molecular fields. II. From the equation of state of a gas. *Proc. R. Soc. London, Ser. A*, Vol. 106, pp. 463–477, 1924.

[A-2] Philip M. Morse, Diatomic molecules according to the wave mechanics. II. Vibrational levels. *Phys. Rev.*, Vol. 34, pp. 57–64, 1929.